

1-16-2015

# Electrochromic Polymer Composites Forming in Solid Gel Matrix and Flexible Electrode for Photonic Application

Amrita Kumar

University of Connecticut - Storrs, [amrita.kumar@uconn.edu](mailto:amrita.kumar@uconn.edu)

Follow this and additional works at: <https://opencommons.uconn.edu/dissertations>

---

## Recommended Citation

Kumar, Amrita, "Electrochromic Polymer Composites Forming in Solid Gel Matrix and Flexible Electrode for Photonic Application" (2015). *Doctoral Dissertations*. 675.  
<https://opencommons.uconn.edu/dissertations/675>

# Electrochromic Polymer Composites Forming in Solid Gel Matrix and Flexible Electrode for Photonic Application

Amrita Kumar

University of Connecticut, 2015

$\pi$ -conjugated electrochromic polymers can undergo reversible oxidation-reduction reaction by application of an external potential and show a change in their electronic property. These polymeric semiconductors have widespread application in electrochromic devices, photovoltaic cells, batteries, thin film transistors, light emitting diodes, radio frequency identification tags and sensors. Among all these possible applications, our research interest is on making electrochromic displays that could be used as smart window, auto dimming rear view mirror, color-changing eye wear, color controlling textile etc. Because of high color efficiency, easy processability, low cost, lightweight, film flexibility and easy control on electronic behavior make the  $\pi$ -conjugated electrochromic polymer a potential candidate for electrochromic devices. Sotzing group has developed a simple one-step method, i.e. *in situ* to assemble electrochromic devices by reducing chemical waste and assembly time along with high success rate. Electrochromic polymer, hereby, generated from small aromatic molecules inside the solid devices, can be used for versatile application purposes. Instead of using one type of monomer, two or more monomers could be dissolved into the liquid polymer gel electrolyte and color of the device could be tuned easily using this *in situ* approach. In **Chapter 3**, this *in situ* fabrication process along with reaction mechanism, reaction kinetics, factors that could affect the rate of reaction as well as on optical behavior were discussed. More specifically, by



changing the concentration of monomers, using different types of monomer and effect of temperature during polymerization were studied. A relationship between device performance parameters such as switch speed and photopic contrast electrochromic polymer thickness, polymerization time, and thickness of the solid gel electrolyte were established. In **Chapter 4**, the effect of ionic conductivity of the polymer gel matrix, by changing the composition of salt and solvent were carried out to maximize the optical performance of electrochromic devices. As for *in situ* method, electrochromic polymers are forming inside the solid cross-linked matrix. Any kind of conformational change of the polymer matrix would affect the conformation of electrochromic polymer as well as their electronic property. In **Chapter 5**, influence of the molecular weight of oligomer, polyethyleneglycol diacrylate used to make the cross-linked matrix, on the resulting electrochromic polymer and the effect on photopic contrast of the device were studied.

As in chapter 3, we have seen that all subtractive colors could be achieved in one step using *in situ* method. Here in **Chapter 6**, neutral-to-neutral colored device was achieved by forming all subtractive colored copolymers orthogonal to electrodes via *in situ* approach. Here, another one step approach was discussed to achieve neutral color in both redox states by using an organic dye along with electrochromic polymer.

In **Chapter 7**, flexible free-standing conductive fiber mat was prepared and the sheet resistance was optimized as a function of color luminance. This fiber mat was made by electrospinning poly (ethylene terephthalate) - silica dispersion. This fiber mat was spun coated with poly [3,4-ethylenedioxythiophene]-poly

[styrene sulfonate (PEDOT-PSS) to achieve low sheet resistivity. This resultant fiber mat was used as electrode to deposit electrochromic polymer on it. And finally, reflective-type electrochromic devices were assembled using this conductive fiber mat and device performance was also characterized.

**Electrochromic Polymer Composites Forming in Solid Gel Matrix and  
Flexible Electrode for Photonic Application**

Amrita Kumar

M.Sc. Vidyasagar University, 2007

A Dissertation

Submitted in Partial Fulfillment of the

Requirements for the Degree of

Doctor of Philosophy

at the

University of Connecticut

2015

Copyright by  
Amrita Kumar

2015

## APPROVAL PAGE

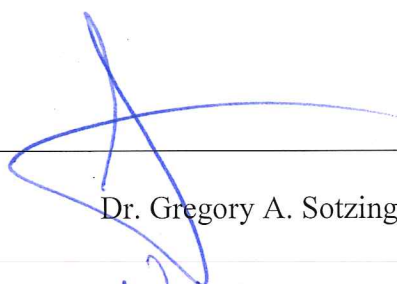
Doctor of Philosophy Dissertation

### **Electrochromic Polymer Composites Forming in Solid Gel Matrix and Flexible Electrode for Photonic application**

Presented by

Amrita Kumar, M.Sc.

Major Advisor



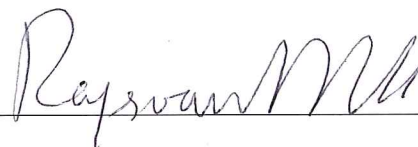
Dr. Gregory A. Sotzing

Associate Advisor



Dr. Douglas Adamson

Associate Advisor



Dr. Rajeswari Kasi

University of Connecticut

2015

## **Acknowledgements**

I want to take the opportunity to thank Dr. Gregory Sotzing being my adviser. I have always got the support and motivation to carry out cutting edge research from him. Beside science I have learnt a lot of things from him. His guidance on career development, improving writing skill and confidence has helped me to develop myself. The work freedom to do research in our group made me an independent researcher. I really appreciate his creative thinking ability.

I think another great experience is working on industrial projects and attending business meetings that prepared myself as a potential candidate for real world. I really have learnt a lot of technical skills from him and the business team, Mark Bertolami and Rob DaPra.

I would like to thank my associate adviser Dr. Douglas Adamson and Dr. Rajeswari Kasi for their support. I would also like to thank Dr. Christian Bruckner and Dr. Yao Lin for their time and support.

I want to thank all IMS and chemistry employees for their help. A special thanks goes to Laura Pinatti, Mark Dudley, Roger Ristau, Lichun Zhang, Gary Lavigne and Marcus Giotto for helping with instruments and their experience. I also want to thank electronic shop, machine shop and glass shop for their help.

I think I was lucky to have Dr. Yujie Ding as my mentor. I really appreciate her help and guidance to understand our research area and academics.

My sincere thanks go to Dr. Tanmoy Dey from whom I came to know the beauty of color changing devices and developed my interest for joining Sotzing group.

I also want to thank Dr. Michael Invernale, for his help with whenever I have asked for. He always helped me at his best. I have enjoyed the support and friendship of Dr. Donna Mamangun, Dr. Aom Kulthida and Dr. Aaron Baldwin. I want to extend my thanks to all group members; Dr. Daminda Navarathne, Dr. ki-ryong Lee, Dr. Fahad Alhashmi Alamer, Michael Otley, Yumin Zhu, Jose Santana, Xiaozheng Zhang, Mengfang Li, Dr. Robert Lorenzini, Whitney Kline, Rui Ma, Esin Eren, Yani Feng, Dr. Chris Asemota, Shahidul Islam, Omer Yassin, Geng Li, Greg Treich and Shamima Nasreen.

I consider myself fortunate for having such a lovely family. They have always encouraged me to fulfill my dreams. I feel myself blessed to uphold my parent's pride. I want to thank my spouse Dr. Rajat Subhra Das for his support, without his help this graduate school journey should not be that easy for me. I also want to thank my little baby Rishik for his patience while I was working on my thesis. I would like to extend my thanks to Dr. Dipak Dey and Rita Dey for their kindness and being here as a loving family friend.

**I dedicate this dissertation to my family**

**Jan 9<sup>th</sup>, 2015**



## LIST OF FIGURES

Figure #	Figure caption	Page #
1.1	Chemical structure of polyacetylene showing $\pi$ conjugation	4
1.2	Band gap change for different materials	5
1.3	Band gap change for semiconductors using different dopants	6
1.4	Band gap change for conductive polymers	7
1.5	PEDOT at two-redox state: neutral and oxidized state	7
1.6	Schematic diagram of conventional ECD	13
1.7	Different ECD at neutral state assembled via <i>in situ</i> method	17
1.8	Color space: xy chromaticity and CIE LUV	24
1.9	Absorption spectra for neutral colored commercially available eye wears	25
1.10	XY color coordinate for neutral color	26
1.11	Typical electrospinning set up	27
2.1	Structures for different chemicals used	38
2.2	Typical linear sweeps of potentials in CV	41
2.3	A typical CV graph for electrodeposition and switching of conductive polymer, PProDOT-Me <sub>2</sub>	42
2.4	A typical example of a chronoabsorpmetry spectrum	44
2.5	A typical Bode plot	45
2.6	Set up for ionic conductivity measurement of gel electrolyte	46

2.7	Set up for two-electrode cell	51
2.8	Instrument used for spray coating	52
2.9	UV chamber	53
2.10	Image of battery box	54
2.11	Schematic diagram for diffusion study	55
3.1	Schematic diagram of an electrochromic device assembled via <i>in situ</i> method	59
3.2	Electrochromic device assembled via <i>in situ</i> method	63
3.3	Representation of a general electrochemical reaction pathway	67
3.4	Photopic transmittance of PProDOT-Me <sub>2</sub> as a function of effective polymer layer thickness	69
3.5	Photopic transmittance of PEDOT as a function of effective polymer layer thickness	70
3.6	Photopic transmittance of PBPMOM-ProDOT as a function of effective polymer layer thickness	71
3.7	Photopic contrast as a function of polymerization time for various concentration of ProDOT-Me <sub>2</sub>	72
3.8	Concentration profile of electroactive species at different time	75
3.9	Diffusion coefficient of ProDOT-Me <sub>2</sub> at different concentration inside solid gel matrix	76
3.10	%T <sub>bleached</sub> as a function of polymerization time	77
3.11	Photopic contrast as a function of polymerization time for different polymer	79
3.12	Image of ruined ITO	85
3.13	Image of 105cm <sup>2</sup> active area electrochromic device	88
3.14	Absorption spectra for three different copolymers	90

	assembled via <i>in situ</i> method	
3.15	Images of three different copolymers assembled via <i>in situ</i> method	91
4.1	Schematic diagram of a device assembled via <i>in situ</i> method	99
4.2	Relation between photopic contrast and ionic conductivity of solid gel electrolyte	102
4.3	Pictures of assembled <i>in situ</i> devices using ionic liquid	103
4.4	Photopic contrast as a function of propylene carbonate loading into gel electrolyte	104
5.1	Chemical structures of different materials	116
5.2	Cross-sectional diagram of an <i>in situ</i> device before and after electropolymerization	121
5.3	Relationship between ionic conductivity as a function of salt loading for PEGDA systems	123
5.4	Absorption spectra of PProDOT-Me <sub>2</sub> in bleached state for different PEGDA systems	126
5.5	Image of an electrochromic device with 54% photopic contrast	127
6.1 (a)	Structures of PProDOT- <i>t</i> Bu <sub>2</sub> , PProDOT- <i>t</i> Bu <sub>2</sub> -co-PProDOT-Me <sub>2</sub> and PProDOT-Me <sub>2</sub>	134
6.1 (b)	Absorption spectra of PProDOT- <i>t</i> -Bu <sub>2</sub> , PProDOT- <i>t</i> -Bu <sub>2</sub> -co-PProDOT-Me <sub>2</sub> and PProDOT-Me <sub>2</sub> in neutral state	134
6.2	Schematic diagram of electrochromic window where subtractive color spectrum is (a) horizontal and (c) orthogonal on ITO	138
6.3	Schematic diagram of stepwise assemble method to achieve neutral color	140
6.4	Color coordinates for neutral colored devices assembled via <i>in situ</i> method	142

6.5	Color coordinates of the ECD in dark state at different diffusion time interval	143
6.6	Absorbance spectra of neutral colored devices assembled via <i>in situ</i> method	145
7.1	SEM images of 15wt% PET fiber mesh with and without silica	159
7.2	TEM image of silica nanoparticles on surface of 15wt% PET fiber mat	160
7.3	PET non woven mat before and after PEDOT-PSS coating	164
7.4	Cyclic voltagrams on ITO and different fabric mat	166
7.5	Images for electrodeposition of poly 2,2' bithiophene on different fiber mesh	167
7.6	Color coordinates of fiber mesh before and after electrodeposition of poly 2,2' bithiophene	168
7.7	SEM images of of conductive fiber mat before and after electrodeposition of poly 2,2' bithiophene	169
7.8	Images at two redox state of poly 2,2' bithiophene on conductive fiber mat	170
7.9	Images of assembled devices using conductive fiber mat as working electrode	171
7.10	Switching cycle of electrochromic device using conductive fiber mat as working electrode	172

### LIST OF SCHEMES

<b>Scheme #</b>	<b>Caption</b>	<b>Page #</b>
1.1	Cathodically and anodically colored polymer	10
1.2	A typical electrochemical (I) reduction and (II) oxidation reaction process	12
1.3	Variables affect the rate of electrochemical reaction	13
1.4	Photochemical reaction of PEGDA	15
3.1	Formation of Polypyrrole following Diaz mechanism	65
3.2	Formation of Polypyrrole following Pletcher mechanism	66
7.1	Schematic diagram for making conductive fiber mat	154

## **LIST OF TABLES**

<b>Table #</b>	<b>Caption</b>	<b>Page #</b>
3.1	Relation between polymerization time required to achieve the saturated photopic contrast and corresponding percentage of conversion	74
3.2	Represents the photopic transmittance value at different redox state at maximum achievable photopic contrast	80
3.3	Effect of gel electrolyte thickness on photopic contrast for <i>in situ</i> method	82
3.4	Photopic contrast of PEDOT devices using different techniques, assembled via <i>in situ</i> approach	83
3.5	Temperature study for <i>in-situ</i> EC device	84
3.6	Redox switching speed for <i>in situ</i> devices	87
4.1	Composition of solvent and PEGDA	105
4.2	Photopic contrast of PEDOT and PProDOT-Me <sub>2</sub> for different solvent systems	106
4.3	Relationship between pulse width and contrast	107
4.4	Relation between ionic conductivities and photopic contrast for (EC+PC) mixture	108
5.1	T <sub>g</sub> , ionic conductivity and optical behavior of three optimized PEGDA systems	124
7.1	Relation between shearing time and sheet resistance	161
7.2	Relation between various concentration of ORGACON PEDOT-PSS with luminance and R <sub>s</sub>	163
7.3	Relation between various concentration of ORGACON PEDOT-PSS with luminance and R <sub>s</sub>	165

## **TABLE OF CONTENTS**

<b>LIST OF FIGURES.....</b>	<b>X</b>
<b>LIST OF SCHEMES.....</b>	<b>XIV</b>
<b>LIST OF TABLES.....</b>	<b>XV</b>
<b>LIST OF CONTENTS.....</b>	<b>XVI</b>

### **Chapter 1: Introduction**

1.1	Electrochromic materials and their applications.....	1
1.2	Conjugated polymers.....	3
1.3	Conjugated polymer as electrochromic materials.....	7
1.4	Electrochromic reactions inside the cell.....	10
1.5	Electrochromic device.....	12
1.6	Optical parameters of ECD.....	17
1.7	Diffusion.....	21
1.8	Color and color coordinate.....	22
1.9	Neutral color.....	25
1.10	Electrospinning.....	26
	References.....	28

### **Chapter 2: Experimental procedure and Instruments**

2.1	Introduction. ....	36
2.2	Chemicals and abbreviation.....	36
2.3	Structure of chemical used. ....	38
2.4	Techniques.....	40
2.4.1	Electrochemical Characterization.....	40
2.4.1.1	Cyclic voltammetry.....	40
2.4.1.2	Chronocoulometry.....	42
2.4.2	Optical Characterization.....	43
2.4.2.1	UV-Vis spectroscopy .....	43
2.4.2.2	Colorimeter.....	44
2.4.3	Ionic conductivity measurement.....	44
2.4.4	Sheet resistance measurement.....	46

2.4.5	Thermal behavior analysis.....	46
2.4.5.1	Differential scanning calorimetry.....	46
2.4.5.2	Thermal mechanical analysis.....	46
2.4.6	Electrospinning.....	48
2.4.7	Characterization of film morphology.....	49
2.4.7.1	Scanning electron microscopy.....	49
2.4.7.2	Transmission Electron Microscopy .....	49
2.4.8	Electrochromic device assembly.....	50
2.4.9	Diffusion coefficient.....	54

### **Chapter 3: Property relationships and characterization of one-step *in situ* method for solid-state electrochromic devices**

3.1	Introduction.....	58
3.2	Experiment.....	61
3.3	Results and discussion.....	63
3.3.1	Photopic contrast as a function of polymer layer thickness.....	67
3.3.2	Photopic contrast as a function of monomer loading.....	71
3.3.3	Photopic contrast as a function of various monomer.....	78
3.3.4	Photopic contrast as a function of gel electrolyte thickness.....	81
3.3.5	Using different techniques to electropolymerize.....	82
3.3.6	Effect of temperature during electropolymerization.....	83
3.3.7	Switching speed of <i>in situ</i> electrochromic devices.....	85
3.3.6	Color tuning using one step method.....	88
3.4	Conclusion.....	92
	Reference.....	93

### **Chapter 4: Optimization of gel electrolyte towards high photopic contrast**

4.1	Introduction.....	96
4.2	Experiment.....	98
4.3	Results and discussion.....	99
4.3.1	Optimization of salt concentration.....	99
4.3.2	Effect of propylene carbonate.....	103
4.3.3	Effect of ethylene carbonate and tetraethylene glycol dimethyl ether on optical performance.....	104
4.3.4	Effect of solvent mixture.....	107
4.4	Conclusion.....	109
	Reference.....	110



# **Chapter 1**

## **Introduction**

## 1.1 Electrochromic materials and their application

Electrochromic materials are demarcated as materials that can reversibly switch between two color states upon application of an external potential. In 1961, J. R. Platt introduced first theoretical discussion about electrochromic materials<sup>1</sup>. First EC device was demonstrated by Deb et al. in 1970s<sup>2</sup>. Colors result from different electronic absorption bands in visible region upon electrochemical redox reaction. These materials can be used for smart windows, auto-dimming mirrors including rear view mirrors, sunroofs, eyewears etc<sup>3-12</sup>. Several companies like Gentex Corp, Donnelly, Sage, Dow Chemical Co, have done commercialization of electrochromic material<sup>13</sup>.

Electrochromic materials can be classified into three categories. Type I is inorganic material. Examples of which are transition metal oxides like nickel oxide<sup>14</sup>, tungsten oxide<sup>15,16</sup>, bismuth oxide<sup>17</sup>, antimony oxide<sup>18</sup>, molybdenum oxide etc<sup>19</sup>. Type II is small organic molecules like bipyridilium, metallophthalocyanines etc<sup>20</sup>. And third category is conjugated polymers, such as polyaniline, polythiophene, polypyrrole etc<sup>21</sup>. To date tungsten oxide ( $\text{WO}_3$ ) and viologen has extensively studied and commercialized<sup>2</sup>. Among the different classes of electrochromic materials, conjugated polymers are of high interest due to reported sub-second switch speeds, offerings of color variety, high optical contrast, film flexibility, open circuit memory, small energy consumption making them

potential candidate for affordable displays, smart windows, eye wears, light emitting diodes, capacitors, batteries, and color controlled textile<sup>7-13,22-40</sup>.

## 1.2 Conjugated polymer

Discovery of conductive polymer, polyacetylene in 1976 by Shirakawa, Heeger and MacDiarmid introduced an interesting area to study and develop new organic conductive polymers. The uniqueness of electrical conductivity arises due to conjugated structure, presence of alternative single and double bond on carbon backbone as shown in **Figure 1.1**. Longer conjugation directed more extended  $\pi$ -conjugation on backbone. This extended  $\pi$ -  $\pi^*$  conjugation allows to move electron through the carbon backbone to conduct electricity<sup>41,42</sup>. This extended  $\pi$ -conjugation causes to lower the band gap<sup>43,44</sup>.

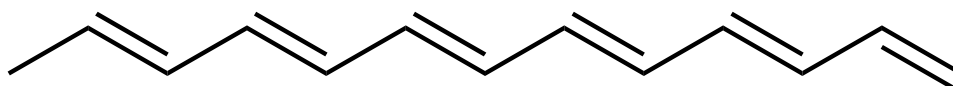


**Figure 1.1** Chemical structure of polyacetylene showing  $\pi$  conjugation

Electronic conductivity results from low energy gap ( $E_g$ ), energy difference between highest point of valence band and lowest point of conduction band. Conduction band is partially or fully empty at ground state. To conduct electricity, electrons or holes need to transfer from valence band to conduction band. Electrons need to overcome the bandgap energy to

conduct electricity. **Figure 1.2** represents the energy diagram of different materials at absolute zero temperature. Metals have no band gap due to the overlap of conduction band with valence band. This makes them good conductors.

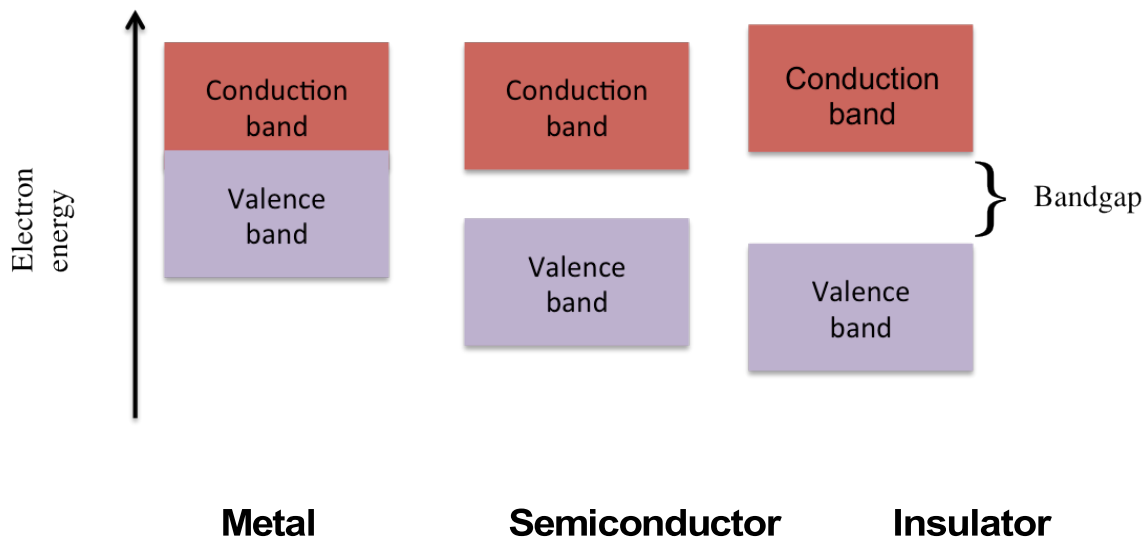


**Figure 1.2** Band gap change for different materials

For insulators energy gap ( $E_g$ ) is too high ( $>3$  eV) to travel charge carrier from valence band to conduction band. For semiconductor energy gap is moderate, falls in between metal and insulators. This band gap is not enough small to conduct electrons in ground state. But excitation or doping can control energy gap, so electrons can be able to move and conduct electricity. A small amount of added impurity into semiconductive materials can change the electronic configuration that helps to conduct electricity<sup>45</sup>. Impurities or dopant can be classified into two categories: electron-rich and electron-deficient. Electron-rich dopants help to lower the conduction band

and electron-deficient dopants helps to extract electrons as shown in **Figure 1.3**. As a result conductivity increases.

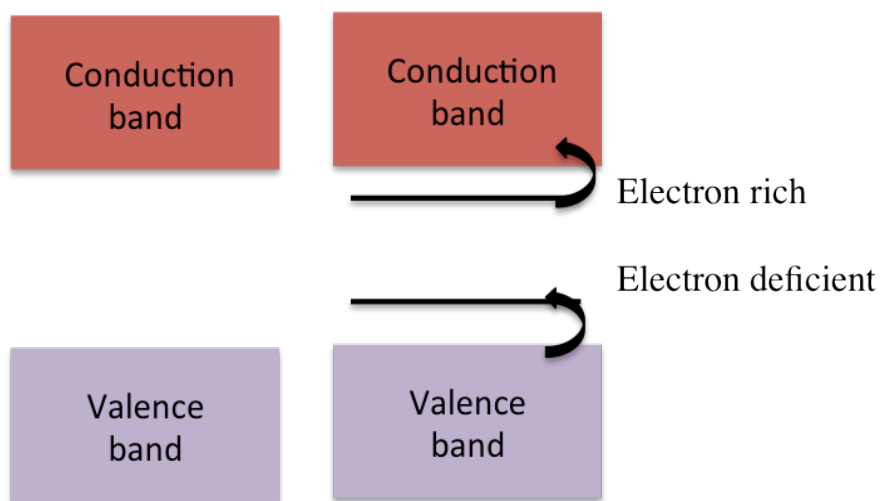


**Figure 1.3** Band gap change for semiconductors using different dopants

For conjugated polymers, highest occupied molecular orbital (HOMO,  $\pi$  orbital) represents the valence band and lowest occupied molecular orbital (LUMO,  $\pi^*$  orbital) represents conduction band. Conjugated polymers are insulating in their neutral states. Upon chemical or electrochemical doping the band structure charge carriers, polarons and bipolarons are produced and lower energy intraband transition takes place. For oxidation process (p-doping), electrons are removed from neutral polymer to produce a radical cation. After removing an electron a polaron forms which is a combination of a radical electron and a charge site. After losing second electron from the polymer chain a bipolaron formed which contains two positive charges. During doping process, these carriers are the main

reason to change the band gap energy as shown in **Figure 1.4**. And this change in the band gap energy results a change in optical behavior of the ECPs between neutral and oxidized state.

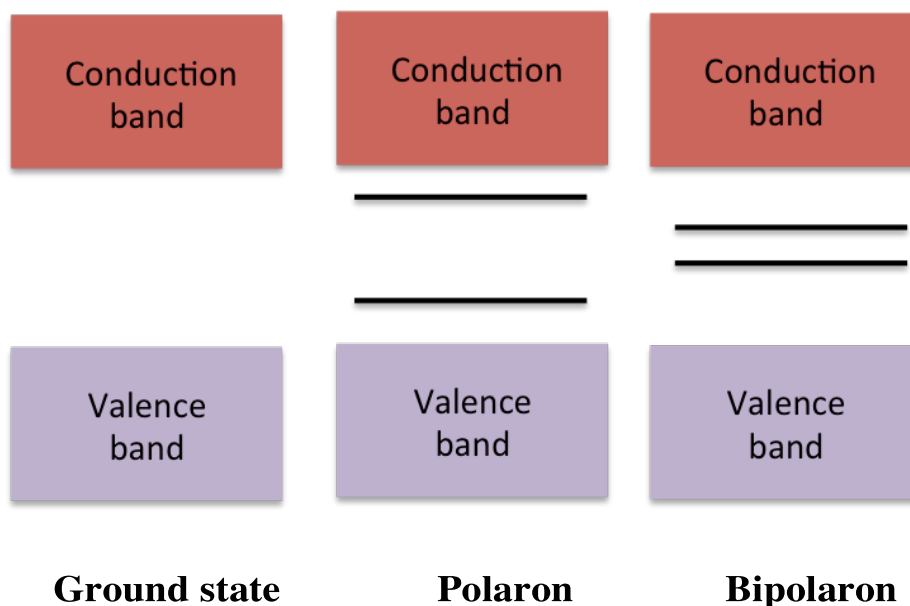


**Figure 1.4** Band gap change for conductive polymers (a) neutral polymer, (b) Polaron generated after an electron removal, (c) Bipolaron generated after an electron removal from polaron (from left to right)

McCullough et al. have studied the effect regioregularity on electronic behavior of polythiophene by synthesizing various regioregular polymer using organometallic catalysts and studied the electrical behavior<sup>46-52</sup>. It was noticed that homogeneity helps to improve the electronic conductivity by increasing charge transportation. Another important factor is the distance between two polymer chains, although the effect of this three-

dimensional charge movement has not been well understood<sup>53,54</sup>. The effect of applied potential, electrolyte solution has impact on formation of conjugated polymers. The physical and electronic properties depend on the morphology of conductive polymers. A more compact polymer chain conformation will have larger number of defects than expanded polymer chain. As a result shorter polymer chain will have lower electronic conductivity. An electrolyte with small counterpart can enhance the doping level due to easy diffusion.<sup>23</sup>

### 1.3 Conjugated polymer as electrochromic material

The most popular conjugated electrochromic polymer is PEDOT. This polymer has extensively studied. It has band gap energy of 1.7 eV<sup>55</sup>. It provides dark blue color at neutral state and light sky blue color upon oxidation as shown in **Figure 1.5**. Polypyrrole has two distinct colors at two redox states. It can switch from blue-violet (doped) to yellow-green (dedoped). Similarly, polythiophene switches from blue to red color upon doping-dedoping process.

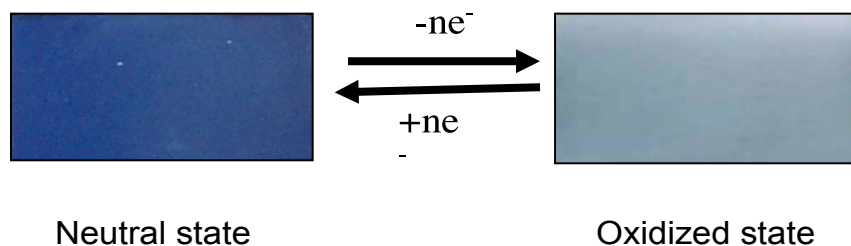


**Figure 1.5** PEDOT at two-redox state: neutral and oxidized state

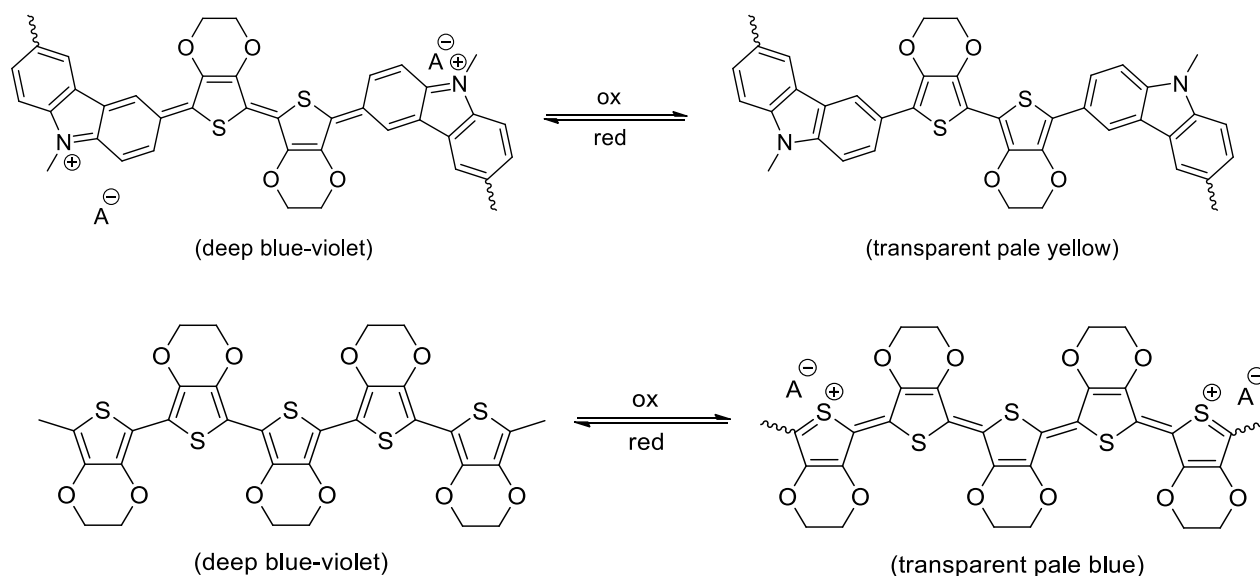
According to Planck's relation:

$$E = h\nu = \frac{hc}{\lambda_{\max}} \text{-----}(1.1)$$

where E is the energy, h is Planck's constant, c is the velocity of light,  $\lambda_{\max}$  maximum absorption wavelength.

From this calculation the wavelength corresponding to 1-3 eV falls in the visible spectrum region<sup>10,37</sup>. Upon chemical or electrochemical oxidation and reduction  $\pi$ -electron go through a reversible insertion and extraction of ions through the polymer film. Conjugated polymers with band gap 1-3 eV, switch between colored state and transmissive state upon doping and dedoping<sup>13,20,27,56</sup>. For conjugated polymers having band gap > 3 eV, absorption will occur at low end <410 nm of the visible region. This makes them transmissive upon reduction. This kind of polymers will produce colored state upon dedoping. Former category is known as cathodically colored polymer and second category is known as anodically colored polymer. Scheme 1.1 shows an example of cathodically colored polymer [poly ethylene dioxythiophene, PEDOT] and anodically colored polymer [poly 3,6-bis(3,4-ethylenedioxythiophene)-N-methyl carbazole, PBEDOT-NMeCz].





**Scheme 1.1** Cathodically colored polymer PEDOT (top) and anodically colored polymer PBEDOT-NMeCz (bottom)

All colors would be obtained from subtractive and additive primary colors by using color-mixing theory. Color of electrochromic polymers can be easily controlled based on three major factors: (i) through controlling the band gap of polymer, by putting different substituent on monomer unit. For example, by increasing the number of thiophene rings band gap energy reduces, as a result  $\lambda_{\max}$  shifted<sup>57</sup>.

(ii) making copolymers, by changing the composition ratio of two or more monomer units<sup>13,58</sup>.

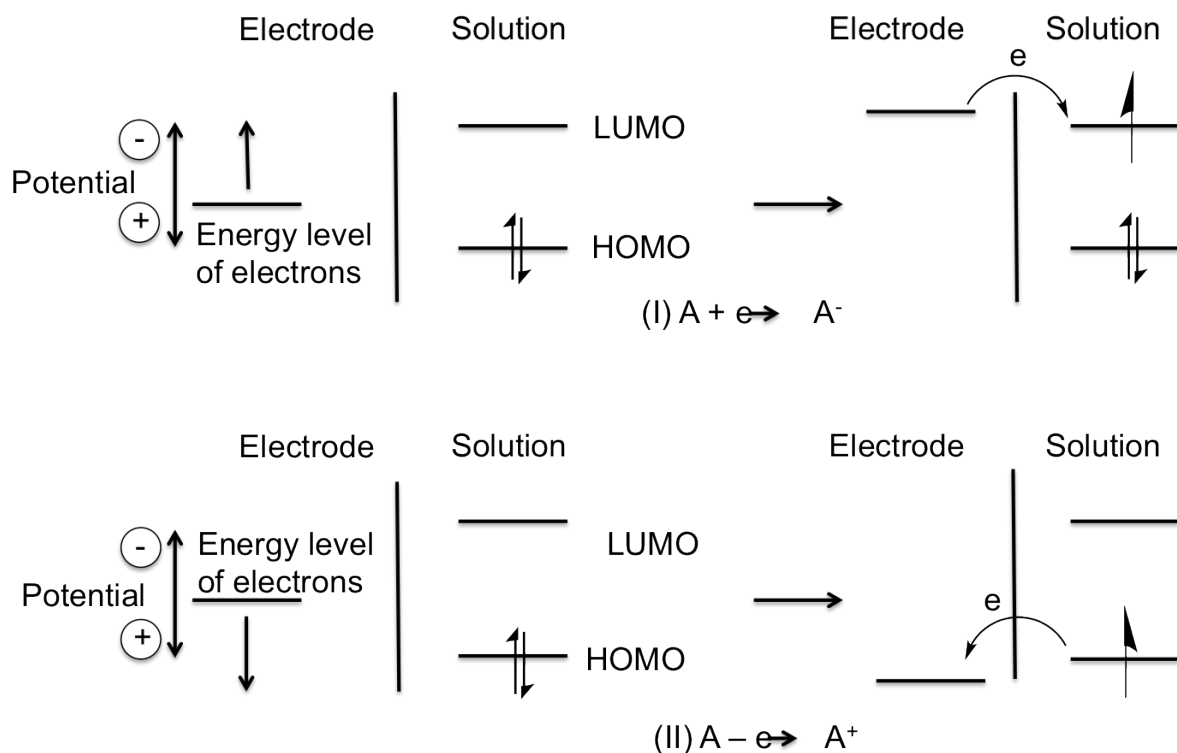
(iii) preparing composites, blends and laminates of electrochromic materials<sup>13</sup>.

Some of electrochromic polymers have intermediate colors. To date red<sup>59</sup>, yellow<sup>59</sup>, purple<sup>36</sup>, green<sup>25,38,60</sup> and black<sup>36,61</sup> colors are reported. Complex

colors can be also achieved by using multilayer of electrochromic polymers<sup>62,63</sup>.

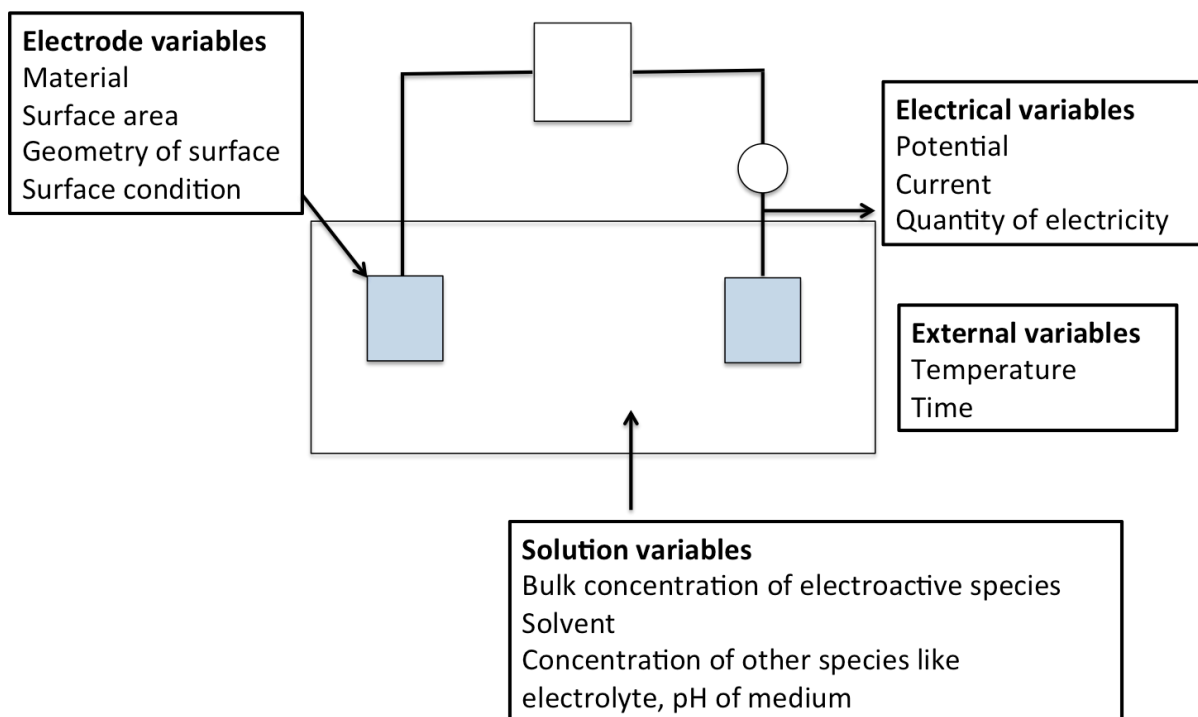
#### **1.4 Electrochemical reactions inside the cell**

Inside the electrochemical cell charges transfer across the interface between the electrode (electronic conductor) and electrolyte (ionic conductor). This charge transfer occurs through the movement of an electron and/or hole. This electrode could be a metal (like Pt, Ag, Au) or semiconductor (like ITO, Si). Electrolyte could be liquid or solid-gel that contains ionic species. For a typical electrochemical cell, electrodes are immersed into an electrolyte solution and by using an external power source the potential difference between electrodes is controlled (shown in chapter 2). **Scheme 1.2** represents the reduction and oxidation reaction of a species A occurred in an electrolyte solution. By supplying more negative potential to the working electrode, energy level of electron are enhanced high enough. So, electron can transfer from electrode to lowest occupied molecular orbital of the electrolyte. Electron will transport from electrolyte to working electrode while more positive potential will be implied and oxidation of electrolyte species will take place.



**Scheme 1.2** Representation of a typical electrochemical (I) reduction and (II) oxidation reaction process of an electroactive species A.

The rate of electrochemical reaction could be affected by several factors as shown in **Scheme 1.3**. Among those variables, some variables like electrode geometry, electrode area, mass transfer etc. have no impact on potential directly. In potentiometric experiment the  $E$  is determined as function of  $C$ . Generally, the objective of this kind of electrochemical experiment is to obtain information about kinetic, thermodynamic, analytical etc. for the system.

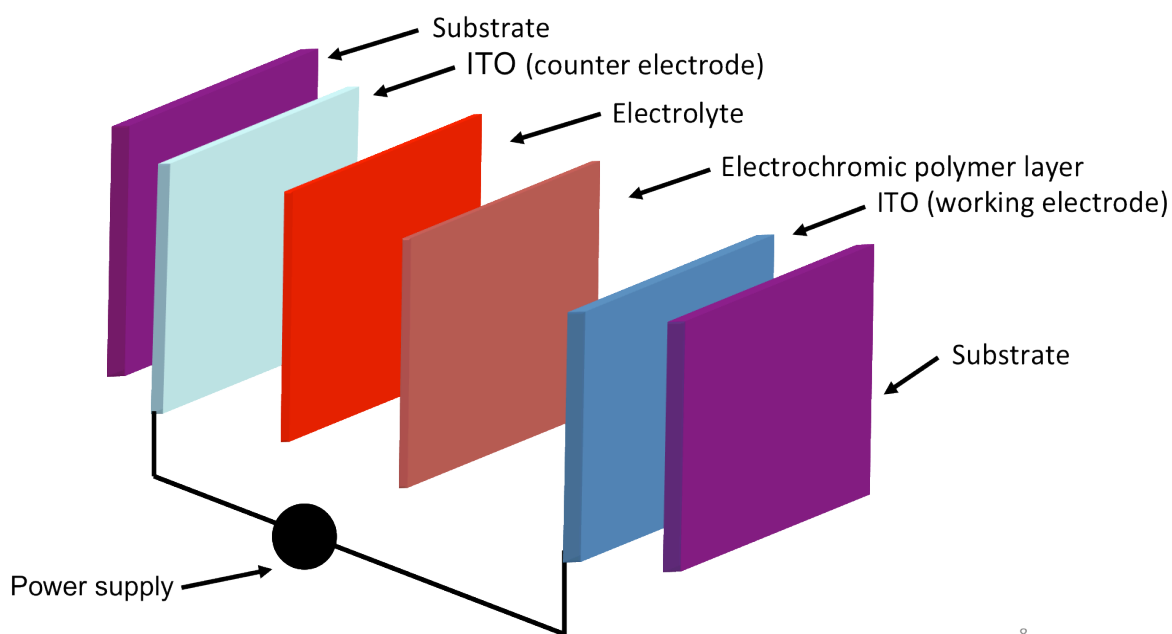


**Scheme 1.3** Variables affect the rate of electrochemical reaction

### 1.5 Electrochromic device

Electrochromic devices are popular because of their fast switching speed and high coloration efficiency<sup>61</sup>. They are mostly used as smart windows, auto-dimming rearview mirrors, eyewear and color controlled textile industry<sup>61</sup>. For window type devices transparent electrodes like glass or PET coated with transparent conductive material ITO are used. One of the electrodes needs to be coated with ECP. This electrode is generally termed as “working electrode”. Other electrode is termed as “counter electrode”. **Figure 1.6** shows the schematic diagram of an ECD assembled via conventional method. Sometimes the counter electrode is also coated with EC materials to balance the charge<sup>4,36,64</sup>, to enhance the contrast<sup>65</sup> or

to get complex color<sup>66-68</sup>. Once the working electrode is coated with ECP, device was assembled by a “sandwich” method. An electrolyte needs to be place in between two electrodes.

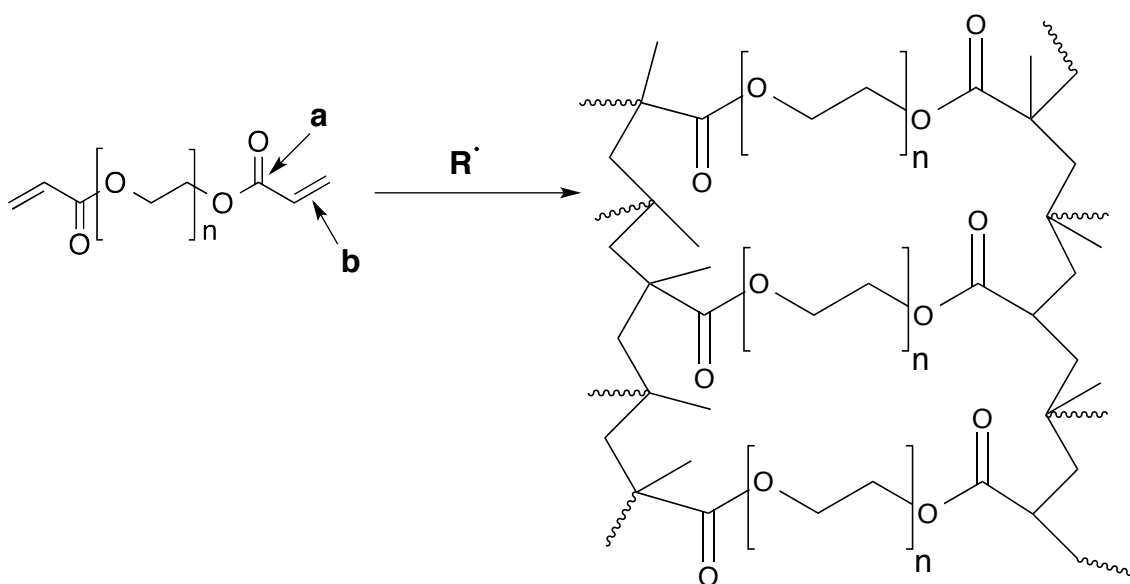


8

**Figure 1.6** Schematic diagram of conventional ECD

For application purpose liquid electrolyte is not desired because of evaporation and leakage. Also high transparency is required for the gel electrolyte. For this purpose, a solid polymer gel electrolyte, composed of some salt that provides ions, plasticizer to dissolve the salt and to enhance the ionic mobility and a polymer matrix to provide the mechanical strength<sup>69</sup>. Polyethylene oxide and its derivatives coordinate with lithium

cations are the most extensively studied solid polymer gel electrolyte matrix.<sup>70</sup> A solution of an acrylate based low molecular weight polyethylene glycol, salt, solvent and initiator can be prepared and placed in between two electrodes, and sealed. By photochemical or thermal irradiation, initiators will produce radical and that will attack the active the site of acrylate group and a solid cross-linked polymer gel matrix can be formed<sup>23,64</sup>.



**Scheme 1.4** Represents the photochemical reaction of PEGDA

Electrochromic polymer (ECP) can be prepared chemically or electrochemically. ECP can be formed onto ITO coated substrates from an electrolyte bath by electrodeposition, or by coating the ECP onto electrode after chemical synthesis.

Due to nucleation growth process, presence of any foreign particles like grease, dirt or defect on ITO causes defect on polymer films. For this reason, rigorously cleaned dust free, defect free ITO substrates are required for electrodeposition method. Also, electrolyte bath needs to be changed frequently to minimize the nucleation growth. This results in enormous waste of chemicals. It is also difficult to make pattern on ITO surface.

For chemical synthesis process, soluble ECP needs to synthesize and following some processing method like spray coating, spin coating, drop casting, electrospinning, printing etc. deposited onto ITO surface. The main problem with this technique is the solubility issue of high molecular weight polymers in organic solvents. This problem can be overcome by introducing different substituent on monomer unit or by changing the polymer structure. A common method to make soluble polymers is by introducing alkyl or alkoxy substitutes like butyl, hexyl, octadecyloxy, 2-ethyloxymethyl into polymer backbone<sup>71,72</sup>. Another method, solid-state conversion (SOC) was developed by Sotzing's *et al.* to solve the aforesaid problem<sup>73</sup> by synthesizing copolymer of electrochromic unit with silane. This precursor polymer is soluble into organic solvents and can be deposited onto ITO surface by following common processing methods. Upon oxidation of the precursor polymer, conjugated polymer is formed upon cleaving the Si-C bond and coupling of aromatic electrochromic units.

It has been shown that this process eliminates the need of dust-free, clean ITO surfaces.

As it has been already shown that it is really hard to make large area defect-free substrate using electrodeposition method, which causes a huge chemical waste. And for later method, chemical synthesis route needs to go through lots of synthetic steps to have a high molecular weight soluble polymer with desired color. To overcome the processability problem and to commercialize the conjugated polymer to make electrochromic devices, our group has developed a novel one step approach, which is called *in situ* method. For this approach, heterocyclic monomers need to dissolve into polymer gel electrolyte (as mentioned before) and the solution needs to be colorless. Here, ECP forms inside the solid device. This process does not need electrolyte bath. A large area,  $> 100 \text{ cm}^2$  defect free window which is equivalent to goggle size is assembled via *in situ* method. A detail of this process is described in chapter 3. This one step method could be an adaptable method to commercialize the ECPs for smart windows, rear view mirrors, eye wears, color changing fabrics, solar cells, OLEDs and other applications. Using this *in situ* approach it is easy to tune colors in one step by changing the feeding ratio of two co-monomers. Even all subtractive colors and neutral colors can be achieved in one step using this new method (described in chapter 6) with minimal waste. **Figure 1.7** shows different colored ECD assemble via *in situ* approach. Another advantage of



the in situ process is that complex patterns can be rapidly formed with relatively high-resolution large area substrates.

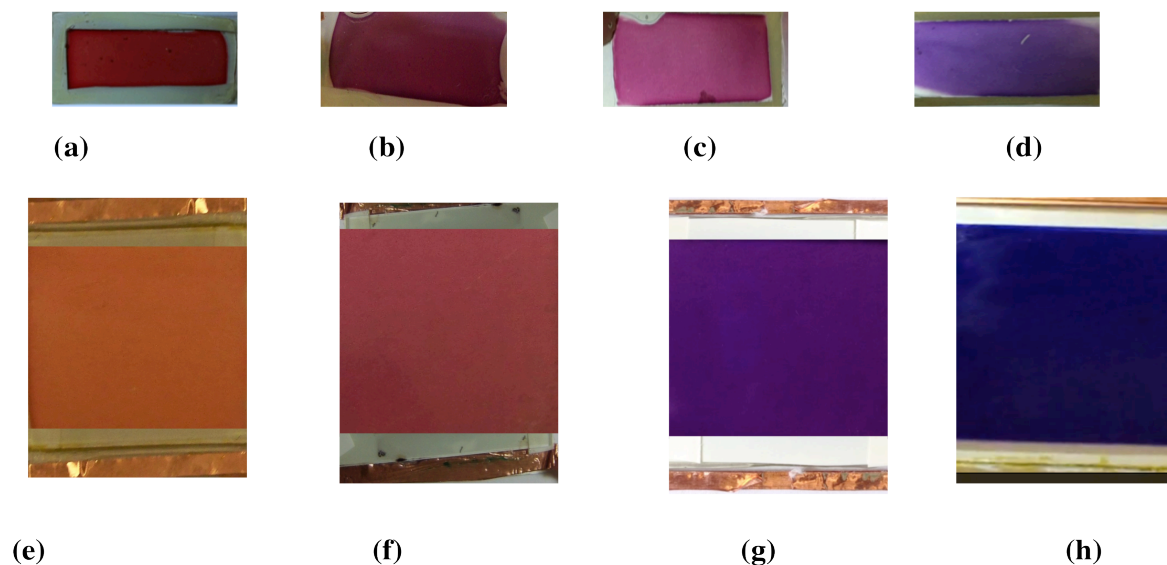


**Figure 1.7** Different ECD at neutral state assembled via *in situ* method; (a) – (f) random copolymer PProDOT-*t*Bu<sub>2</sub>-co-PProDOT-Me<sub>2</sub>, (g) PProDOT-Me<sub>2</sub> and (h) PEDOT

## 1.6 Optical parameters of ECD

Photopic contrast, color efficiency, optical memory, color uniformity, and switching speed are essential requirements for EC devices. The essential terminologies are briefly discussed in literatures<sup>55,56,65,74</sup>. These parameters are briefly reviewed in this section.

## (I) Photopic contrast

Contrast is defined as the change in transmittance between the two extreme redox states of an electrochromic material. Often in literature, contrast is reported at a single-wavelength ( $\lambda_{\max}$ ). However, the best representation for reporting contrast is photopic contrast, which consists of a full-spectrum calculation because it's weighted to the sensitivity of the human eye<sup>64</sup>. For best accuracy, photopic contrast ( $\Delta T_{\text{photopic}}$ ) is calculated using the transmittance values in the spectral range of 350-850 nm. For both bleached ( $T_{\text{photopic,b}}$ ) and colored state ( $T_{\text{photopic,c}}$ ) in according to the following equation,

$$T_{\text{photopic}} = \frac{\int_{380}^{780} T(\lambda) \cdot S(\lambda) \cdot P(\lambda) \cdot d\lambda}{\int_{380}^{780} S(\lambda) \cdot P(\lambda) \cdot d\lambda} \quad \text{-----(1.1)}$$

$$\text{and Photopic contrast, } (\Delta T_{\text{photopic}}) = \%T_{\text{photopic,b}} - \%T_{\text{photopic,c}} \quad \text{-----(1.2)}$$

where  $P(\lambda)$  is the normalized spectral response of the human eye,  $S(\lambda)$  is the normalized spectral emittance of a blackbody (at 6000°K), and  $T(\lambda)$  is the spectral transmittance of the device.

## II. Optical density (OD)

Optical density at a particular wavelength can be calculated using following equation

$$\text{OD} = \log_{10} \left( \frac{1}{T} \right) \quad \text{-----(1.3)}$$

### III. Color efficiency ( $\eta$ )

To determine the power requirements during redox switching of an electrochromic material, the color efficiency needs to be calculated. It can be determined by knowing the charge ( $Q_d$ ) required during each redox switch. It can be given by following equation,

$$\eta = \frac{\Delta OD}{Q_d} = \log_{10} \left( \frac{T_b}{T_c} \right) / Q_d \text{ -----(1.4)}$$

where  $\eta$  ( $\text{cm}^2/\text{C}$ ) is reported at a specific wavelength,  $T_b$  and  $T_c$  are the transmittance value of bleached and colored state at a specific wavelength, respectively.

### IV. Optical memory / Open circuit memory

As per display application purpose EC materials should retain their color upon termination of current. An EC material that does not need further charge under open circuit for months/ years can be considered as a potential candidate for displays. The time requires maintaining the color of each state that is measured, as the absorption intensity of that particular state after under open circuit is known as optical memory. Unfortunately, most of the ECD has some charge leakage problem due to some unavoidable reasons like unwanted side reactions, manual error during device construction. By application of small amount of electric stimuli can help to restore the color intensity.

## **V. Color uniformity**

For making a better optical display color uniformity is an essential requirement. Nucleation is of the main reason to cause this problem. Other problems like presence of grease or foreign particle may affect the uniformity of ECP film. For *in situ* method (which is discussed in chapter 3), slow diffusion of electroactive species could be a potential reason.

## **VI. Switching speed**

The time required switching between two redox states of an ECD upon application of suitable potential. Switching speed is measured by monitoring the charge needed during switching or by monitoring the change of transmittance value. Detailed is explained in chapter 2. Generally ECPs have sub seconds switching time. This switching speed, the doping and dedoping process depends on several factors such as the thickness of the ECP, morphology of ECP, ionic conductivity of the electrolyte system, and applied potential.

## **VIII. Stability**

Stability of an ECD means after how many redox switching cycles the device could be able to retain the initial absorption intensity of each state. The maximum switching cycle with a minimum loss of color intensity is acceptable. Because of some irreversible redox side reactions and  $iR$  loss of electrolyte or electrode, each system has some to extent of stability.

Although the stability can be increased by proper sealing, using suitable electrolyte, reducing the presence of impurity specially moisture by the system. Upto  $10^6$  cycles switching stability without any significant performance loss has been reported. The stability of an ECD is measured either by monitoring the charge loss or %T loss after each redox cycle.

### 1.7 Diffusion

For formation of ECP, electroactive species or monomers need to diffuse from electrolyte solution or solid polymer gel matrix towards working electrode to get oxidized. For polymer deposition an external potential needs to be applied. The time required to apply the potential depends on the rate of diffusion of the electroactive species. This diffusion behavior of the electroactive species could be explained based on Fick's first and second law.

Fick's first law is applicable for steady state diffusion where concentration does not change with time. Equation **1.5** represents the one dimensional relation of steady state diffusion.

$$J = -D \left( \frac{dc}{dx} \right) \text{-----(1.5)}$$

Where J is the net flow of the particle, D ( $\text{m}^2/\text{s}$ ) is the diffusion coefficient of the particle,  $(dc/dx)$  is the concentration gradient (variation of concentration with distance). This concentration gradient is the driving force for the diffusion. The negative sign of equation **1.5** implies the direction of the flow from high concentration to low concentration.

Fick's second law implies for non-steady state situation where concentration changes with time. Here diffusion occurs from a finite space into a specific volume. Diffusion coefficient does not depend on time. It can be written as,

$$\frac{dc}{dx} = D \left( \frac{d^2c}{dx^2} \right) \text{ -----(1.6)}$$

This second order linear partial differential equation **1.6** requires some boundary conditions to calculate the concentration in a specific volume. Concentration can be calculated as follows,

$$(C_2 - C)/(C_2 - C'_2) = \text{erf} (x/2\sqrt{Dt}) \text{ -----(1.7)}$$

$C_2$  is the initial concentration at the starting point while the distance  $x = 0$ ,  $C$  is the concentration at distance  $x$  after time  $t$ ,  $C'_2$  is concentration of the electrolyte before penetration and erf is the Gauss error-function, is available from literature.

To calculate the diffusion coefficient of monomers inside the solid polymer gel matrix to understand the optoelectronic behavior of ECD (in chapter 3) non-steady state diffusion nature was used. Here monomers diffused from a reservoir to the surrounding solid polymer gel matrix. The concentration  $C(x,t)$ , at distance  $x$  (after time  $t$ ) changes with time.

## **1.8 Color and color coordinate**

The sources of light perceives by our eye can be classified into two categories: by emission and by reflection. Light can directly entered into eye from a light source before hitting an object or it can hit an object and

reflect light. Sunlight is a combination of all visible lights. Human eye is sensitive towards 350 nm to 800 nm that corresponds to violet and red color respectively. When a light hits an object, it absorbs all wavelengths except the particular wavelength corresponding to the color. When that emitted light enters into our eye, light sensitive rod and cone cells absorb it. This light is then converted to electromagnetic signals and our brain gets the signal to interpret the color. If an object absorbs all visible wavelengths, the resultant color will be black. Our eyes react differently with different colors. It has different sensitivity at different colors. Our eye is most sensitive to 550 nm. Generally, on going both sides from 550 nm, the sensitivity of our eye decreases.

Primary additive colors are red, green and blue (RGB) and cyan, magenta and yellow (CMY) are the primary colors of subtractive color. By mixing all additive colors will give white color and by mixing all subtractive colors create black.

As different people have different sensitivity to different color, it was needed to specify a color more scientifically. For this purpose, Commission of Internationale de l'Eclairage has established a method in 1931 to recognize colors. Our eye process colors as a mixture of all primary colors of RGB and is expressed as tristimulus values X, Y and Z. In 1976, both CIE  $L^*u^*v^*$  (CIELUV) and  $L^*a^*b^*$  (CIELAB) were established to transform the tristimulus values. Former system mostly used for display applications and later one used for fabric type industry<sup>55</sup>. A parallel two-dimensional

Cartesian system – “xy chromaticity” has been used where x and y value can be calculated from tristimulus values. Similarly, CIELUV has a two-dimensional Cartesian system where  $u'$  and  $v'$  represents two axes. To describe the color of an object it is important to mention the light source or standard illuminant.  $D_{65}$  is the most common illuminant used in color measurement<sup>75,76</sup>. It is also important to pronounce the viewing angle. By increasing the viewer angel larger visual field will be covered. For this reason CIE 1931 Standard Observer angle was used  $2^\circ$  view angle. Later CIE 1964  $10^\circ$  view angle was used since it provides more accurate data for distance viewer.

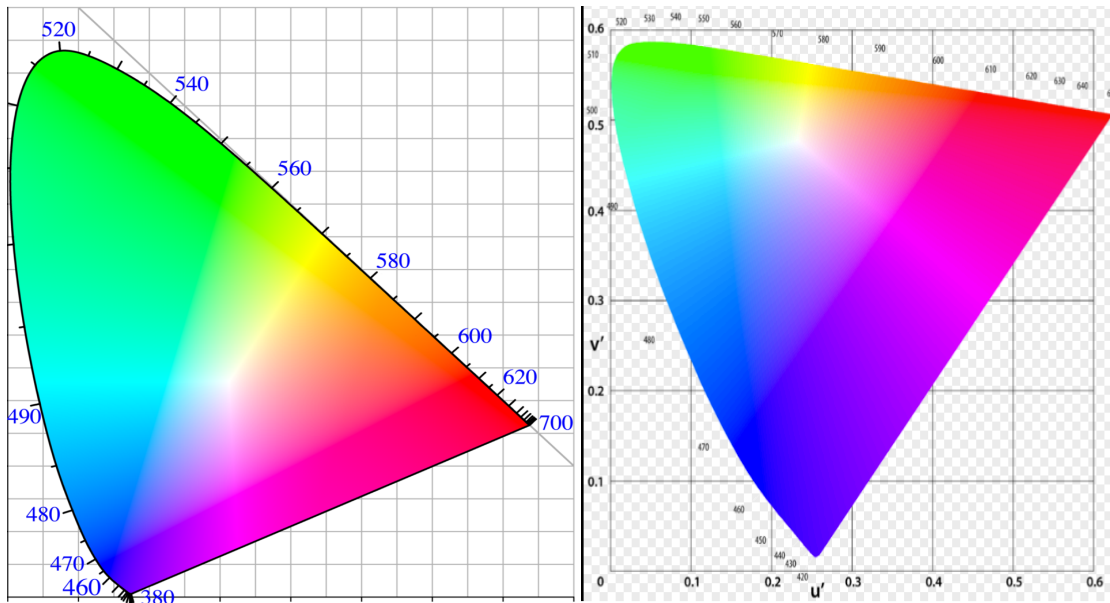


**Figure 1.8** Color space xy chromaticity (left) and CIE LUV (right)



## 1.9 Neutral color

For window type application purpose neutral-to-transmissive color transition is most desirable for EC materials. Common neutral colors are black, white, grey, ivory and taupe. According to the 1931 and 1964 CIE XYZ color spaces the chromaticity coordinates  $[x,y]$  for achromatic colors  $[0.333, 0.333]$  based on standard D65 illuminant.<sup>16-18</sup> From the spectroscopic viewpoint, a chromophore, which is able to absorb the entire visible light homogeneously, will exhibit the black or neutral color. **Figure 1.10** shows the neutral color region in XY color coordinate that was obtained from army lab standard specs.

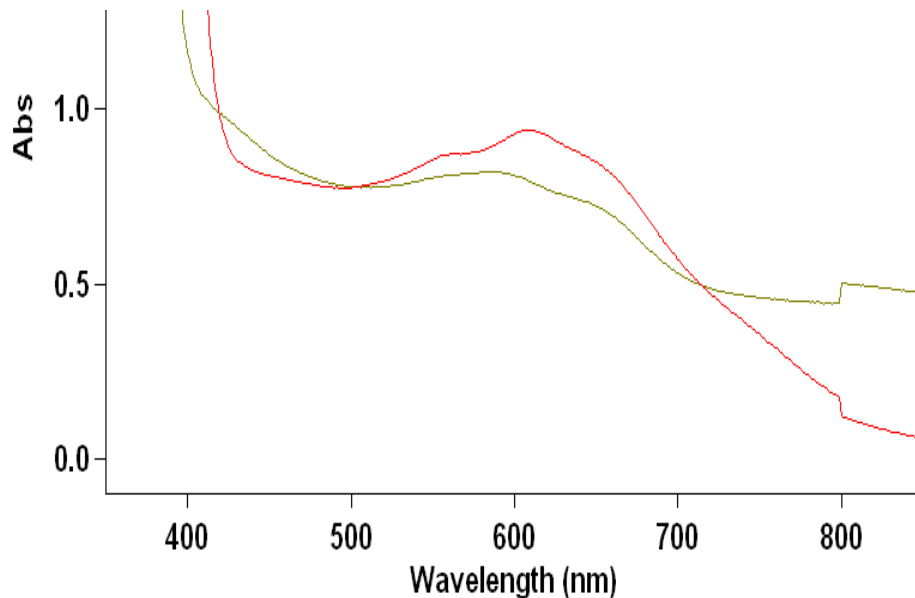


**Figure 1.9** Absorption spectra for two neutral colored commercially available eye wears

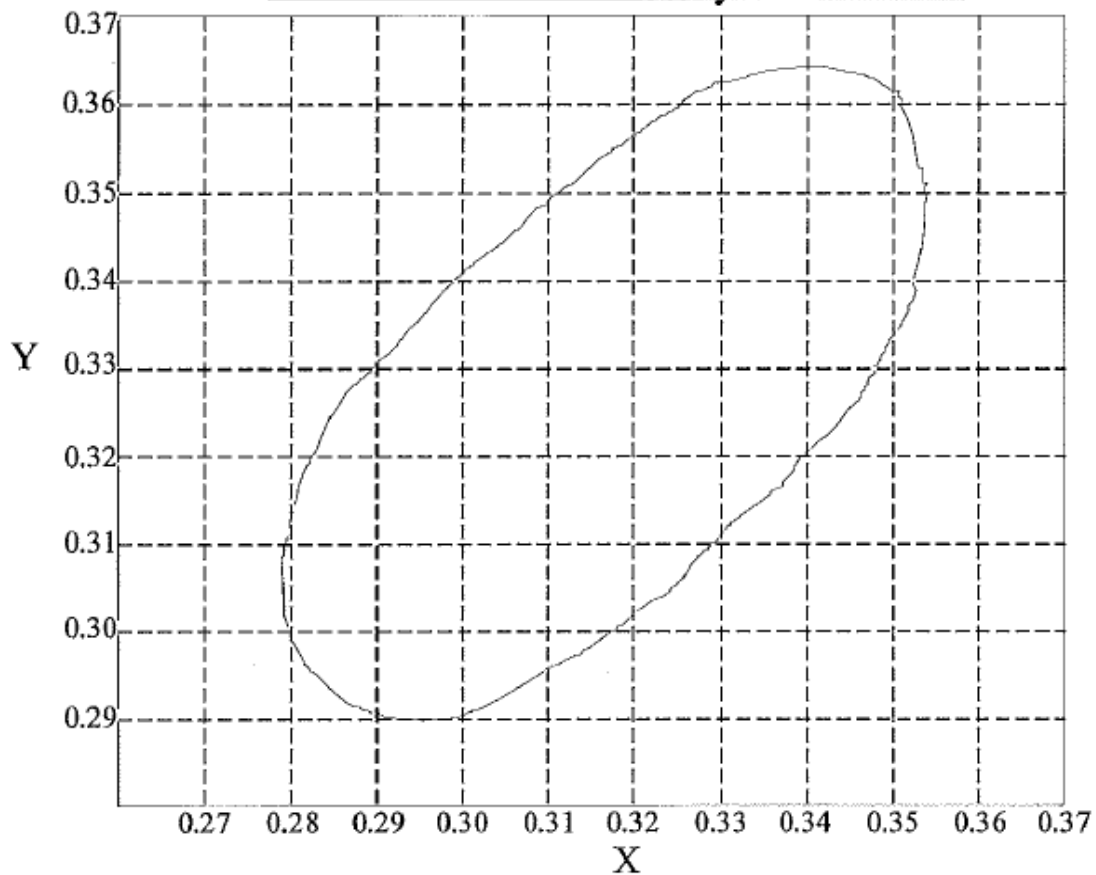


**Figure 1.10** Region for neutral colored in XY color coordinate

### 1.10 Electrospinning

Electrospinning is an easy technique to make fibers using polymer solution or melted polymer. This technique has several advantages<sup>77,78</sup>

- (a) Unidirectional fiber mat can be easily made
- (b) Wide range of fiber diameter can be prepared by changing processing parameters
- (c) Non woven fiber can be prepared in short period
- (d) Easily scalable

(e) Encapsulation of different water soluble and insoluble material can be easily done.

A typical setup for electrospinning is shown in **Figure 1.11**. Here a controlled syringe is needed to control the flow of polymer solution and is placed horizontally above the collector. A high voltage is applied to jet polymeric solution. A threshold potential is needed to overcome the surface tension to form the Taylor cone. Concentration of the polymer solution is another important parameter to create a stable jet. Otherwise, Taylor cone breaks the solution and results to small droplets. Major disadvantage of the electrospinning technique is slower formation rate of fiber mat. This could be overcome by using multiple spinnerets but there could be interference between multiple spinnerets.

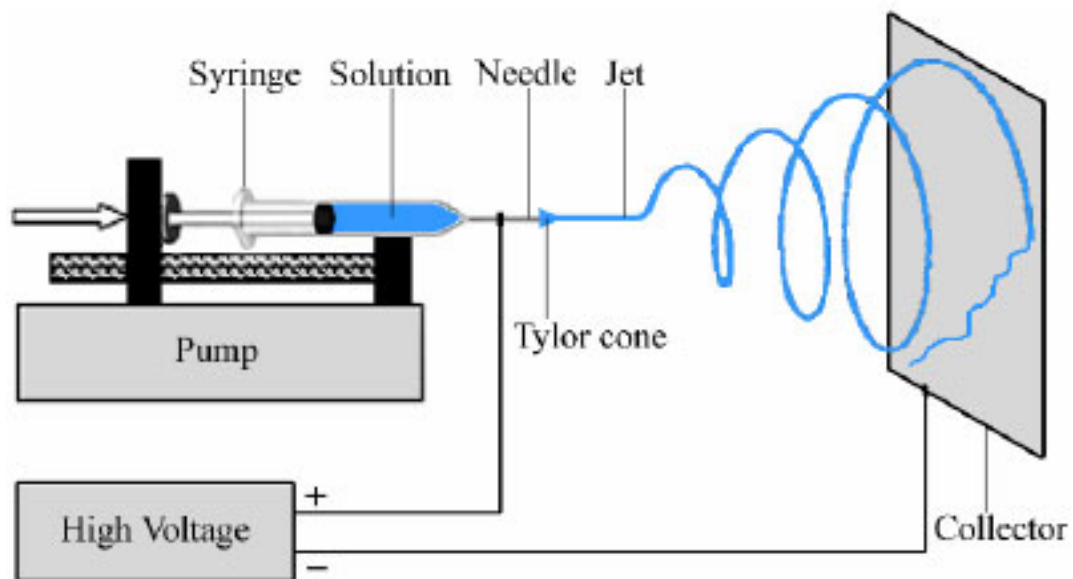


**Figure 1.11** Typical electrospinning set up<sup>79</sup>

## References

- (1) Platt, J. R. *J. Chem. Phys.* **1961**, 34.
- (2) Deb, S. K. *Appl. Opt., Suppl.* **1969**, 3, 192.
- (3) Somani, P. R.; Radhakrishnan, S. *Materials Chemistry and Physics* **2003**, 77, 117.
- (4) Sapp, S. A.; Sotzing, G. A.; Reddinger, J. L.; Reynolds, J. R. *Adv Mater* **1996**, 8, 808.
- (5) Ananthakrishnan, N.; Padmanaban, G.; Ramakrishnan, S.; Reynolds, J. R. *Macromolecules* **2005**, 38, 7660.
- (6) Henckens, A.; Knipper, M.; Polec, I.; Manca, J.; Lutsen, J.; Vanderzande, D. *Thin Solid Films* **2004**, 451, 572.
- (7) Invernale, M. A.; Ding, Y.; Sotzing, G. A. *ACS Appl. Mater. Interfaces* **2010**, 2, 296.
- (8) Sonmez, G.; Shen, C. K. F.; Rubin, Y.; Wudl, F. *Angewandte Chemie (International ed. in English)* **2004**, 43, 1498.
- (9) Kim, W. H.; Mäkinen, A. J.; Nikolov, N.; Shashidhar, R.; Kim, H.; Kafafi, Z. H. *Applied Physics Letters* **2002**, 80, 3844.
- (10) Hu, B.; Li, D.; Ala, O.; Manandhar, P.; Fan, Q.; Kasilingam, D.; Calvert, P. D. *Advanced Functional Materials* **2011**, 21, 305.
- (11) Xu, J.; Yang, Y.; Yu, J.; Jiang, Y. *Applied Surface Science* **2009**, 255, 4329.
- (12) Choi, M. R.; Woo, S. H.; Han, T. H.; Lim, K. G.; Min, S. Y.; Yun, W. M.; Kwon, O. K.; Park, C. E.; Kim, K. D.; Shin, H. K.; Kim, M. S.; Noh, T.; Park, J. H.; Shin, K. H.; Jang, J.; Lee, T. W. *ChemSusChem* **2011**, 4, 363.
- (13) Argun, A. A.; Aubert, P. H.; Thompson, B. C.; Schwendeman, I.; Gaupp, C. L.; Hwang, J.; Pinto, N. J.; Tanner, D. B.; MacDiarmid, A. G.; Reynolds, J. R. *Chem. Mater.* **2004**, 16, 4401.

- (14) Chen, W.; Wu, S.; Ferng, Y. *Materials Letters* **2006**, 60, 790.
- (15) Granqvist, C. G. *Sol. Energy Mater. Sol. Cells* **2000**, 60, 201.
- (16) Granqvist, C. G.; Avendano, E.; Azens, A. *Thin Solid Films* **2003**, 442, 201.
- (17) Shimano, K. *Solid State Ionics*. **2002**, 147, 129.
- (18) Naghavi, N. *Solid State Ionics* **2003**, 156, 463.
- (19) Lee, S. *Solid State Ionics* **2002**, 147, 129.
- (20) Sonmez, G. *Chemical communications (Cambridge, England)*. **2005**, 5251.
- (21) Mortimer, R. J. *Electrochim. Acta* **1999**, 44, 2971.
- (22) Mortimer, J. A.; Dyer, A. L.; Reynolds, J. R. *Displays* **2006**, 27, 2.
- (23) Cihaner, A.; Alg, F. *Adv. Funct. Mater.* **2008**, 18, 3583.
- (24) Yang, W.; Zhao, J.; Kong, Y.; Kong, T.; Cui, C. *J. Electrochem. Sci.* **2012**, 7, 2764.
- (25) Beaujuge, P. M.; Ellinger, S.; Reynolds, J. R. *Adv. Mater.* **2008**, 20, 2772.
- (26) Zhang, F.; Johansson, M.; Andersson, M. R.; Hummelen, J. C.; Inganäs, O. *Adv Mater* **2002**, 14, 662.
- (27) Gonzaleztejera, M.; Delablanca, E.; Carrillo, I. *Synthetic Metals*. **2008**, 158, 165.
- (28) Baek, M.; Lee, J.; Zong, S. H.; Lee, K. *Synthetic Metals*. **2010**, 160, 1197.
- (29) Li, G.; Shrotriya, V.; Huang, J.; Yao, Y.; Moriarty, T.; Emery, K.; Yang, Y. *Nature Materials*. **2005**, 864.
- (30) Hamedi, M.; Forchheimer, R.; Inganäs, O. *Nat Mater* **2007**, 6, 357.
- (31) Sirringhaus, H.; Bird, M.; Zhao, N. *Adv Mater* **2010**, 22, 3893.
- (32) Lu, K.; Liu, Y. *Current Organic Chemistry*. **2010**, 14, 2017.

- (33) Yan, F.; Li, J.; Mok, S. M. *Journal of Applied Physics*. **2009**, *106*, 74501.
- (34) Bell, J.; Matthews, J. P.; Skryabin, I. L.; Wang, J.; Monsma, B. G. *Renewable Energy*. **1998**, *15*, 312.
- (35) Seshadri, V.; Padilla, J.; Bircan, H.; Radmard, B.; Draper, R.; Wood, M.; Otero, T. F.; Sotzing, G. A. *Organic Electronics*. **2007**, *8*, 367.
- (36) Vasilyeva, S. V.; Beaujuge, P. M.; Wang, S.; Babiarz, J. E.; Ballarotto, V. W.; Reynolds, J. R. *ACS Appl. Mater. Interfaces*. **2011**, *3*, 1022.
- (37) Tehrani, P.; Hennerdal, L. O.; Dyer, A. L.; Reynolds, J. R.; Berggren, M. *Journal of Materials Chemistry*. **2009**, *19*, 1799.
- (38) Gunbas, G. E.; Durmus, A.; Toppare, L. *Adv Mater* **2008**, *20*, 691.
- (39) Calvert, P.; Duggal, D.; Patra, P.; Agrawal, A.; Sawhney, A. *Molecular Crystals and Liquid Crystals*. **2008**, *484*, 291.
- (40) Lange, U.; Mirsky, V. M. *Analytica chimica acta*. **2011**, *687*, 105.
- (41) Molapo, K. M.; Ndangili, P. M.; Ajayi, R. F.; Mbambisa, G.; Mailu, S. M.; Njomo, N.; Masikini, M.; Baker, P.; Iwuoha, E. I. *Int. J. Electrochem. Sci*. **2012**, *7*, 11859.
- (42) Rehman, M.; Kumar, A.; Su-Park, D.; Shim, Y. *Sens*. **2008**, *8*, 118.
- (43) *Conducting polymers, fundamentals and applications: a practical approach*; Chandrasekhar, P., Ed.; Springer, 1999.
- (44) Baughman, R.; Shacklette, L. *Physical review. B, Condensed matter*. **1989**, *39*, 5872.
- (45) Koenraad, P. M.; Flatté, M. E. *Nature Materials*. **2011**, *10*, 91.
- (46) Mudigonda, D. S. K.; Boehme, J. L.; Brotherston, I. D.; Meeker, D. L.; Ferraris, J. P. *Chem. Mater*. **2000**, *12*, 1508.
- (47) Loewe, R. S.; Mccullough, R. D. *Chem. Mater*. **2000**, *12*, 3214.
- (48) Loewe, R. S.; Ewbank, P. C.; Liu, J.; Zhai, L.; Mccullough, R. D. *Macromolecules* **2001**, *34*, 4324.

- (49) Liu, J.; Sheina, E.; Kowalewski, T.; McCullough, R. D. *Angew Chem Int Ed Engl* **2002**, *41*, 329.
- (50) Zhai, L.; Pilston, R. L.; Zaiger, K. L.; Stokes, K. K.; Mccullough, R. D. *Macromolecules* **2003**, *36*, 61.
- (51) Jeffries, E. M.; Sauvé, G.; McCullough, R. D. *Adv Mater* **2004**, *16*, 1017.
- (52) Sheina, E. E.; Liu, J.; Iovu, M. C.; Laird, D. W.; Mccullough, R. D. *Macromolecules* **2004**, *37*, 3526.
- (53) Gartshtein, Y. N.; Zakhidov, A. A. *Journal of Molecular Electronics*. **1987**, *3*, 163.
- (54) Heeger, A. J. *Angew Chem Int Ed Engl* **2001**, *40*, 2591.
- (55) Monk, P. M. S.; Mortimer, R. J.; Rosseinsky, D. R.; Cambridge University Press: 2007, p 483.
- (56) Carpi, F.; Derossi, D. *Optics & Laser Technology* **2006**, *38*, 292.
- (57) Lee, K.; Sotzing, G. A. *Macromolecules* **2013**, *34*, 5746.
- (58) Mudigonda, D. S. K.; Meeker, D. L.; Loveday, D. C.; Osborn, J. M.; Ferraris, J. P. *Polymer* **1999**, *40*, 3407.
- (59) Dey, T.; Invernale, M. A.; Ding, Y.; Buyukmumcu, Z.; Sotzing, G. A. *Macromolecules* **2011**, *44*, 2415.
- (60) Gunbas, G. E.; Durmus, A.; Toppare, L. *Adv. Funct. Mater.* **2008**, *18*, 2026.
- (61) Beaujuge, P. M.; Ellinger, S.; Reynolds, J. R. *Nat Mater* **2008**, *7*, 795.
- (62) Unur, E.; Beaijuge, P. M.; Ellinger, S.; Jung, J. H.; Reynolds, J. R. *Chem. Mater.* **2009**, *21*, 5145.
- (63) Shin, H.; Kim, Y.; Bhuvana, T.; Lee, J.; Yang, X.; Park, C.; Kim, E. *ACS Appl. Mater. Interfaces*. **2012**, *4*, 185.
- (64) Invernale, M. A.; Seshadri, V.; Mamangun, D. M. D.; Ding, Y.; Eilorama, J.; Yavuz, M. S.; Sotzing, G., A. *Chem. Mater.* **2009**, *21*, 3332.

- (65) Seshadri, V.; Padilla, J.; Bircan, H.; Radmard, B.; Draper, R.; Wood, M.; Otero, T. F.; Sotzing, G. A. *Org. Electron.* **2007**, *8*, 367.
- (66) Camurlu, P.; Cirpan, A.; Toppare, L. *Journal of Electroanalytical Chemistry.* **2004**, *572*, 61.
- (67) Lin, T.; Ho, K. *Solar Energy Materials and Solar Cells* **2006**, *90*, 506.
- (68) DeLongchamp, D. M.; Hammond, P. T. *Chemistry of Materials* **2004**, *16*, 4799.
- (69) Henderson, W. A. *Solid State Ionics* **2012**, *217*, 1.
- (70) Fenton, D. E.; Parker, J. M.; Wright, P. V. *Polymer* **1973**, *14*, 589.
- (71) Reeves, B. D.; Grenier, C. R. G.; Argun, A. A.; Cirpan, A.; McCarley, T. D.; Reynolds, J. R. *Macromolecules* **2004**, *37*, 7559.
- (72) Zong, K.; Reynolds, J. R. *The Journal of Organic Chemistry* **2001**, *66*, 6873.
- (73) Invernale, M. A.; Ding, Y.; Mamangun, D. M. D.; Yavuz, M. S.; Sotzing, G., A. *Adv Mater* **2010**, *22*.
- (74) Padilla, J.; Seshadri, V.; Filloramo, J.; Mino, W.; Mishra, S.; Radmard, B.; Kumar, A.; Sotzing, G. A.; Otero, T. *Syn Metals.* **2007**, *157*, 261.
- (75) Ohta, N.; Robertson, A. R.; Robertson, A. A.; John Wiley and Sons,: 2005, p 334.
- (76) Zollinger, H.; 1st ed.; WILEY-VCH: 1999, p 66.
- (77) Huang, Z. M.; Zhang, Y. Z.; Kotaki, M.; Ramakrishna, S. *Composites Science and Technology* **2003**, *63*, 2223.
- (78) Li, D.; Xia, Y. *Adv Mater* **2004**, *16*, 1151.
- (79) Ziabari, M.; Mottaghitalab, V.; Haghi, A. K. *Braz. J. Chem. Eng.* **2009**, *26*, 53.
- (80) Li, D., Xia, Y. *Adv Mater* **2004**, *16*, 1151.
- (81) ZIABARI, M., MOTTAGHITALAB, V., HAGHI, A. K.. *Braz. J. Chem. Eng.* **2009**, *26*, 53.



- (82) Gunbas, G.; Toppare, L. *Chem Commun (Camb)* **2012**, 48, 1083.
- (83) Beaujuge, P. M.; Reynolds, J. R. *Chem Rev* **2010**, 110, 268.
- (84) Westenhoff, S.; Howard, I. A.; Hodgkiss, J. M.; Kirov, K. R.; Bronstein, H. A.; Williams, C. K.; Greenham, N. C.; Friend, R. H. *J Am Chem Soc* **2008**, 130, 13653.
- (85) Liu, R.; Duay, J.; Lee, S. B. *ACS Nano* **2010**, 4, 4299.
- (86) Bijleveld, J. C.; Zoombelt, A. P.; Mathijssen, S. G.; Wienk, M. M.; Turbiez, M.; de Leeuw, D. M.; Janssen, R. A. *J Am Chem Soc* **2009**, 131, 16616.
- (87) Shi, P.; Amb, C. M.; Knott, E. P.; Thompson, E. J.; Liu, D. Y.; Mei, J.; Dyer, A. L.; Reynolds, J. R. *Adv Mater* **2010**, 22, 4949.
- (88) Hamedi, M.; Forchheimer, R.; Inganas, O. *Nat Mater* **2007**, 6, 357.
- (89) Sonmez, G.; Shen, C. K.; Rubin, Y.; Wudl, F. *Angew Chem Int Ed Engl* **2004**, 43, 1498.
- (90) Mortimer, J. R., ; Dyer, A. L.; Reynolds, J. R.; *Displays* **2006**, 27, 2.
- (91) Roncali, J. *Chem. Rev.* **1992**, 92, 711.
- (92) Ding, Y., ; Invernale, M. A.; Mamangun, D. M. D.; Kumar. A.; Sotzing, G, A.; *J. Mater. Chem.* **2011**, 21, 11873.
- (93) Kumar, A. O., M.T.; Alamar, F. A.; Zhu. Y.;Sotzing, G, A.; *J. Mater. Chem. C* **2014**, 2, 2510.
- (94) Otley, M. T. A., F. A.; Zhu. Y.; Singhviranon, A.; Zhang, X.; Li, M.;Kumar, A.;Sotzing, G, A.; *Appl. Mater. Interfaces* **2014**, 6, 1734.
- (95) Zhu. Y, O., M.T.; Alamar, F. A.; Kumar, A.; Zhang. X.; Mamangun. D. M. D.; Li. M.; Arden. B. G.; Sotzing, G, A.; *Org. Electron.* **2014**, 15, 1378.
- (96) Alamar, F. A. O., M.T.; Zhu, Y.; Kumar. A.; Sotzing, G.A.; *Solar Energy Materials and Solar Cells* **2015**, 132, 131.
- (97) Welsh.A, K. A., ; Meijer,E.W.; Reynolds, J.R.; *Adv Mater* **1999**, 11.
- (98) Bamford, B., ; Reiche, A.; Dlubek, G.; Allion, F.; Sanchez; Alam, M.A.; *J. Chem. Phys.* **2003**, 118, 9420.

- (99) Miyamoto, T., ; Shibayama,K;; *J. Appl. Phys.*, **1973**, 44, 5372.
- (100) Pas, S. T., ; Ingram, M. D.; Funke, K; Hill. A.J;; *Electrochimica Acta* **2005**, 50, 3955.
- (101) Forsyth, M., ; Meakin, P;; MacFarlane, D. R.; Hill, A. J;; *J. Phys. Condens. Matter* **1995**, 7, 7601.
- (102) MacCallum, M. A., ; Vincent, C.A;; *Polymer Electrolyte Reviews*, **1989**, 2, 1989.
- (103) Hardy, L. C., ; Shriver, D. F;; *J. Am. Chem. Soc.* **1985**, 107, 3823.
- (104) Avlyanov, K. J., ; Min, Y;; MacDiarmid, A. G;; Epstein, A. J;; *Syn Metals*. **1995**, 72, 65.
- (105) Avlyanov, K. J., ; Kuhn, H.H;; Josefowicz, J.Y;; MacDiarmid, A. G;; *Syn Metals*. **1997**, 84, 15

## **Chapter 2**

### **Experimental procedure and Instruments**

## **2.1 Introduction**

To have a better performing electrochromic device the electrochemical and optical behavior of electrochromic polymers needs to be tested. This chapter is going to introduce the instruments and general experimental procedures that were carried out to study the electrochemical and optical properties of electrochromic conjugated polymers in this dissertation. More specific experiments are discussed in the corresponding chapters.

General assemble method for fabricating electrochromic devices and preparation of polymer gel electrolyte were also discussed into this chapter.

## **2.2 Chemicals and abbreviation**

### **2.2.1 Electrode**

Platinum (Pt), silver wire (Ag), Indium dopped tin oxide (ITO) coated glass ( $R_s = 8-12 \text{ Ohm/sq}$ ) and polyethylene terephthalate (PET) ( $R_s = 60-80 \text{ Ohm/sq}$ ) were purchased from Delta Tech Inc and Bay View Inc, respectively.

### **2.2.2 Preparation of polymer gel electrolyte**

Propylene carbonate (PC), ethylene carbonate (EC), poly(ethylene glycol) diacrylate (PEG-DA)  $M_n = 700, 500 \text{ and } 250$ , lithium trifluoromethanesulfonate (LiTRIF), 2,2-dimethoxy-2-phenyl-acetophenone

(DMPAP) and 1-butyl-3-methylimidazolium hexafluorophosphate were purchased from Sigma Aldrich and used as received.

### **2.2.3 List of monomers used**

3,4-ethylenedioxythiophene was purchased from Heraeus Cleviuos GmbH and vacuum distilled before use. 2,2' bithiophene was purchased from Sigma Aldrich. Biphenylmethyloxymethyl-3,4 propylene dioxythiophene (BPMOM-ProDOT), 1,3-di-tert-butyl-3,4 propylene dioxythiophene (ProDOT-tBu<sub>2</sub>), 2,2-dimethyl-3,4 propylene dioxythiophene (ProDOT-Me<sub>2</sub>), 1,3-di-isopropyl-3,4 propylene dioxythiophene (ProDOT-IP<sub>2</sub>), were synthesized according to reported procedure.

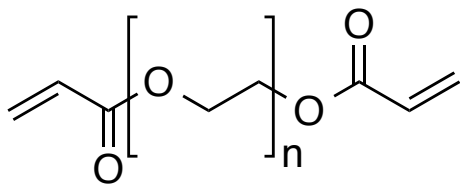
### **2.2.4 Preparation conductive fiber mat**

Polyethylene terephthalate (Mv=30,000)(PET) was bought from Scientific Polymer. Silica nanoparticles with surface area 200m<sup>2</sup>/g, average particle size 12nm was purchased from AEROSIL. ORGACON S300 and CLEVIOS PH1000 PEDOT-PSS were bought from Agfa and Heraeus, respectively. The metal mesh was a generous gift from ITP GmbH. Dichloromethane (DCM) & trifluoroacetic acid (TFA) was from Fisher.

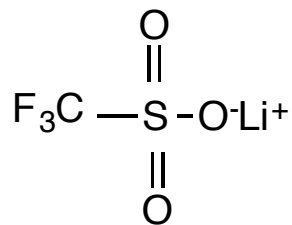
### **2.2.5 Assembly of ECD**

Copper tape was purchased from Newark. Norland UV curable glue, UVS-91 was purchased from Products Inc.

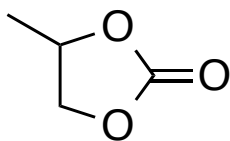
## 2.3 Structure of chemicals used



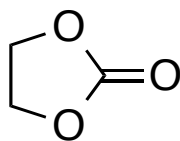
(a)



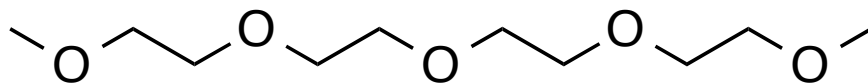
(b)



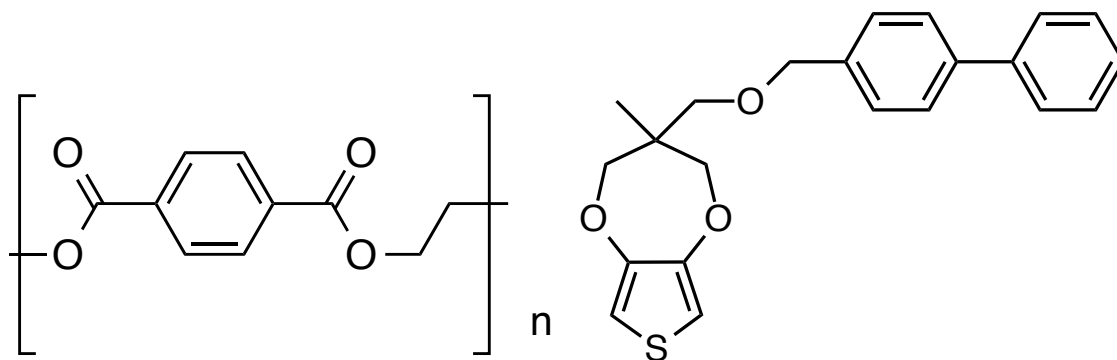
(c)



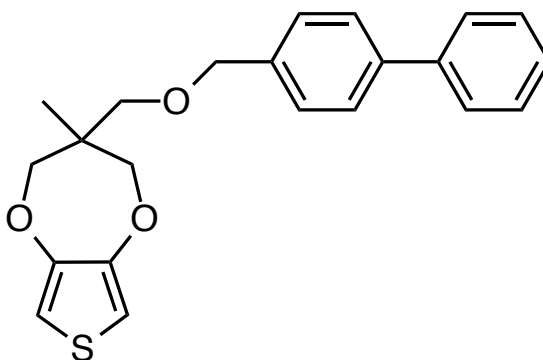
(d)



(e)



(f)



(g)

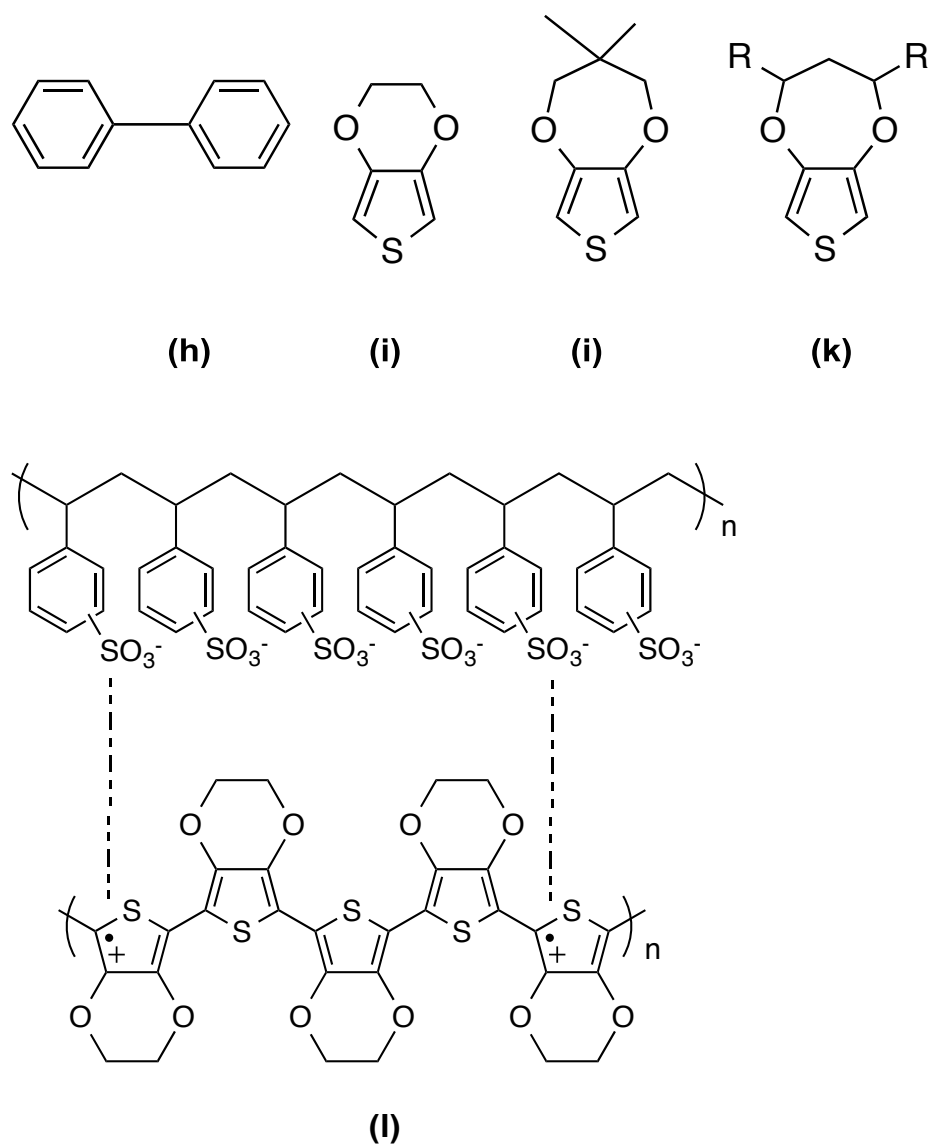


**Figure 2.1** Chemical structures of (a) PEGDA, (b) LiTRIF, (c) PC, (d) EC, (e) tetraethylene glycol dimethyl ether, (f) PET, (g) BPOM-ProDOT, (h) biphenyl, (i) EDOT, (j) ProDOT-Me<sub>2</sub>, (k) 1,3 disubstituted-ProDOT and (l) PEDOT-PSS

## 2.4 Techniques

### 2.3.1 Electrochemical characterization

The electrochemical study was carried out using CHI 720c, 660a and 400a potentiostats. Generally cyclic voltammetry and chronocoulometry techniques were used to characterize the electrochemical behavior of the electrochromic polymers.

#### 2.4.1.1 Cyclic voltammetry (CV)

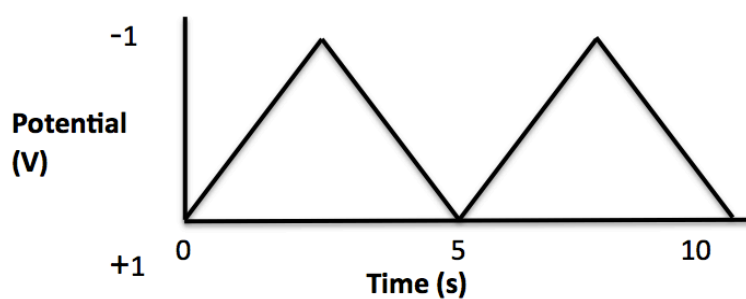
In this technique a linear sweep of potential is applied and a change in current with applied potential at working electrode. The change in voltage over time is shown in **Figure 2.2** and the ramping is known as scan rate. A CV can provide the following information about a conjugated polymer: (i) the monomer oxidation potential, (ii) oxidation and reduction potential of redox switching, (iii) oxidation and reduction peak current. **Figure 2.3** is an example of a typical CV for polymerization of ethylene dioxythiophene and its redox cycles. It can be seen that the oxidation potential for this monomer is about 1.3V using Pt as working, Ag as reference and ITO as counter electrode in a 0.1M lithium triflate in acetonitrile solution. From Randles and Sevcik equation peak current of a reversible electrolyte can be given as,

$$i_p = 2.69 \times 10^5 n^{3/2} A D^{1/2} v^{1/2} C_o \text{-----(2.1)}$$

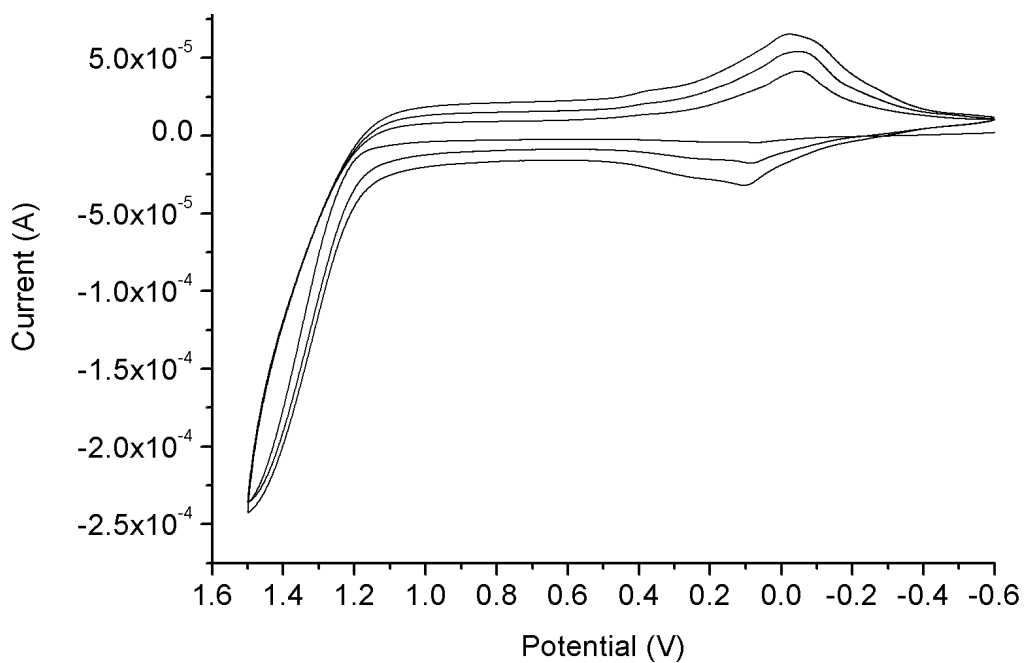
n is the number of electrons involve, A is the active area of the working electrode (cm<sup>2</sup>), D is the diffusion coefficient of the electrolyte (cm<sup>2</sup>/s), v is



the scan rate (V/s) and  $C_o$  is the concentration of the electroactive species ( $\text{mol}/\text{cm}^3$ ) in bulk solution. From this above equation it can be seen that the peak current is related to the scan rate and concentration of the electroactive species. By knowing the peak current diffusion coefficient can be calculated.



**Figure 2.2** Typical linear sweeps of potentials in CV



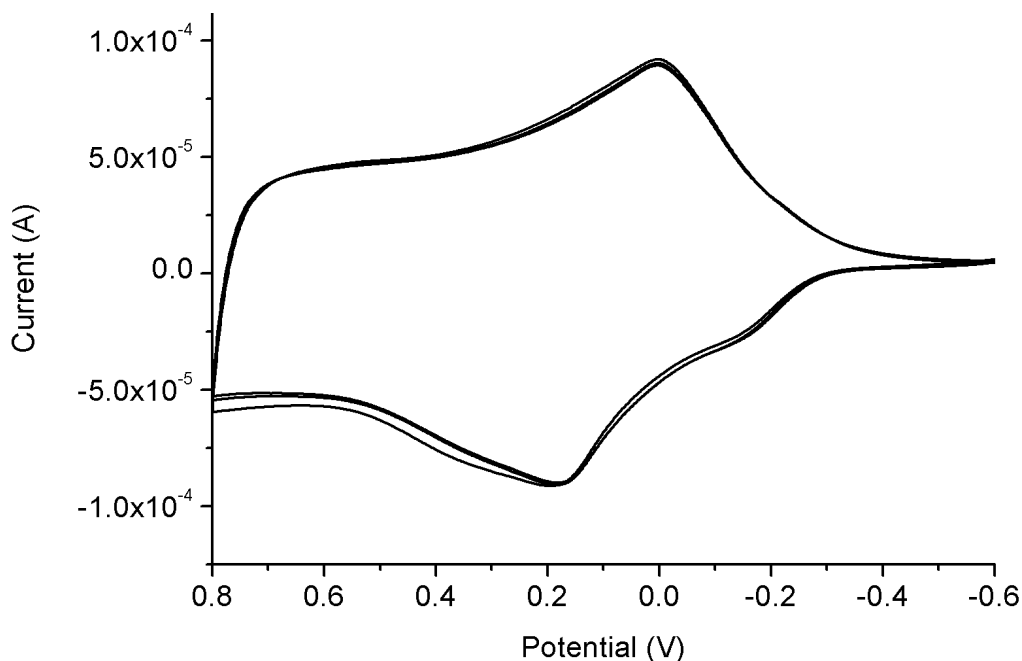


**Figure 2.3** Example of a typical CV graph for electrodeposition of conductive polymer (PProDOT-Me<sub>2</sub>) (top) and switching (bottom) using electrolyte bath

#### 2.4.1.2 Chronocoulometry (CC)

In this technique initial and final potentials are two constant values and the charges passed for a certain time is plotted as a function of time. Generally, for electrochemical study after determining the oxidation potential of the monomer using CV, chronocoulometry is used to electropolymerize for a certain period of time with a constant potential. CC is also a helpful tool to switch EC devices between two redox states and to measure the switching speed. Charge consumption during electropolymerization or switching can also be calculated from CC, which

could be helpful for more fundamental studies like calculating doping level, percentage of yield etc.

## **2.4.2 Optical characterization**

The optical performance study was carried out using spectrophotometer Cary 5000i UV-Vis-NIR. All spectra were performed without background correction. Color research PR 670 was used to determine the color coordinates.

### **2.4.2.1 UV-Vis-NIR spectrophotometry**

Spectrometry is an important tool to evaluate the optical performance of an electrochromic device. By taking the absorbance spectra photopic transmittance value can be evaluated. It gives us the idea of darkness or transparency of an electrochromic device. By knowing the onset of the absorption spectra band gap energy can be calculated. Fast switching speed of an electrochromic device is very important. Some of the devices have  $<1$  s response time. This switching speed can be calculated by monitoring the switching of the device between two redox states at a certain wavelength. Long-term stability of an ECD can be calculated by monitoring the transmittance loss during switching. **Figure 2.6** shows a typical chronoabsorpmetry spectrum of an ECD while monitoring at 555nm by subjecting to  $\pm 2$ V potential.

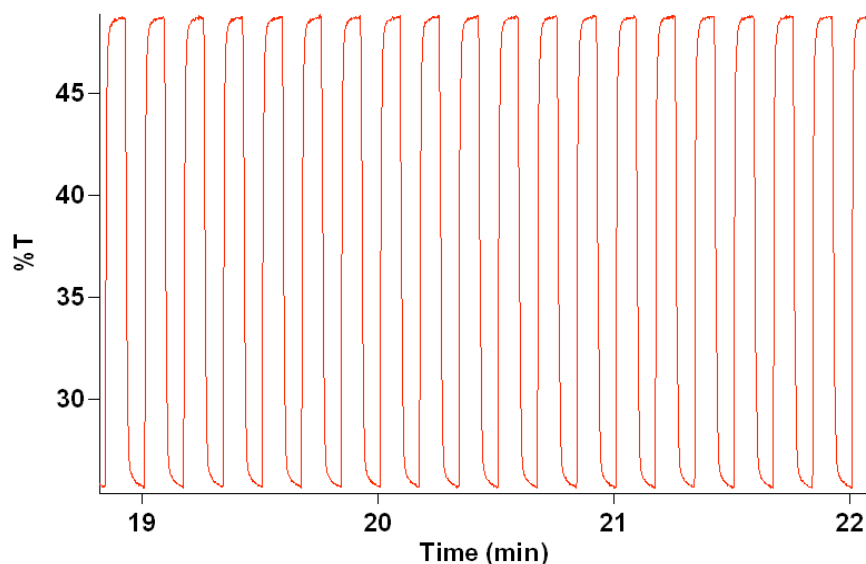


**Figure 2.4** A typical example of a chronoabsorpmetry spectrum where %T is monitored at 555 nm.

#### **2.4.2.2 Colorimeter**

A PR-670 colorimeter was used to analyze the colors and the luminance of different samples. A reference was run on white background under D65 standard illuminant lamp inside a black box. 360-860 nm measurement range with 1 nm intervals and a ½ degree aperture MS-5X zoom lens was used.

#### **2.4.3 Ionic conductivity measurements**

To evaluate the highest ionic conductivity of each PEG acrylate system, different weight percentage of LiTRIF salt was dissolved into 1:1 weight

ratio of plasticizer : PEG-acrylate and cured using photoinitiator. The ionic conductivity,  $\sigma$ , was measured by placing the solid polymer gel electrolyte in between two stainless steel electrodes using Agilent 4284A LCR meter, an AC impedance spectroscopy over a 20 to 10000 Hz frequency range. Using the Bode plot where impedance is plotted as function of frequency (as shown in **Figure 2.5**), the resistance (R) of the solid electrolyte was calculated and  $\sigma$  was calculated using the following equation,

$$\sigma = t/RA \text{ -----2.2}$$

where t is the thickness of the polymer gel electrolyte and A is the area of the electrodes. A typical experimental set up for measuring ionic conductivity of solid gel electrolyte is shown in **Figure 2.6**.

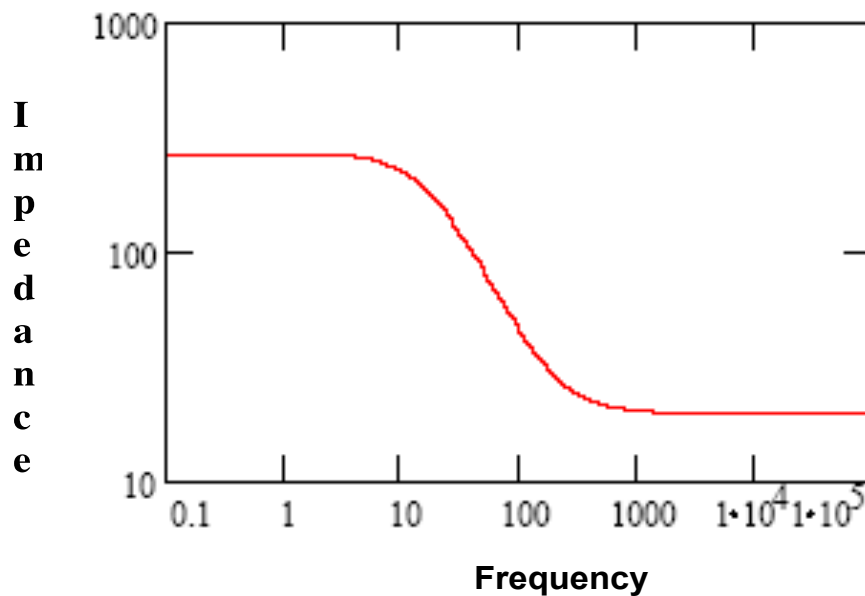


**Figure 2.5** A typical Bode plot: impedance at different frequency

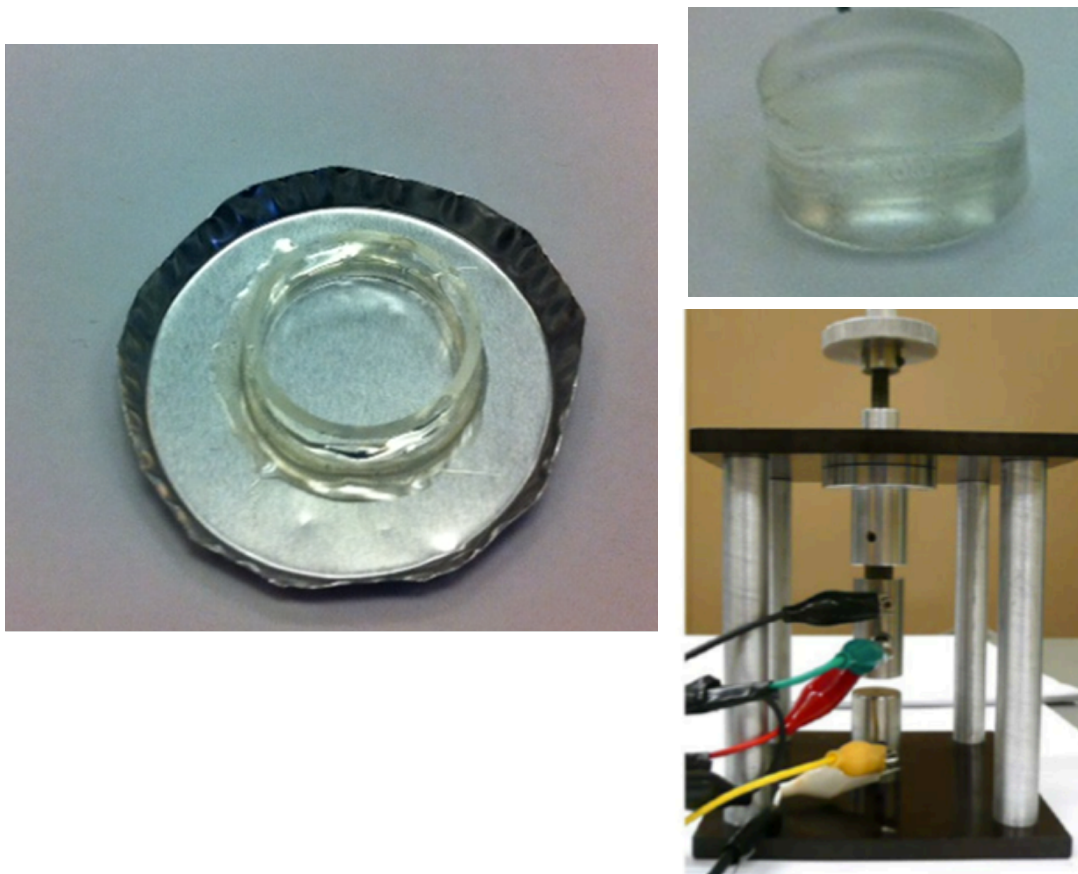


**Figure 2.6** Shows an example of (a) set of sample preparation (top left), (b) a solid polymer gel electrolyte (top right), (c) set up for placing polymer gel electrolyte in between two electrodes for Agilent 4284A LCR meter (bottom).

#### **2.4.4 Sheet resistance measurement**

As two-point probe is not appropriate to calculate the sheet resistance of a semiconductor, four-line was used to measure the sheet resistance to minimize the parasitic resistance. In case of four-line probe system, current

is sent through outer probes and voltage between inner probes is measured. Here the voltage is measured at different applied current. Sample must touch all four probes and to have a consistency between different samples. The four electrodes are equispaced. Keithley 224 was used as current source. At least 10 data points were taken per sample.  $I$  is plotted against  $V$  and resistance ( $R$ ) is calculated from the slope and sheet resistance ( $R_s$ ) is calculated from **equation 2.3**.

$$R_s = R (w/l) \text{ -----2.3}$$

where  $w$  is the width of the sample and  $l$  is the distance between the probes.

## **2.4.5 Thermal analysis**

### **2.4.5.1 Differential Scanning Calorimetry (DSC)**

Differential scanning calorimetric studies were carried out on Q-100. First heating scan was from  $-90^{\circ}\text{C}$  to  $50^{\circ}\text{C}$ , then cooling back to  $-90^{\circ}\text{C}$  at  $20\text{min}/^{\circ}\text{C}$  and again heating up to  $50^{\circ}\text{C}$  at  $5^{\circ}\text{C}/\text{min}$ .

### **2.4.5.2 Thermal Mechanical Analysis (TMA)**

Thermal mechanical analysis experiment was carried out on TMA Q-400. For this study  $0.0200\text{ N}$  force was applied and final temperature was  $50^{\circ}\text{C}$ . A scanning rate of  $5^{\circ}\text{C}/\text{min}$  was used.

#### **2.4.6 Electrospinning**

Objective of electrospinning is to make fibers with uniform diameter. A typical electrospinning set up was arranged using a stable polymer solution, high voltage power supply and a control syringe pump to inject the polymer solution. Polymer solution can be prepared by dissolving polymers into appropriate solvent or by melting the polymer. Spellman CZE 1000R is used to apply the voltage. It is capable to supply voltage from 0 to 30 kV and 0 to 300  $\mu$ A DC output. This polymer solution becomes charged by application of voltage. A KD scientific automated syringe pump was used to control the flow rate. This pump can control the flow rate of polymer solution in between 0.001  $\mu$ L/hr to 999 mL/hr. typically 1ml hypodermic syringe was used. The collector was orthogonally placed below the syringe. Depending upon the utility of the fibers the collectors were chosen. It could be a conductive substrate like aluminum foil or non-conductive like glass, PET or Kapton. Fiber diameter and morphology of depends on several parameters. These parameters can be divided into three categories; (i) solution parameters, (ii) process parameters and (iii) environmental parameters. Details of these parameters are given below.

(i) Solution parameters:

- Concentration of polymer solution
- Viscosity
- Dielectric constant
- Solvent volatility



(ii) Process parameters:

- Electric field strength
- Distance between collector and nozzle tip
- Nozzle diameter and size
- Flow rate of feeding

(ii) Environmental parameters:

- Temperature
- Pressure
- Humidity
- Air flow

Fiber diameter can be tuned by controlling the solution and process parameters. Like, fiber diameter can be increased by increasing the concentration of polymer solution or flow rate or nozzle diameter. To minimize environmental effect the whole set up was kept inside a glass box.

## **2.4.7 Characterization of film morphology**

### **2.3.7.1 Scanning Electron Microscopy (SEM)**

SEM imaging was done on the Jeol JSM-6335F at 2.5 kV, probe current: 14  $\mu$ A to induce charging on the surface of a sample. Charging allowed differentiation between the conducting and non-conducting regions via charge contrast imaging.

Cross-sectioning was done by cutting the free-standing fiber mesh submersed in liquid nitrogen with a razor blade.

#### **2.4.7.2 Transmission Electron Microscopy (TEM)**

Bright field TEM images were taken using a FEI Tecnai-T12 at 80 kV. EDS measurements were performed on a EDAX silicon crystal detector (30 mm<sup>2</sup>) operated by FEI TIA software. EDS was used to identify the SiO<sub>2</sub> within the PET fiber cross-sections.

PET fiber mesh was cut into 2 mm X 6 mm sections that were then embedded into an epoxy resin (SPI-Chem Araldite 6005 kit), and cured at 80°C for at least 12 hours. Next, samples were cut into ultrathin sections, 20 µm, slices using 45° Diatome diamond blade on a Reichert–Jung Ultra Cut E microtome and collected on a 400 mesh carbon coated copper grids. Excess water was wicked off of the copper grid/sample then TEM was immediately done.

#### **2.4.8 Electrochromic device assembly**

Electrochromic conjugated polymers are made either by electrochemical or chemical synthesis procedure. For electrodeposition method an electrolyte bath is needed. A typical electrolyte solution has 0.1M salt concentration; here in this dissertation 0.1M lithium triflate in acetonitrile solution was used. Generally, 10mM monomer concentration was used and the polymers were deposited onto the working electrode. For a typical three-

electrode system, ITO coated glass/PET surface was used as working and counter electrode, Ag/Ag<sup>+</sup> non-aqueous was used as reference. Here, to match the active area between both electrodes ITO was used for electrode. For fabric devices, conductive fiber mat was used as working electrode. For window type devices, reference electrode was shorted with counter electrode to keep the simplicity. **Figure 2.7** shows a set-up for two-electrode cell.

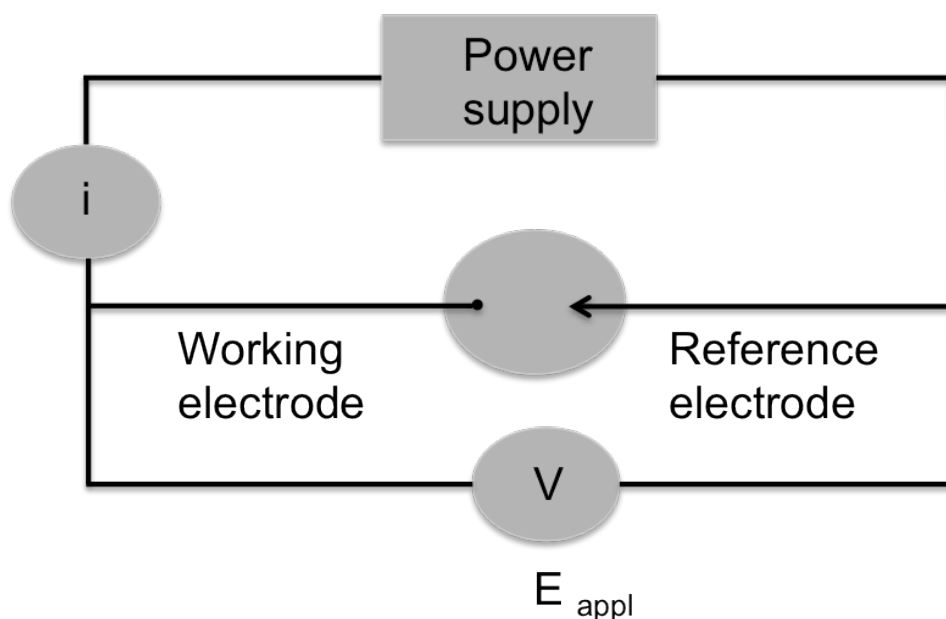


**Figure 2.7** Represents set-up for two-electrode cell

For chemical synthesis procedure, first electrochromic polymer needs to be synthesized, then make a processable solution, finally deposit the polymer onto ITO surface. Here in this dissertation any chemically synthesized electrochromic polymers were not used.

For chemical synthesis process, EC polymers or high molecular weight precursors were synthesized and were coated on ITO surface by using some processing technique. Generally, spin coating, spray coating or dip coating techniques was used to deposit the soluble polymers on electrode.



**Figure 2.8** Instrument used for spray coating technique

After depositing the electrochromic polymer onto working electrode surface, polymer gel electrolyte was placed in between two electrodes. UV curable glue was used to seal the edges of the devices. Polymer electrolyte and the glue is cured by irradiating the assembled device with 365 nm UV light. For large active area, goggle sized devices,  $>100 \text{ cm}^2$  adhesive Cu tape were used around the whole perimeter to lower the Iris effect.

## UV chamber

A UV crosslinker CL-1000 equipped with UV lamp with 365 nm wavelength, 5.8 W/cm<sup>2</sup> as shown in **Figure 2.9**, was used to form cross linked matrix.



**Figure 2.9** UV chamber, CL-1000 used to perform photochemical reaction

Upon application of suitable potential EC devices can be switched between two redox states. A  $\pm 2$  V potential is applied for redox switching either by CC or by using small battery box. For battery box, two 3 V watch battery were used and diodes were used to get desired potential as shown in **Figure 2.10**.

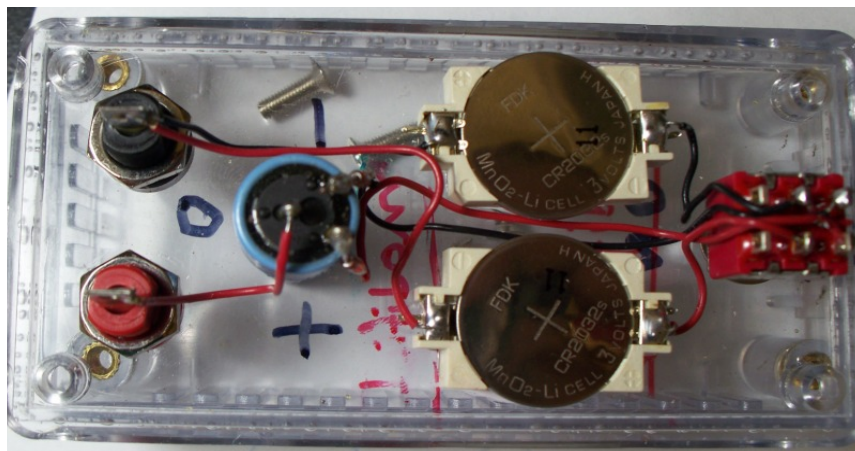


**Figure 2.10** Image of battery box used to switch ECD at  $\pm 2$  V

#### 2.4.9 Diffusion coefficient

To measure the diffusion of monomers inside the solid polymer gel matrix, ECD were assembled as mentioned earlier. The only exception was, the polymer matrix was made with out any monomer. A hole was made inside the solid polymer gel matrix and monomer electrolyte solution was added into it. ITO coated PET was used as counter electrode. **Figure 2.11** shows the schematic diagram of an assembled system. Initially, there were no monomers inside the solid matrix, as time goes monomers travel through the solid matrix. Concentration of monomer decreases with increasing the distance from the reservoir at a fixed time. After time  $t$  monomer solution from the hole pipetted out and the device was activated and switched by suitable potential. The distance traveled by EC material was measured by the color of the ECP at neutral state. Using the equation **2.4** the diffusion coefficient of the monomers inside the solid polymer matrix was calculated.

$$x = (2Dt)^{1/2} \text{ -----2.4}$$

where x is the diffusion length at time t and D is the diffusion coefficient of the monomer<sup>5</sup>

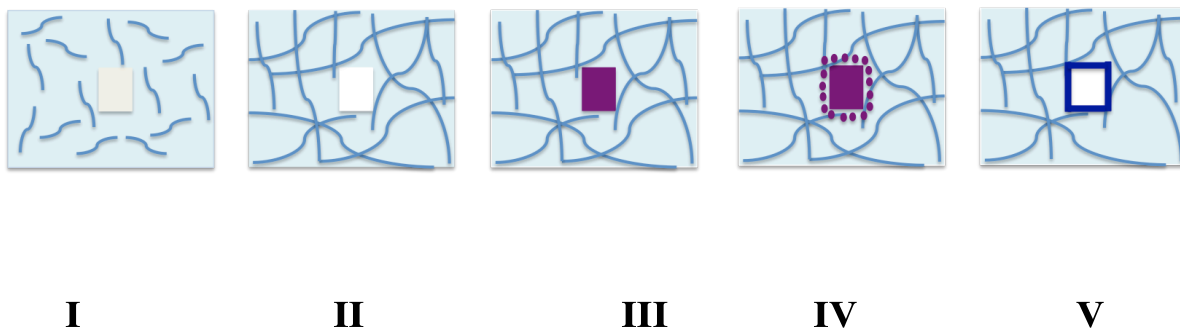


**Figure 2.11** Schematic diagram of ECD for diffusion study: (I) Liquid gel electrolyte without any monomer, (II) solid polymer gel matrix without any monomer, (III) monomer solution inside the reservoir, (IV) monomer diffused into the solid gel matrix and (V) monomers converted to conjugated polymer

## **Chapter 3**

### **Property relationships and characterization of one-step *in situ* method for solid-state electrochromic devices**



**Abstract:** Electrochromic polymer, hereby, generated from monomer after device construction, i.e. *in situ*, simplifying the fabrication of electrochromic devices by reducing waste generation and assembly time as well as increasing the versatility of device manufacturing in open atmosphere. Here, *in situ* fabrication process along with reaction mechanism, reaction kinetics, factors that could affect the rate of reaction as well as on optical behavior were discussed. The establishment of a relationship between device performance parameters such as switch speed and photopic contrast with device composition and electrochromic polymer thickness is reported here for a versatile one-step preparation method of relatively large area, 105 cm<sup>2</sup>, solid-state electrochromic devices. Photopic contrast is a critical property for electrochromic displays, windows, and lenses. Necessitating the study of how changing selected material and device properties affects the rate of polymerization as well as their optical behavior. More specifically photopic contrast performance is evaluated as a function of polymerization time, effective electrochromic polymer layer thickness, monomer concentration, thickness of gel electrolyte, and *in situ* conversion temperature. The percentage of the monomer conversion can also be calculated. Photopic contrast of 47% for poly biphenylmethyloxymethyl-3,4-propylenedioxythiophene (PBPMOM-ProDOT), 46% for poly 2,2-dimethyl-3,4-propylenedioxythiophene

(PProDOT-Me<sub>2</sub>), and 40% for poly(3,4-ethylenedioxythiophene) (PEDOT) without background correction were achieved.

### 3.1 Introduction

Electrochromic materials can reversibly change from one color state to another upon supplying a suitable charge and can be classified into three categories; inorganic materials, small organic molecules, and conductive polymers<sup>1</sup>. Among the different classes of electrochromic materials, conjugated polymers are of continued interest due to reported sub-second switch speeds, offerings of color variety, and high optical contrast<sup>1,2</sup> making them potential candidates for affordable displays, smart windows, eye wear and color controlled textile<sup>1, 2-10</sup>.

Electrochromic devices can be prepared by electrodeposition of the electrochromic polymer onto ITO coated substrates from an electrolyte bath, or by deposition of the processable polymers and then assembled by a “sandwich” method<sup>11-13</sup>. For this purpose, rigorously cleaned dust free, defect free ITO substrates are required. Here a new one-step assembly method (*in situ*) is described where electrochromic polymers are grown inside the solid gel matrix. As a result there is no need of electrolyte bath that can increase the success rate and minimize the amount of chemical waste. Only criteria for this method is that monomer needs to be soluble into the liquid polymer gel electrolyte and after mixing the solution needs to be colorless to minimize the color interference to achieve a good photopic

contrast. Gel electrolyte is a composition of plasticizer, salt, acrylate functionalized low molecular weight poly (ethylene glycol) (PEG) and some photo initiator or thermal initiator. Like sandwich method this liquid polymer gel electrolyte with monomer is placed in between two ITO coated substrates, under proper circumstances like UV light or heat the initiators produces radicals and a radical polymerization of acrylate poly (ethylene glycol) occurs to form a cross-linked solid gel matrix where the monomers are imbedded uniformly. By applying the proper oxidation potential monomers get oxidized and form conductive polymers inside the solid gel matrix close to the working electrode. A schematic diagram is shown in **Figure 3.1**.

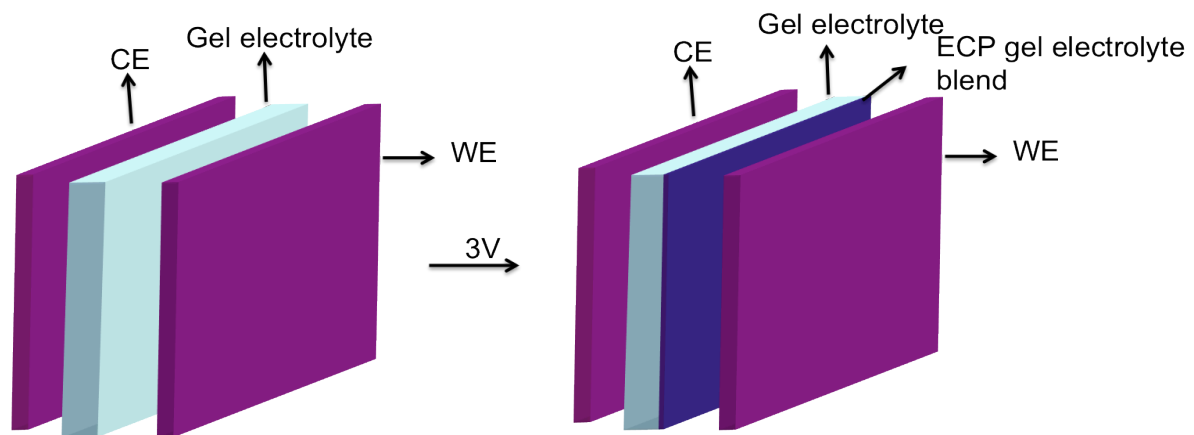


**Figure 3.1** Schematic diagram of an ECD assembled via *in situ* method

Instead of mixing one type of monomer, two or monomers could be added into polymer gel electrolyte solution. As a result a random copolymer will

be formed upon applying suitable monomer oxidation potential. Photopic contrast, optical memory, color uniformity, and switching speed are essential requirements for EC devices. Contrast can be defined as the change in the transmittance between the two extreme redox states of the electrochromic polymer. The transmittance value is related to the charge density and the thickness of the conductive polymer layer.<sup>14</sup> Lim *et al.* have reported that the intensity of the color change for each redox state is both a device characteristic and a material characteristic<sup>15</sup>.

For the *in situ* approach, as the conductive polymers are forming inside the solid matrix the thickness of the electrochromic polymer, concentration of the monomer, distance between two electrodes have to be considered in order to achieve maximum contrast. Also, the concentration of electroactive species will affect the polymerization rate. To see the effect of monomer concentration on rate of the polymerization as well as on the optical behavior, concentration of 2,2-dimethyl-3,4-propylenedioxythiophene was varied. Here, three different thiophene based monomers 3,4-ethylenedioxythiophene (EDOT), 2,2-dimethyl-3,4-propylenedioxythiophene (ProDOT-Me<sub>2</sub>), biphenylmethyloxymethyl ProDOT (BPMOM-ProDOT) were used wherein the highest contrast of 48% was achieved using PBPMOM-ProDOT without background correction. This value is higher than previously reported using the traditional *ex situ* electrodeposition method<sup>10</sup>. According to the Stokes-Einstein equation, the rate of monomer diffusion is temperature dependent.

To evaluate the effect of temperature on the assembled device during electropolymerization, the temperature was varied from 22 °C to 35 °C and the effect of photopic contrast was investigated. Herein, after introducing all the optimized parameters relatively large area, 105cm<sup>2</sup> optical defect free EC devices have been fabricated using the *in situ* method. These devices were fully characterized for switching speed and photopic contrast using absorptiometry and chronocoulometry.

Using different types of monomers into the gel electrolyte random copolymers were formed inside the solid matrix using *in situ* assemble method. By changing the concentration of each monomer with different band gap energy color of the resultant polymer could be achieved.

## **3.2 Experimental**

### **3.2.1 Materials**

Propylene carbonate (PC), poly(ethylene glycol) diacrylate ( $M_n = 700$ ) (PEG-DA), Lithium trifluoromethanesulfonate (LITRIF), 2,2-dimethoxy-2-phenyl-acetophenone (DMPAP) were purchased from Sigma Aldrich and used as received. ITO

coated glass (resistance 8-12 Ohm/sq) and polyethylene terephthalate (PET) were purchased from Delta Tech Inc and Bay View Inc, respectively.

Norland UV curable glue, UVS-91 was purchased from Products Inc. ProDOT-Me<sub>2</sub> and BPMOM-ProDOT were synthesized according to

reported procedures<sup>16-18</sup>. EDOT was purchased from Heraeus Clevios GmbH and vacuum distilled before use.

### **3.2.2 Instrumentation**

The electrochemical study was carried out using CHI 720c and 400a potentiostats. A Varian Cary 5000i UV-Vis-NIR was used for all optics studies. A UVP CL-1000 was used for UV curing.

### **3.2.3 Electrochromic Device Fabrication**

The electrolyte solution was prepared according to reported procedure<sup>19,20</sup>. Different weight percentages of various monomers were added to the electrolyte gel as specified in the result and discussion section. The gel electrolyte (with monomer) was then drop cast between two ITO coated substrates. Using copper tape and a rubber gasket controlled the thickness of the gel. The EC device was cured by UV irradiation at 365nm (5.8mW/cm<sup>2</sup>) for 5 minutes to provide a solid matrix, and UV curable glue was used to seal the device. 4 cm<sup>2</sup> active area EC devices were used to optimize each parameter. Once optimized, devices with 105 cm<sup>2</sup> active area were made to demonstrate that these features could be translated to goggle-sized devices for a real-world application. To reduce the iris effect for large area devices, adhesive Cu tape was used around the entire perimeter of both ITO substrates. 3V potential bias was used to oxidise the

monomers and  $\pm 2$  V potential was used to switch the ECDs from one state to other state.

**a)**



**b)**



**Figure 3.2** Left neutral state and right oxidized state for a) PEDOT and b) PPr0DOT-Me<sub>2</sub> an electrochromic window using the *in situ* procedure

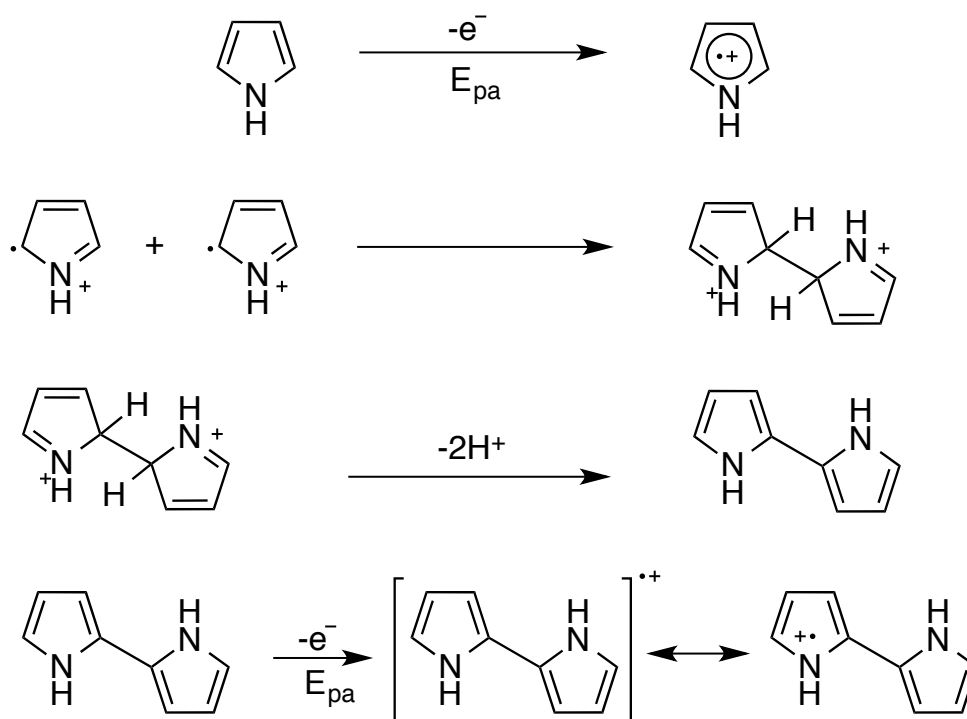
### 3.3 Results and Discussion

For the formation of conductive polymer inside the electrochemical cell, an external potential needs to be applied to overcome the energy barrier. This energy barrier depends on the electronic structure of the monomer unit. Like, EDOT has a band gap about 1.7 eV. By putting electron rich and electron deficient substituent on monomer unit the energy gap can be changed. Once the suitable potential is applied, monomers get oxidized by losing an electron.

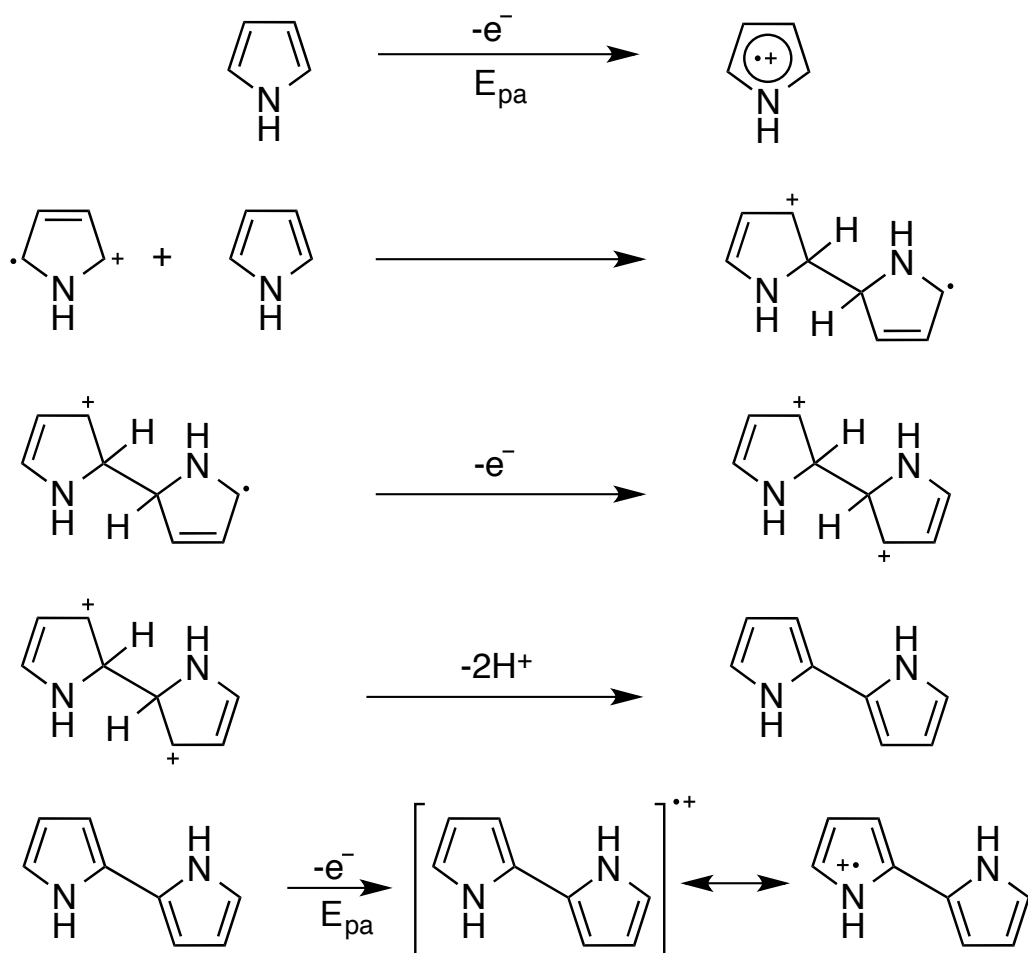
This has been well established for conventional electrochemical polymerization from oxidation of monomer in the bulk solution onto various electrodes. It has already established that two electrons are needed per monomer unit during electropolymerization<sup>21</sup>, though the mechanism is not well established. According to Diaz mechanism<sup>21</sup>, monomers get oxidized and form radical-cation upon application of a proper potential. Two radical-cations get coupled and it regains the aromaticity by losing two protons. Again a dimer gets oxidized and forms a radical-cation, which coupled with other radical cation and the form a stable trimer by losing two protons. Propagation takes place by losing electrons from a neutral oligomer that couples with another radical-cation and regains its aromaticity by losing protons. But dimer formation could be harder because two likely charged species come close proximity to couple. According to the alternate proposed mechanism by Pletcher<sup>22</sup>, neutral monomer/oligomer forms radical-cation by losing an electron upon application of proper potential,



this radical cation attacks another neutral monomer and gain aromaticity by losing two protons. But it has been already shown that rate of electron diffusion is much faster than monomer diffusion<sup>21</sup>. So, it could be possible that initially small oligomers are formed by attacking the radical-cation to a neutral monomer, once the chain is long enough to separate the likely charges, it follows Diaz mechanism. **Scheme 3.1** and **scheme 3.2** shows the stepwise formation of polypyrrole following Diaz and Pletcher mechanism.



**Scheme 3.1** Formation of Polypyrrole following Diaz mechanism



**Scheme 3.2** Formation of Polypyrrole following Pletcher mechanism

After formation of the EC polymers onto or close to the working electrode, electron exchange takes place between EC polymer and electrode by subjecting proper amount of switching potential. As a result two or more distinct color state appears. The general pathway of formation of EC polymer is shown in **Figure 3.3**.

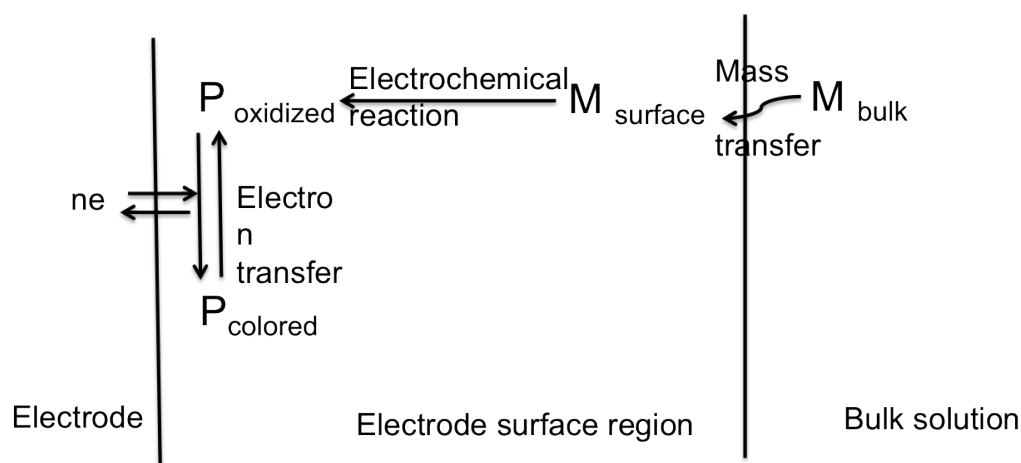


**Figure 3.3** Representation of a general electrochemical reaction pathway of EC polymer.

### 3.3.1 Photopic contrast as a function of polymer layer thickness

Generally, the film thickness for a conjugated polymer prepared by electrochemical polymerization is directly proportional to the charge density that passes during electrochemical polymerization.<sup>17</sup> The transmittance of an anodically coloring electrochromic polymer in both the bleached and colored states corresponding to the oxidized and neutral states, respectively, is proportional to thickness in accordance to Beer's law. As conjugated electrochromic polymers are growing inside the solid gel matrix for *in situ* method, it is hard to calculate the accurate thickness of the electrochromic layer. An effective polymer layer thickness can be calculated using total amount of charge consumption during

polymerization. This charge consumption can be calculated from chronocoulometry.

Effective thickness of electrochromic layer and % of conversion

$$e = Q / (6.023 \times 10^{23}) \times (1.6 \times 10^{-19})$$

where  $e$  = # of electrons involved

$Q$  is the charge consumed

$$\text{\# of monomers reacted} = \frac{1}{2} \times e$$

Effective electrochromic polymer layer thickness =

$$\frac{(\text{\# of monomers reacted} \times \text{molar mass} \times \text{density})}{(\text{active area})}$$

$$\% \text{ of conversion} = \frac{(\text{\# of monomers reacted}) \times 100\%}{(\text{number of monomer loaded})}$$

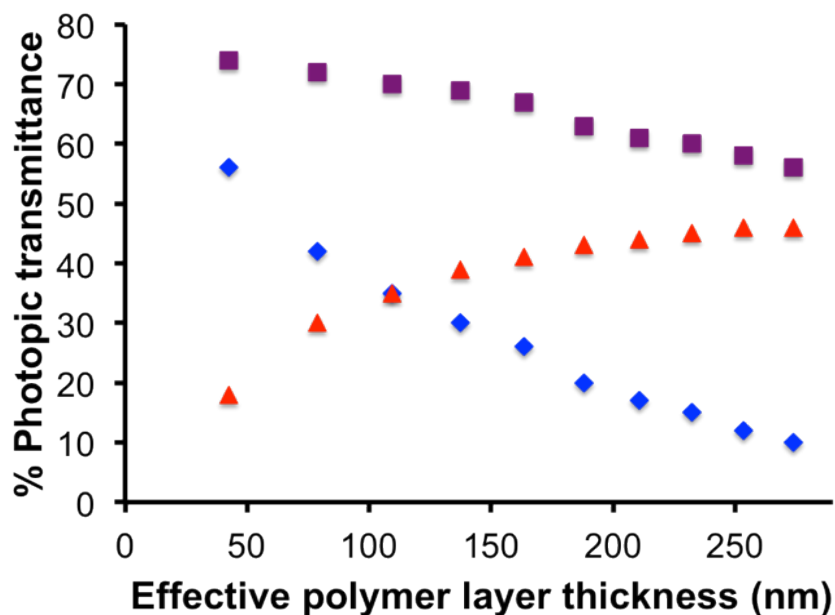


**Figure 3.4** Photopic transmittance of PProDOT-Me<sub>2</sub> for neutral state (shows in blue diamond), oxidized state (shows in dark purple square) and respective contrast (shows in red triangle) as a function of for 2.5 wt% of ProDOT-Me<sub>2</sub> monomer loaded ECD using *in-situ* method.

The photopic transmittance (%T<sub>photopic</sub>) of bleached and colored states of an electrochromic device as a function of the effective electrochromic layer thickness wherein the conjugated polymer is PProDOT-Me<sub>2</sub> prepared from a gel electrolyte containing 2.5 wt% ProDOT-Me<sub>2</sub> is shown in **Figure 3.4**. The %T<sub>photopic</sub> of the colored and bleached states decrease upon increasing effective PProDOT-Me<sub>2</sub> thickness, corresponding photopic contrast initially increased and reached a saturated value at 46% at *ca.* 200 nm. Same trend was observed for the other two electrochromic polymers, PEDOT and PBPMOM-ProDOT and is shown in **Figure 3.5** and **3.6**.

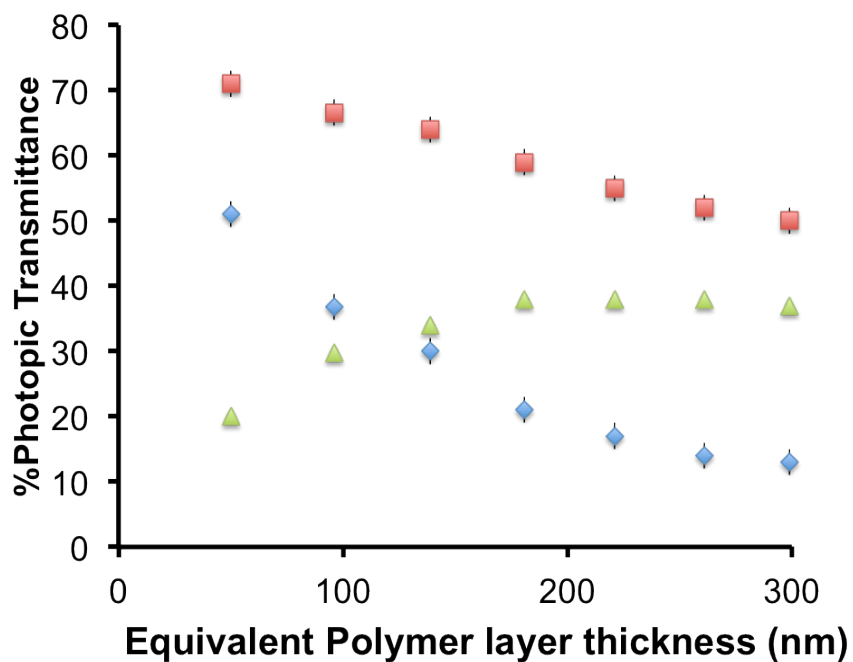


**Figure 3.5** Photopic transmittance of PEDOT for neutral state (shows in sky blue diamond), oxidized state (shows in red square) and respective contrast (shows in green triangle) as a function of effective EC polymer layer thickness for 2.5 wt% of EDOT monomer loaded ECD using *in-situ* method.

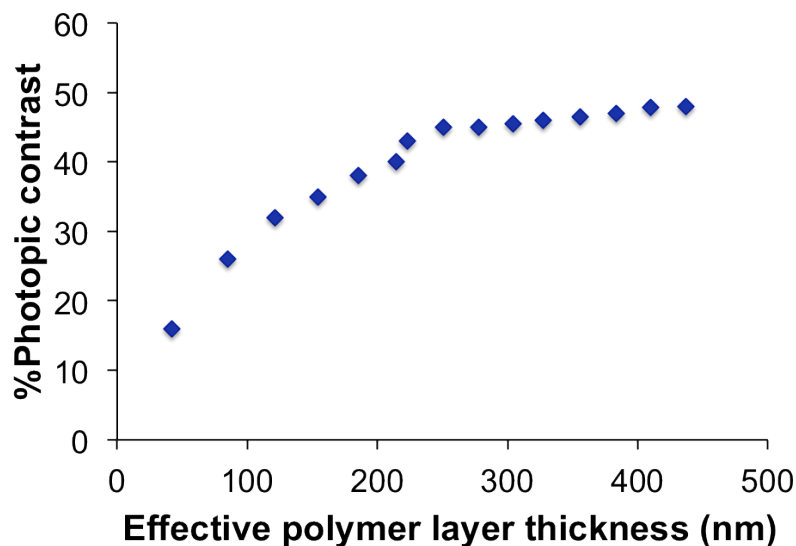


**Figure 3.6** Photopic contrast (shows in blue diamond) as a function of effective EC polymer layer thickness for 2.5 wt% of PBPMOM-ProDOT monomer loaded ECD using *in-situ* method.

### 3.3.2 Photopic contrast as a function of Monomer loading

We have seen that the rate of electrochemical reaction depends on the concentration of electroactive species (in **Figure 1.5**). To see the effect of monomer concentration on the optical performance of the devices, initial concentration of ProDOT-Me<sub>2</sub> was varied from 1 wt% to 5 wt%. Photopic contrast of EC devices at different concentration were measured as a function of polymerization time and the results are shown in **Figure 3.7**.

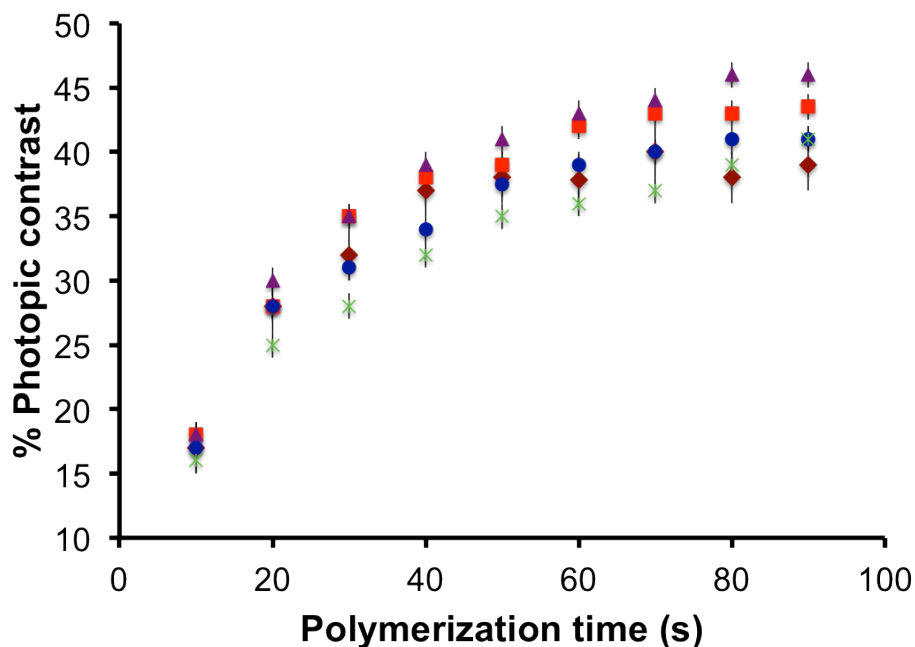


**Figure 3.7** Plot of Photopic contrast as a function of polymerization time for 1, 2, 2.5, 3 and 5 wt% ProDOT-Me<sub>2</sub> in gel electrolyte using the *in-situ* method (represented by purple square, red circle, blue triangle, green star and dark red diamond respectively)

For each system same trend was noticed. By increasing the polymerization time photopic contrast increased as more ECP are forming and reached a saturated value. The maximum photopic contrast was achieved for 2.5 wt% ProDOT-Me<sub>2</sub> system. The maximum achievable photopic contrast and the time required achieving that particular contrast is reported in **Table 3.1**. By increasing the monomer concentration from 2.5 wt% to 5 wt% the maximum photopic contrast value decreased from 46 %T to 39%T.

At shorter conversion time like for 30s all of them has pretty close contrast value. By increasing the polymerization time the bleached state loses



transmittance possibly due to formation of more oligomers. Devices with a higher concentration of ProDOT-Me<sub>2</sub> were found to reach maximum contrast faster than those with lower concentration. Effective thickness of the ECP layer for maximum achievable photopic contrast was calculated and it has been found that the thickness for all systems (1, 2, 2.5, 3 and 5 wt% ProDOT-Me<sub>2</sub>) were around 200 to 250 nm. Although the time required achieving those value is different. Corresponding polymerization time is 110s, 100s, 80s, 70s, 70s, and 60s respectively. And % of conversion of monomers for each system were calculated and the values are about 1.05%, 0.73%, 0.36%, 0.38%, 0.38% and 0.31 respectively.

**Table 3.1** Relation between polymerization time required to achieve the saturated photopic contrast and corresponding percentage of conversion for different concentration of ProDOT-Me<sub>2</sub> inside the ECDs

Initial [monomer]		Maximum photopic contrast	Polymerization time (s)	% of conversion
1wt%	0.054 (M)	42	110	1.05
2wt%	0.108 (M)	43	100	0.73
2.5wt%	0.135 (M)	<b>46</b>	80	0.36
3wt%	0.163 (M)	44	70	0.38
4wt%	0.216 (M)	40	70	0.38
5wt%	0.272 (M)	39	60	0.31

According to the electropolymerization mechanism, the rate of the ECP formation is second order with respect to monomer concentration, the rate of polymerization suppose to be increased 25 times by increasing the concentration from 1wt% to 5 wt%. But in practice, polymerization time decreased only  $P_{t5}/P_{t1} = 60 / 110 = 0.55$  times

#s of monomer reacted:  $m_5/m_1 = (6.87E-07)/(3.7 E-07) = 1.86$

That means there is some other factor affecting the reaction rate. In **Figure 1.5**, it has been mentioned that the rate of reaction depends on the mode of transportation. To have a spontaneous reaction, monomers need to be diffused from bulk to the close proximity of working electrode as shown in **Figure 3.3**. In literature, it has reported that once the electroactive species started to undergo electrochemical reaction, concentration at the electrode surface becomes smaller than the bulk. For system where no stirring of the electrolyte solution involve, the concentration of the electroactive species decreases gradually by increasing the distance from electrode over time as shown in **Figure 3.8**. For our solid-state devices, monomers need to diffuse toward the working electrode from solid gel matrix. As a result the rate of polymerization depends on the diffusion coefficient of the monomers. Diffusion coefficient of ProDOT-Me<sub>2</sub> was calculated at different concentration inside the solid gel electrolyte and reported in **Figure 3.9**.

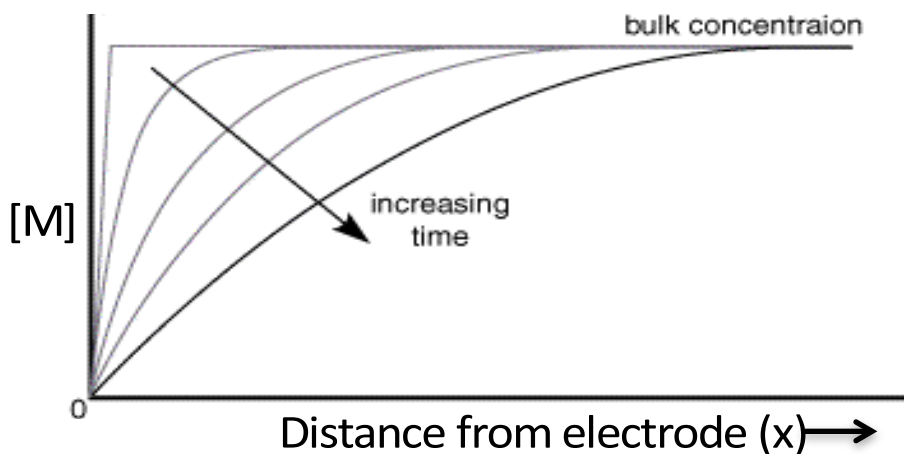


**Figure 3.8** Concentration profile electroactive species at different time

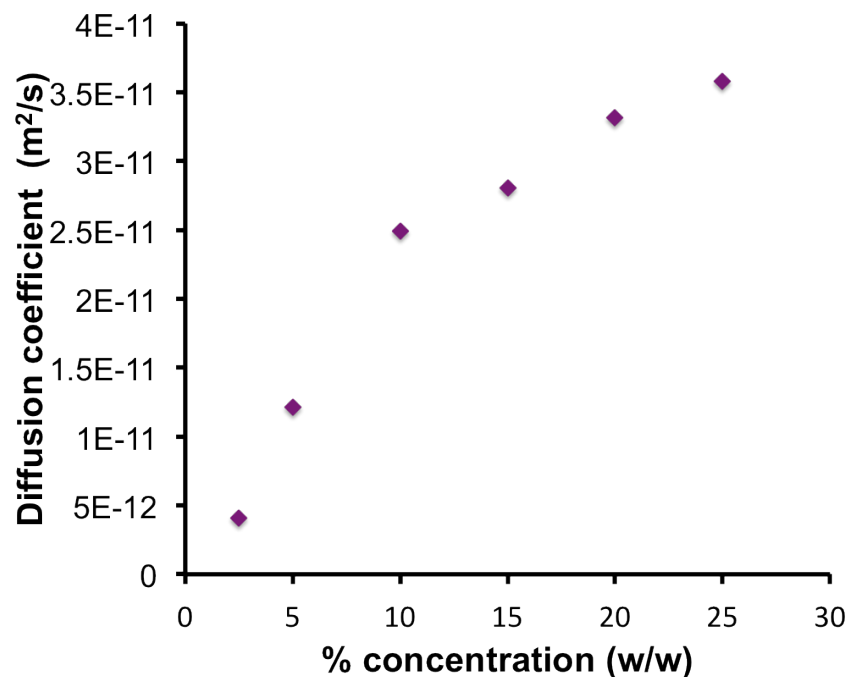


**Figure 3.9** Diffusion coefficient of ProDOT-Me<sub>2</sub> at different concentration (w/w) inside the gel matrix

By changing the concentration of monomers the rate of diffusion of the electroactive species towards the working electrode will be different and different amount of charge will consume during polymerization. This results different transmittance value of each redox state. As a result the contrast of the device is different. Maximum achievable photopic contrast for higher monomer loaded ECD, 5 wt% is smaller than 2.5 wt% ProDOT-Me<sub>2</sub> loaded ECD. It could be because of slow diffusion rate of 5 wt% system leads to more bleached state as they have almost same transmittance value at their

colored state.  $\%T_{\text{bleached}}$  of both 2.5 wt% and 5 wt% ProDOT-Me<sub>2</sub> loaded ECD are shown in **Figure 3.10**. This slow diffusion could affect the packing of EC polymer composite inside the solid gel matrix, that enhanced interchain distance possibly results transmissivity. This high diffusion coefficient could also control the length of conjugation. Formation of more oligomers could be a possible reason for lower photopic contrast.

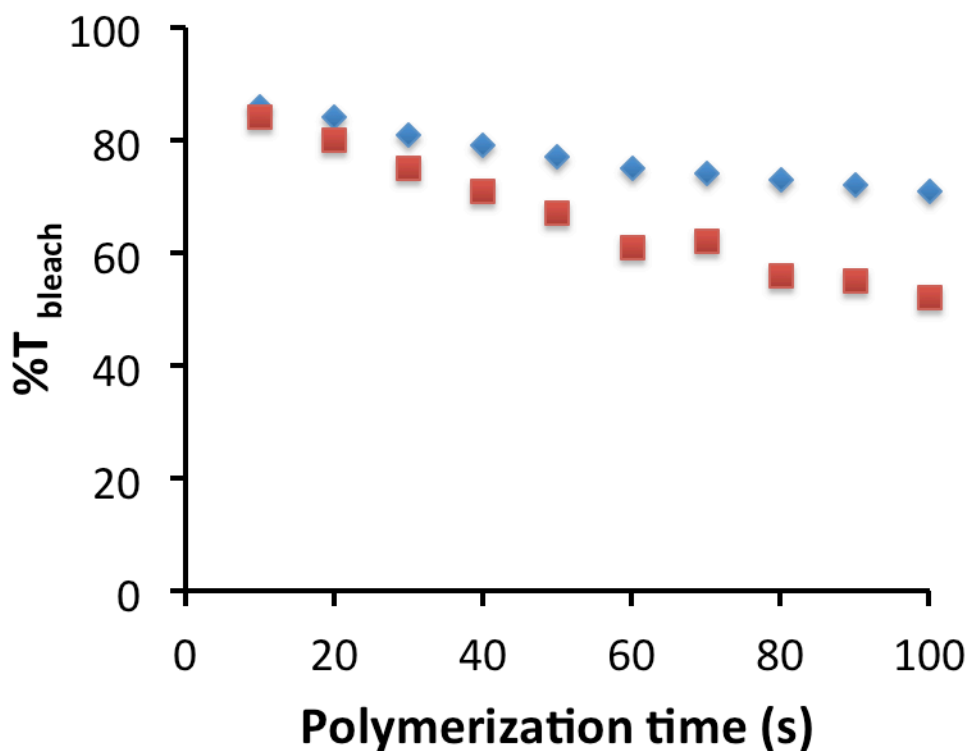


**Figure 3.10**  $\%T_{\text{bleached}}$  as a function of polymerization time of both 2.5 wt% and 5 wt% ProDOT-Me<sub>2</sub> loaded ECD assembled via *in situ* method

As mentioned above that the % of conversion is very low for *in situ* method, like only 0.36% monomer was converted to polymer after 80 s for 2.5 wt% ProDOT-Me<sub>2</sub> monomer concentration. The question arises is it possible to increase the % of conversion by increasing the polymerization time. Applying 3V potential for longer period, initially more monomer will get polymerized and will produce a thicker layer. By increasing the polymer layer thickness more potential needed to be applied according to Ohm's law, as  $V=IR$ . As ITO coated substrates are used as electrode material, it could not be possible to apply higher potential, >3V; otherwise ITO will start to degrade.

### 3.3.3 Photopic contrast as a function of various monomer

To study the effect of different monomers on photopic contrast 0.07 M EDOT, ProDOT-Me<sub>2</sub> and BPMOM-ProDOT loaded devices were prepared and % photopic contrast is plotted as a function of polymerization time in **Figure 3.11**. It can be seen that for each system photopic contrast achieve a saturated value but the only difference is the polymerization time needed to achieve saturation and the maximum achievable photopic contrast.

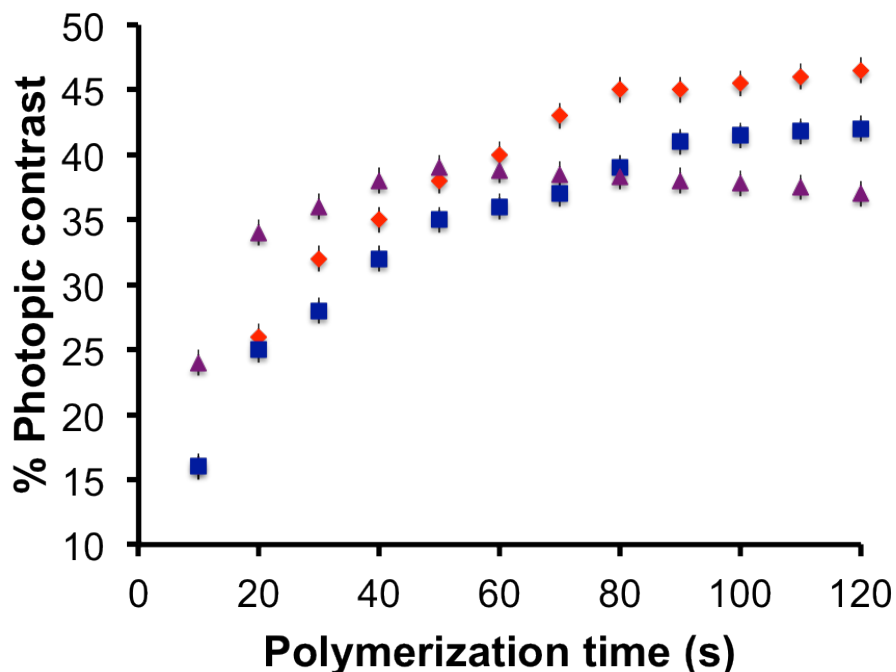


**Figure 3.11** Photopic contrast as a function of polymerization time for PBPMOM-ProDOT using *in-situ* method (top), Photopic contrast of PEDOT (shows in dark purple triangle), PProDOT-Me<sub>2</sub> (shows in blue square) and PBPMOM-ProDOT (shows in red diamond) as a function of polymerization time for 0.07 mM concentrated monomer in gel electrolyte using *in-situ* method (bottom)

Polymerization time to achieve the maximum photopic contrast is dependent upon the monomer diffusion rate in solid electrolyte gel. Diffusion coefficients of EDOT, ProDOT-Me<sub>2</sub> and BPMOM-ProDOT within this specific gel matrix at 0.07M loadings are reported to be  $8.6 \times 10^{-11} \text{ m}^2/\text{s}$ ,  $1.11 \times 10^{-12} \text{ m}^2/\text{s}$  and  $3.89 \times 10^{-13} \text{ m}^2/\text{s}$  respectively. Because of the size of monomers, diffusion coefficients would fit the order that  $D_{\text{EDOT}} > D_{\text{ProDOT-Me}_2}$

>  $D_{\text{BPMOM-ProDOT}}$ . Therefore, the polymerization of EDOT to produce an effective polymer film thickness at photopic saturation is expected to happen on a shorter time scale than that of ProDOT-Me<sub>2</sub> and BPMOM-ProDOT. Like, at 20s polymerization time, % of conversion is highest for PEDOT and produces highest photopic contrast. Among these three polymers, maximum photopic contrast was obtained for PBPMOM-ProDOT due to the high photopic transmissivity of the clear state. %  $\Delta T_{\text{photopic}}$  for PBPMOM-ProDOT is 46% which is 8% and 4% higher than that of PEDOT and PProDOT-Me<sub>2</sub>, respectively while their color state has close value as shown in **Table 3.2**.

**Table 3.2** Represents the photopic transmittance value at different redox state at maximum achievable photopic contrast

EC polymer	%T <sub>photopic, b</sub>	%T <sub>photopic, c</sub>	Max. $\Delta T_{\text{Photopic}}$
PEDOT	55%	17%	38%
PProDOT-Me <sub>2</sub>	58%	16%	42%
PBPOMProDOT	62%	16%	46%



The general enhancement of bleached state transmissivity has been explained by Reynolds, et al.<sup>23</sup> in earlier reports and is related to an increase in distance between conjugated polymer chains which translates to a reduced absorbance in the near infrared. A lower absorbance in the near infrared means a lower absorption tail for this transition in the visible region translating to a higher bleach state transmissivity. It could be possible that for *in situ* devices due to bulkier substituent and slower diffusion of monomer the interchain distance between ECPs increased and affect the transmissivity of the bleached state.

#### **3.3.4 Photopic contrast as a function of gel electrolyte thickness**

To study the effect of solid gel electrolyte layer thickness with respect to photopic contrast of electrochromic devices, several devices were made having thicknesses ranging from 0.34 mm to 2.54 mm. According to the data listed in **Table 3.3** for a constant monomer concentration of 2.5 wt% ProDOT-Me<sub>2</sub>, it is apparent that thicker gel electrolyte consumed less charge comparison to the thinner gel electrolyte for a certain conversion time by increasing the distance between two electrodes. As a result thinner effective conductive polymer layer formed which results lower photopic contrast. By increasing the polymerization time, more monomer will be converted and desired effective polymer layer thickness can be achieved to get the maximum photopic contrast. Like the EC device with 2.54mm has

about 10% lower photopic contrast than the maximum achievable contrast but by increasing the conversion time.

**Table 3.3** Effect of gel electrolyte thickness on photopic contrast of PProDOT-Me<sub>2</sub> using *in situ* method

Thickness of the gel electrolyte (mm)	Charge consumed (C/cm <sup>2</sup> )	PProDOT-Me <sub>2</sub> thickness (nm)	% Photopic contrast
0.34	$1.83 \times 10^{-2}$	$175 \pm 5$	$45.5 \pm 1 \%$
0.54	$1.50 \times 10^{-2}$	$140 \pm 5$	$39.5 \pm 1 \%$
1.19	$1.41 \times 10^{-2}$	$135 \pm 5$	$37 \pm 1 \%$
2.54	$8.60 \times 10^{-1}$	$132 \pm 5$	$34.5 \pm 1 \%$

### 3.3.5 Effect of different techniques during polymerization on photopic contrast

Different pulse techniques were used to grow electrochromic polymers inside the gel electrolyte matrix to check the effect on the contrast. A gel electrolyte with 1 wt% EDOT was prepared and several EC devices were built using *in situ* approach and polymerize them for 60 s using different techniques like: chronocoulometry, chronoamperometry, normal pulse

voltammetry and different pulse voltammetry. Photopic contrast for each devices were measured and is reported in **Table 3.4**. The photopic contrasts were in  $(49 \pm 2)\%$  with background correction.

**Table 3.4** Photopic contrast (with background correction) of PEDOT devices assembled via *in situ* approach and polymerized for 60s

Techniques	Photopic Contrast
Chronocoulometry	51%
Chronoamperometry	47%
Normal Pulse Voltammetry	48%
Differential Pulse voltammetry	49%

### 3.3.6 Effect of temperature during polymerization

The photopic contrast holding the concentration of ProDOT-Me<sub>2</sub> constant at 2.5 wt% and the gel electrolyte layer thickness constant at 0.55 mm, and the photopic contrast data for electrochromic polymers prepared from ProDOT-Me<sub>2</sub> for a polymerization time of 20 seconds at 22°C, 25°C, 28°C, 30°C and 35°C is listed in **Table 3.5**. Temperature beyond 35°C could not be used due to the degradation of ITO as shown in **Figure 3.9**. Photopic

contrast data was obtained for these devices at room temperature, approximately 25°C, high contrast devices were obtained upon raising the temperature of the gel during device preparation since the diffusion rate of the monomer as well as the rate of polymerization increased. Thereby allowing for thicker conductive polymer layer formation for the same polymerization time. Temperature experiments were also done to activate devices using longer conversion times, yet the maximum contrast achieved remained to be 46% for PProDOT-Me<sub>2</sub>. Temperature serves as only an optimization in the time it would take to make a device of a given contrast, not as a means to increase the contrast value beyond that obtained by changing the other variables studied here.

**Table 3.5** Temperature study for *in-situ* EC device electrochromic polymer preparation using 2.5 wt% ProDOT-Me<sub>2</sub> in gel-electrolyte at a constant polymerization time of 20s.

<b>T°C</b>	<b>Bleached (%T)</b>	<b>Colored (%T)</b>	<b>Photopic contrast (ΔT)</b>
22	73	44	29
25	73	37	36
28	69	32	37
30	67	28	39
35	67	27	40

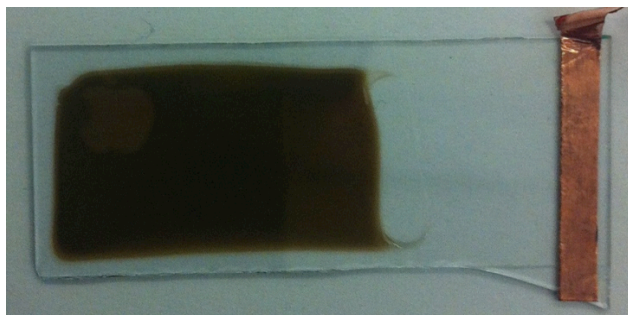


**Figure 3.12** Picture of ruined ITO at 35°C for 30 min after disassembling the ECD

### 3.3.7 Switching speed of the *in situ* EC devices

Transitioning or switching an electrochromic device from the bleached to colored state or vice versa is an electrochemical process involving electron transfer between the electrochromic polymer and the electrode coupled with the diffusion of charge compensating ions. Of special regard considering that the electrochromic polymer is a conjugated one, in one state the conjugated polymer is electrically conductive, whereas in the alternate state, it is an electrical insulator. Generally, reported switching speed is the time required for 95% of the transmittance change to take place at  $\lambda_{\max}$  from one state to the other<sup>24,25</sup>. To determine the switching speed, %T was monitored during application of a square wave potential.

Devices were subjected to +2 to -2V and the transmittance value recorded at the  $\lambda_{\text{max}}$  by a spectrophotometer.

The time required to switch the thicker PProDOT-Me<sub>2</sub> film (>160 nm) was higher than thinner films, 1.8 s to obtain the colored state ( $26 \pm 1$ )%T to ( $67 \pm 1$ )%T while bleaching takes 3.5s. Thinner films (<100 nm) switch faster with times of 1.5 s from ( $35 \pm 1$ )% T to ( $70 \pm 1$ )% T for the same EC devices. Table 3 shows the switching speeds for maximum achievable photopic contrast of different electrochromic polymers using *in situ* method. For three different EC systems the switching speed for bleaching is different while the coloring speed is almost same, 1.8s to achieve the maximum contrast. For bleaching process PEDOT can switch faster than PProDOT-Me<sub>2</sub> and PBPOMProDOT. As the polymer structures are more compact in neutral state compare to oxidised state more time required for bleaching to undergo the conformational relaxation than coloring process<sup>25,26</sup>. The switching speed also changes with the viscosity of the system. For more viscous ionic liquid system the switching speed is 4.2s for PEDOT bleaching whereas it takes only 1.8s to fully bleach for LITRIF system.

**Table 3.6** Redox switching speeds for maximum achievable photopic contrast EC devices using *in situ* method

<b>EC polymer</b>	<b>%T<sub>photopic, b</sub></b>	<b>%T<sub>photopic, c</sub></b>	<b>Coloring(s)</b>	<b>Bleaching(s)</b>
PEDOT	55%	16%	1.8	1.8
PProDOT-Me <sub>2</sub>	58%	12%	1.8	3.5
PBPOMProDOT	60%	12%	1.8	3.2

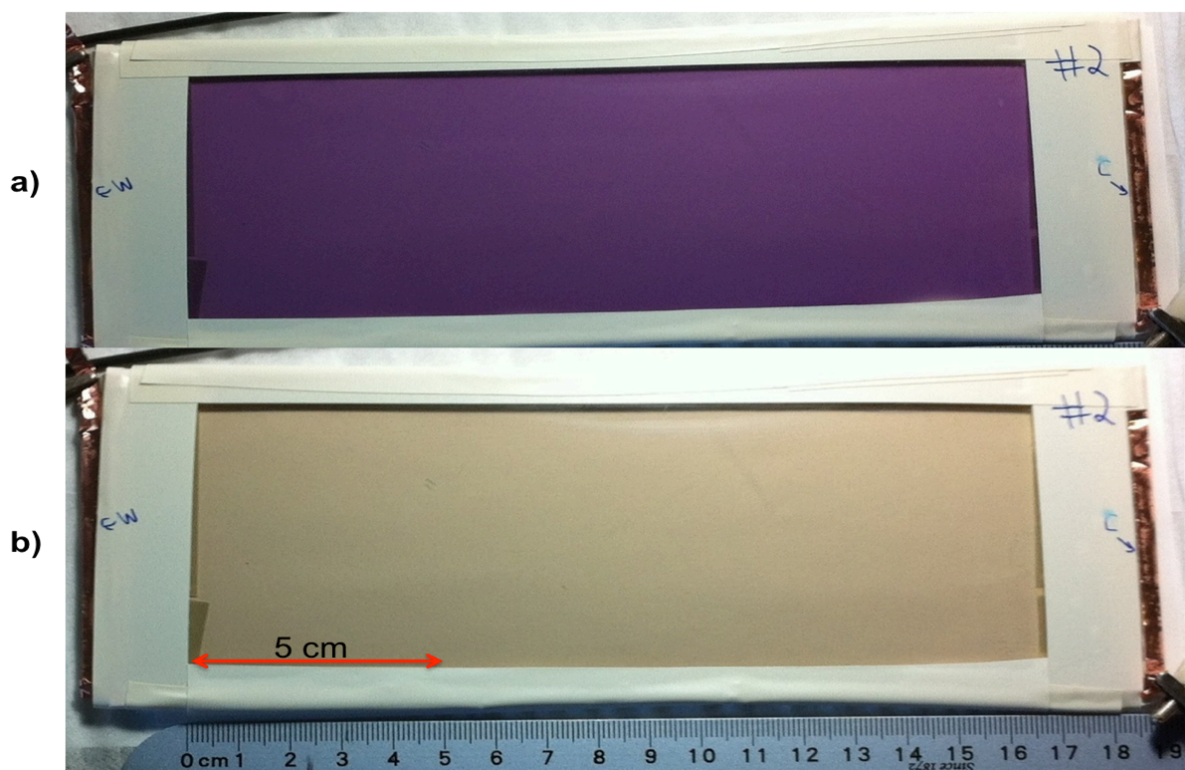


**Figure 3.13** a) Colored state and b) Bleached state for an electrochromic window of  $105\text{cm}^2$  active area using the *in situ* procedure having 2.5 wt% PrODOT-Me<sub>2</sub> in the electrolyte gel

### 3.3.6 Tuning color by formation of copolymer in one step assemble method

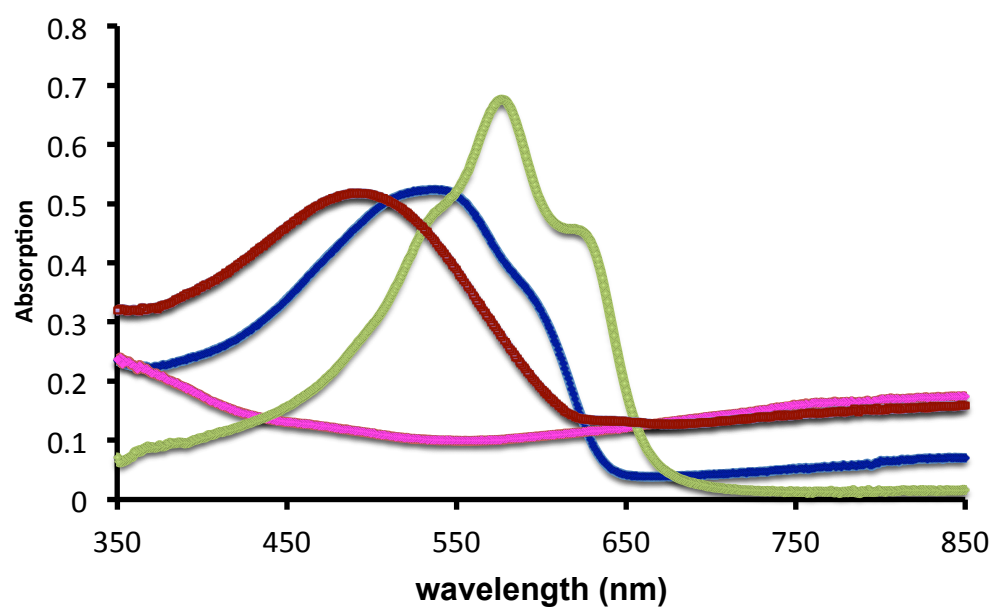
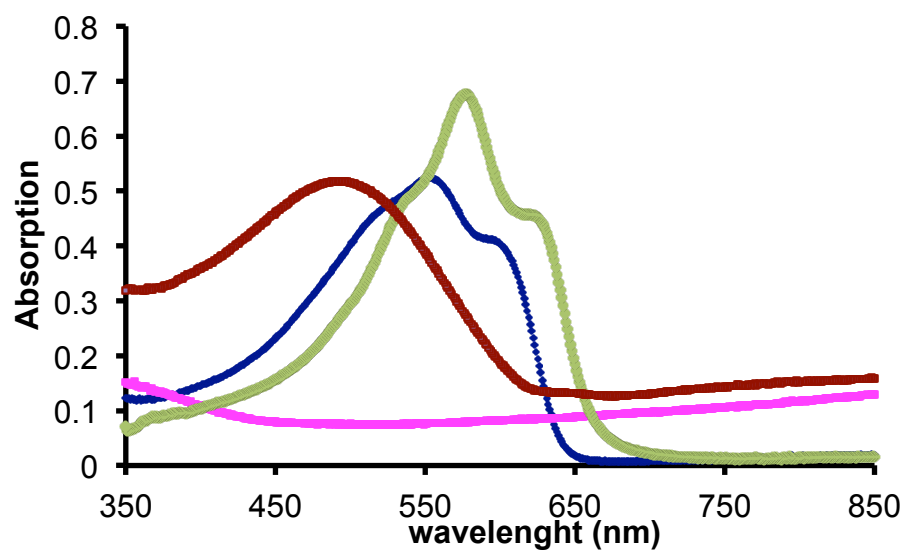
In general color can be tuned by forming copolymer. By changing the monomer ratio inside the random copolymer  $\lambda_{\text{max}}$  shifted and desired color could be achieved. Copolymers can be formed in one-step by mixing two co-monomers into the polymer gel electrolyte. Color could be tuned by changing the fed ratio of two co-monomers. Different monomer has



different diffusion coefficient and by changing the concentration of monomer the rate of diffusion will be different. During electropolymerization the composition of each monomer unit inside the copolymer depends on diffusion coefficient of each monomer. Different repeating units leads to modulation of different band gap energy that corresponds to different electronic properties. This change in band gap energy provides different optical properties. By mixing ProDOT-Me<sub>2</sub> with ProDOT-IP<sub>2</sub> in different ratio copolymers will formed. Homopolymer of ProDOT-Me<sub>2</sub> and ProDOT-IP<sub>2</sub> have  $\lambda_{\text{max}}$  around 570 nm and 505 nm respectively. But by changing the fed ratio of ProDOT-Me<sub>2</sub> and ProDOT-IP<sub>2</sub> color of copolymer can be tuned.

**Figure 3.11** shows the absorption spectra for copolymers formed via *in situ* method for (i) 40 : 60, (ii) 25 : 75 and (iii) 10 : 90 weight ratio of ProDOT-Me<sub>2</sub> and ProDOT-IP<sub>2</sub>. Here it is noticed that by decreasing the amount of ProDOT-Me<sub>2</sub> into total 2.5 wt% of monomer concentration,  $\lambda_{\text{max}}$  shifted towards high-energy region. Optical contrasts of the assembled devices were optimized following abovementioned characterization methods. Using this method, complicated synthesis process could be avoided to tune color.

**Figure 3.12** shows the picture of three assembled ECDs and the photopic contrast for corresponding ECDs are 45%T, 38%T and 31%T respectively. Same experiment has carried out using ProDOT-Me<sub>2</sub> and ProDOT-*t*-Bu<sub>2</sub>. And full subtractive color spectrum was achieved by changing the monomer fed ratio and corresponding absorption spectra is giving in chapter 6.



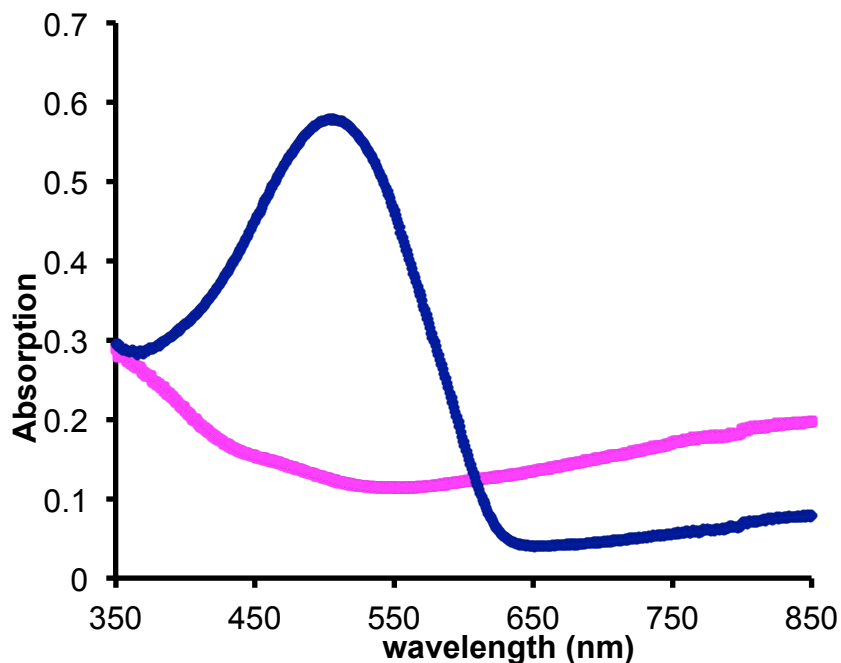


**Figure 3.14** Absorption spectra for three different copolymers assembled via *in situ* method with ProDOT-Me<sub>2</sub> to ProDOT-IP<sub>2</sub> ratio (i) 40 : 60, (top) (ii) 25 : 75 (middle) and (iii) 10 : 90 (bottom) weight ratio respectively. Here dark red, green and blue represent the neutral color of PProDOT-Me<sub>2</sub>, PProDOT-IP<sub>2</sub> and corresponding copolymer respectively. Pink color represents the clear state for copolymer.

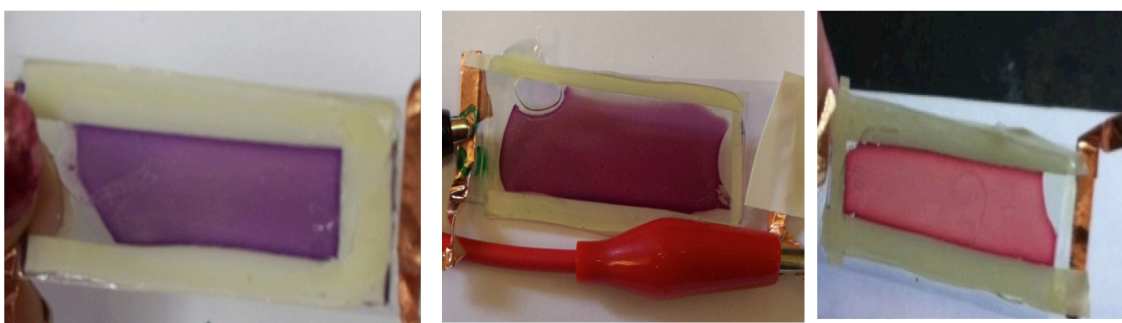


**Figure 3.15** Assembled ECD with monomer fed ratio ProDOT-Me<sub>2</sub> to ProDOT-IP<sub>2</sub> ratio 40 : 60, 25 : 75 and 10 : 90 weight ratio respectively (from left to right)

### 3.4 Conclusions

As electrochromic polymer is formed inside the solid gel matrix in case of *in situ* approach, both material and device characteristics have impact on optical property of the electrochromic devices. Some important factors such as thickness of the electrochromic polymer, polymerization time, diffusion coefficient of the electroactive species, thickness of the gel electrolyte and effect of temperature during polymerization are studied and established a relationship with photopic contrast. By optimizing the above-mentioned parameters large defect free electrochromic window of 105 nm<sup>2</sup> active area were successfully made using one step *in situ* approach. Color tuning could be possible by formation of random copolymer using *in situ* method. This method could reduce cost and waste as well as be adapted for large area devices.

## References

- (1) Argun, A. A.; Aubert, P. H.; Thompson, B. C.; Schwendeman, I.; Gaupp, C. L.; Hwang, J.; Pinto, N. J.; Tanner, D. B.; MacDiarmid, A. G.; Reyanols, J. R. *Chem. Mater.* **2004**, *16*, 4401.
- (2) Beaujuge, P. M.; Reynolds, J. R. *Chem Rev* **2010**, *110*, 268.
- (3) Hamedi, M.; Forchheimer, R.; Inganas, O. *Nat Mater* **2007**, *6*, 357.
- (4) Sonmez, G.; Shen, C. K.; Rubin, Y.; Wudl, F. *Angew Chem Int Ed Engl* **2004**, *43*, 1498.
- (5) Liu, R.; Duay, J.; Lee, S. B. *ACS Nano* **2010**, *4*, 4299.
- (6) Tehrani, P.; Hennerdal, L. O.; Dyer, A. L.; Reynolds, J. R.; Berggren, M. *Journal of Materials Chemistry*. **2009**, *19*, 1799.
- (7) Carpi, F.; Derossi, D. *Optics & Laser Technology* **2006**, *38*, 292.
- (8) Zhang, F.; Johansson, M.; Andersson, M. R.; Hummelen, J. C.; Inganäs, O. *Adv Mater* **2002**, *14*, 662.
- (9) Invernale, M. A.; Ding, Y.; Sotzing, G. A. *ACS Appl. Mater. Interfaces*. **2010**, *2*, 296.
- (10) Ding, Y.; Invernale, M. A.; Mamangun, D. M. D.; Kumar, A.; Sotzing, G., A. *J. Mater. Chem.* **2011**, *21*, 11873.
- (11) Verge, P.; Mallouki, M.; Beouch, L.; Aubert, P. H.; Vidal, F.; Tran-Van, F.; Teyssiach, D.; Chevrot, C. *Mol. Cryst. Liq. Cryst* **2010**, 522.
- (12) Alexander, S. S.; Laurent, G.; Frédéric, V.; Elena, I. L.; Franck, M. I., A. M. ; Claude, C.; Dominique, T.; Irina, L. O. Y., S. V. *J. Polym. Sci., Part A: Polym. Chem* **2009**, 47.
- (13) Verge, P.; Beouch, L.; Aubert, P. H.; Vidal, F.; Tran-Van, F.; Teyssiach, D. C., C. *Adv. Sci. Technol.* **2008**, *55*, 18.
- (14) Padilla, J.; Seshadri, V.; Filloramo, J.; Mino, W.; Mishra, S.; Radmard, B.; Kumar, A.; Sotzing, G. A.; Otero, T. *Syn Metals*. **2007**, 157, 261.
- (15) Lim, J. Y.; Ko, H. C.; Lee, H. *Syn Metals*. **2005**, *155*, 595.

- (16) Krishnamoorthy, K.; Ambade, A. V.; Kanunga, M.; Contractor, A. Q.; Kumar, A. *J. Mater. Chem.* **2001**, *11*, 2909.
- (17) Mishra, S. P.; Sahoo, R.; Ambade, A. V.; Contractor, A. Q.; Kumar, A. *J. Mater. Chem.* **1998**, *10*, 896.
- (18) Mishra, S. P.; Krishnamoorthy, K.; Sahoo, R.; Kumar, A. *J. Polym. Sci., Part A: Polym. Chem* **2005**, *43*, 419.
- (19) Invernale, M. A.; Ding, Y.; Mamangun, D. M. D.; Yavuz, M. S.; Sotzing, G. A. *Adv Mater* **2010**, *22*.
- (20) Invernale, M. A.; Seshadri, V.; Mamangun, D. M. D.; Ding, Y.; Eilorama, J.; Yavuz, M. S.; Sotzing, G., A. *Chem. Mater.* **2009**, *21*, 3332.
- (21) Roncali, J. *Chem. Rev.* **1992**, *92*, 711.
- (22) Asavapiriyant, S.; Chandler, G. K.; Gunawardena, G. A.; Pletcher, D. *J. Electroanal. Chem* **1984**, *177*, 229.
- (23) Welsh, A.; Kumar, A.; Meijer, E. W.; Reynolds, J. R. *Adv Mater* **1999**, *11*.
- (24) Seshadri, V.; Invernale, M. A.; Sotzing, G., A. *Org. Electron.* **2007**, *8*, 367.
- (25) Otero, T. F.; Grande, H. J.; Rodriguez, J. *J Physical Chemistry B* **1997**, *101*, 3688.
- (26) Otero, T. F.; Bengoechea, M. *Langmuir* **1999**, *15*, 1323.

## **Chapter 4**

### **Optimization of gel electrolyte towards high photopic contrast**

**Abstract:** Polymeric electrochromic devices (ECDs) have aroused significant interest due to their energy-saving functions and low power consumption in applications such as smart windows and eyewear. With an electrochromic window, the amount of light passing through the device can be limited; hence it can play an important role in reducing energy costs. High contrast smart windows with fast switching speeds and low power consumption have been the main demands in the development of polymeric ECDs. We have optimized a one-step *in situ* device fabrication to improve performance towards meeting the demands of commercialization. Comparing with conventional device fabrication processes, where polymer films are electrodeposited from solution, the *in situ* monomer technique utilizes open-air fabrication, minimizes cost and waste, shortens device construction time, and facilitates large window production. Polymers formed by this approach are highly dependent on the properties of the gel electrolyte. Herein, extensive studies on ionic conductivity of the polymer gel matrix, by changing the composition of salt and solvent were carried out to maximize the optical performance of electrochromic devices.

#### 4.1 Introduction

Electrochromic device changes from one color state to other color state upon applying a small external potential. The origin of this color is from the electronic structure of the electrochromic materials. Different types of EC materials like viologen<sup>1</sup>, tungsten oxide<sup>2-4</sup> etc. are already commercialized. Because of color variability, high optical contrast, open circuit memory, film flexibility conjugated polymers have gained high interest<sup>5-12</sup>. Several research groups are working to



make different colors to commercialize the ECDs using conjugated polymers. But the major problem towards commercialization is the processability. Our group has recently developed a new one-step assembly technique called *in situ* method<sup>13</sup>. For this method there is no need to synthesize the EC polymer before assembling the device. Here EC polymer grows inside the solid gel matrix in close proximity of the working electrode. This method reduces the chemical waste, assembly time and cost. As the polymer is growing inside the polymer electrolyte matrix, ionic conductivity of the gel has an important role on device performance<sup>14</sup>. This gel electrolyte is a composition of salt, solvent and cross-linked PEO based polymer matrix. The role of salt is to provide ions that help to counter balance the charge of the EC polymer chain during doping-dedoping. To enhance the ionic mobility suitable solvents need to be used that could help to dissolve the salt as well. Generally, solvents with high dielectric constant and low viscosity are desired. As per application purpose, solvents with high boiling point that provides low vapor pressure at room temperature are preferred. Here in this chapter, ionic conductivity was optimized for different system and a relation with photopic contrast is established.

For window type devices highest photopic contrast is one of the most important criteria. Here in this study our goal is to have a better performing ECD without any compromise with photopic contrast. Three different solvents propylene carbonate, ethylene carbonate and tetraethylene glycol dimethyl ether were used. As ionic liquid could be used as plasticizer, to see the effect ionic liquid on ECD performance 1-butyl-3-methylimidazolium hexafluorophosphate was used. To

observe the device parameter two most common ECPs, PProDOT-Me<sub>2</sub> and PEDOT were used.

## **4.2 Experimental**

### **4.2.1 Materials**

Propylene carbonate, ethylene carbonate, poly(ethylene glycol) diacrylate ( $M_n = 700$ ) (PEG-DA), Lithium trifluoromethanesulfonate (LITRIF), 2,2-dimethoxy-2-phenyl-acetophenone (DMPAP), Tetraethylene glycol dimethyl ether and 1-butyl-3-methylimidazolium hexafluorophosphate were purchased from Sigma Aldrich and used as received. ITO coated glass (resistance 8-12 Ohm/sq) and polyethylene terephthalate (PET) were purchased from Delta Tech Inc and Bay View Inc, respectively. Norland UV curable glue, UVS-91 was purchased from Products Inc. ProDOT-Me<sub>2</sub> was synthesized according to reported procedures.<sup>20-22</sup> EDOT was purchased from Heraeus Clevios GmbH and vacuum distilled before use.

### **4.2.2 Instrumentation**

The electrochemical study was carried out using CHI 720c potentiostat. A Varian Cary 5000i UV-Vis-NIR was used for all optics studies. A UVP CL-1000 was used for UV curing.

### **4.2.3 Preparation of Polymer gel electrolyte**

The electrolyte solution was prepared as mentioned in previous chapter<sup>15,16</sup>

#### 4.2.4 Electrochromic Device Fabrication

ECDs are assembled as mentioned in previous chapter<sup>13</sup>.

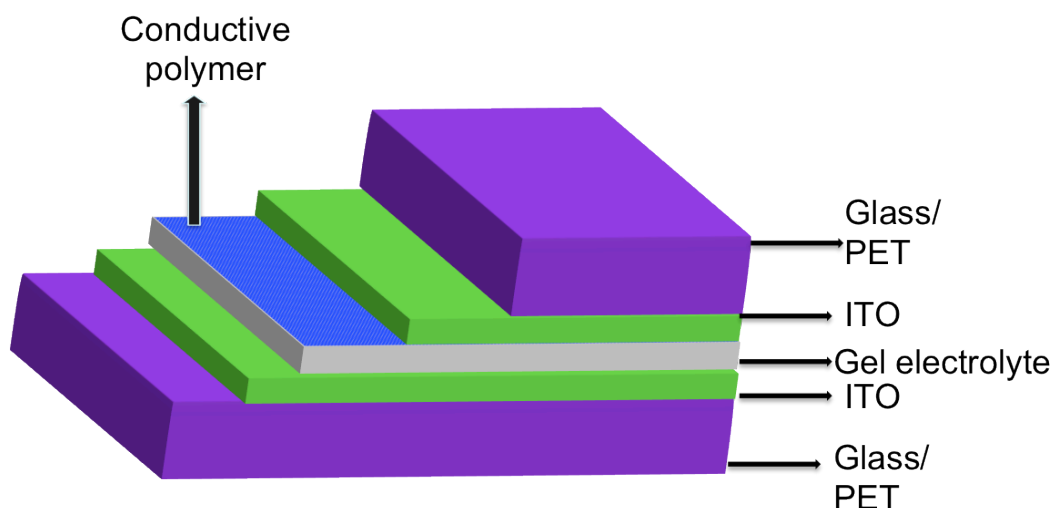


**Figure 4.1** Schematic diagram of a an ECD assembled via *in situ* method

### 4.3 Results and discussion

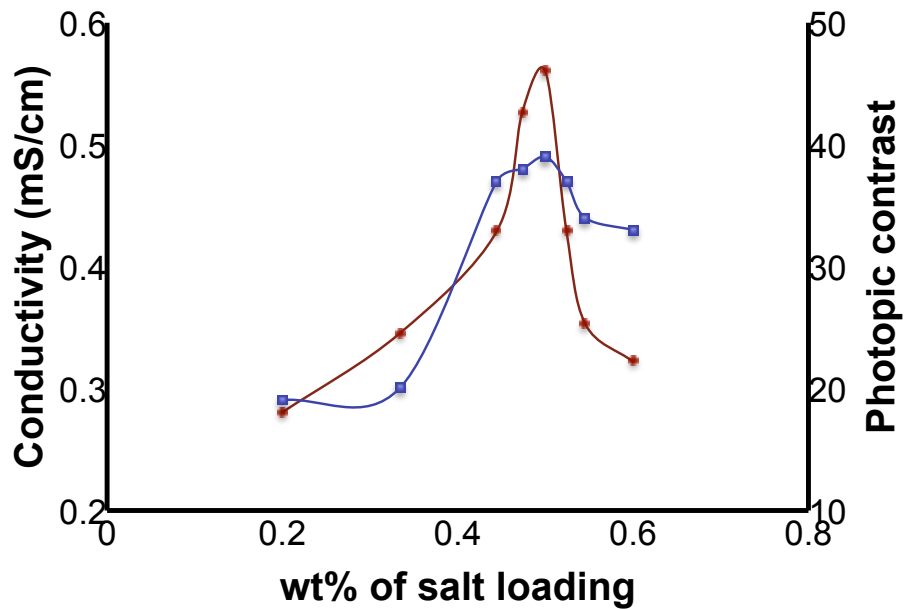
#### 4.3.1 Optimization of salt concentration

Upon increasing the salt concentration in a gel, the ionic conductivity will increase until a maximum is achieved. Upon further increase of salt concentration beyond this maximum, the ionic conductivity has been reported to drop due to issues such as aggregation of the salt and/or crystallization<sup>17</sup>. Higher ionic conductivities contribute to a higher contrast

since more mobile electrolyte leads to an increased doping level during polymerization, thus affecting polymer formation. As %T for both neutral and oxidised states decays exponentially by increasing the charge densities<sup>18</sup>, hence a maximum contrast achieved. Increasing ionic conductivity will also increase the speed of an electrochromic polymer switching between the bleached and colored states, which in turn can lead to an observed change in photopic contrast based upon the fixed time that the contrast is observed. Different concentrations of LITRIF salt, 2.38 %wt to 13 wt% LITRIF were put into 1:1 PC: PEG-DA and the conductivity was measured. The ionic conductivity doubled for 9 wt% salt ( $\sigma = 0.56 \text{ mS/cm}^2$ ) with respect to 2.4 wt% salt ( $\sigma = 0.28 \text{ mS/cm}^2$ ), due to an increase in number of ionic charge carriers while maintaining solubility in the gel matrix. Addition of more salt into the electrolyte causes the conductivity to decrease because of slower segmented motion of the polyelectrolyte chain due to ion aggregation<sup>19</sup>. Photopic contrast was measured as a function of salt loading using a constant concentration of 2.5 wt% of EDOT, for constant gel matrix thickness of 0.5 mm. Electrochromic devices prepared using 9 wt% salt achieved the highest photopic contrast 39% (55%T to 16%T).

The salt concentration study was also performed using an ionic liquid, 1-butyl-3-methylimidazolium hexafluorophosphate (IL), and the same relationship was established between ionic conductivity and photopic contrast. **Figure 4.2** shows the plots for ionic conductivity and percent

photopic contrast as a function of percent salt in the gel electrolyte for both the LITRIF and ionic liquid systems. The maximum ionic conductivity for the gel layer containing ionic liquid ( $\sigma = 1.29 \text{ mS/cm}^2$ ) is higher than that for the LITRIF system ( $\sigma = 0.56 \text{ mS/cm}^2$ ), and, as a result, the photopic contrast is higher *ca.* 2%.



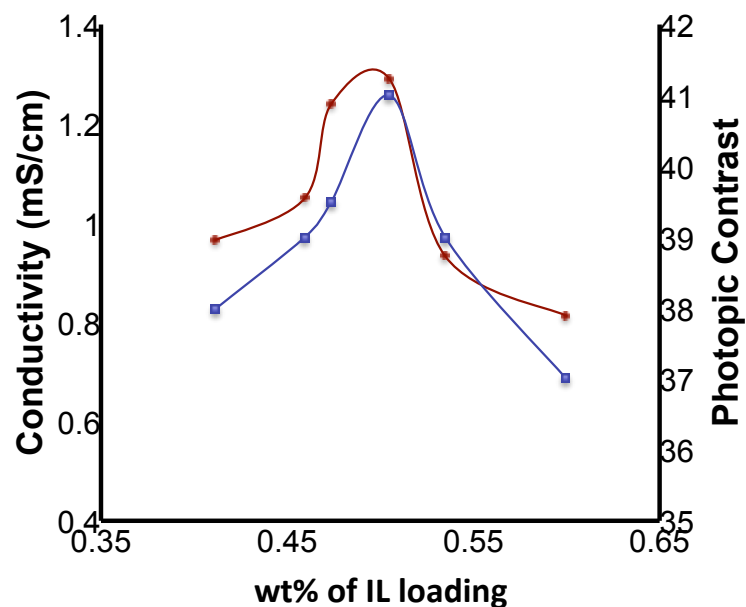


**Figure 4.2** Relation between photopic contrast of PEDOT (shows in dark purple diamond) and ionic conductivity of solid gel electrolyte (shows in blue square) as a function of LITRIF (top) and ionic liquid 1-butyl-3-methylimidazolium hexafluorophosphate, (b) concentration for the *In situ* method of making electrochromic devices.

As the viscosity of the gel electrolyte increases by incorporation of ionic liquid<sup>20</sup> less uniform EC polymer was observed in case of PProDOT-Me<sub>2</sub>. But for liquid monomers like EDOT and pyrrole, always got uniform polymer composite<sup>21</sup>. This behaviour can be explained by the diffusion coefficient of the monomers. As reported earlier<sup>14</sup>, the diffusion coefficient of EDOT ( $9.57 \times 10^{-11} \text{ m}^2/\text{S}$ ) is 8 times higher than ProDOT-Me<sub>2</sub> ( $1.21 \times 10^{-11} \text{ m}^2/\text{S}$ ) inside the cross-linked gel electrolyte matrix. Higher viscosity does

not interfere to make a uniform polymer for PEDOT but it does with PProDOT-Me<sub>2</sub>.

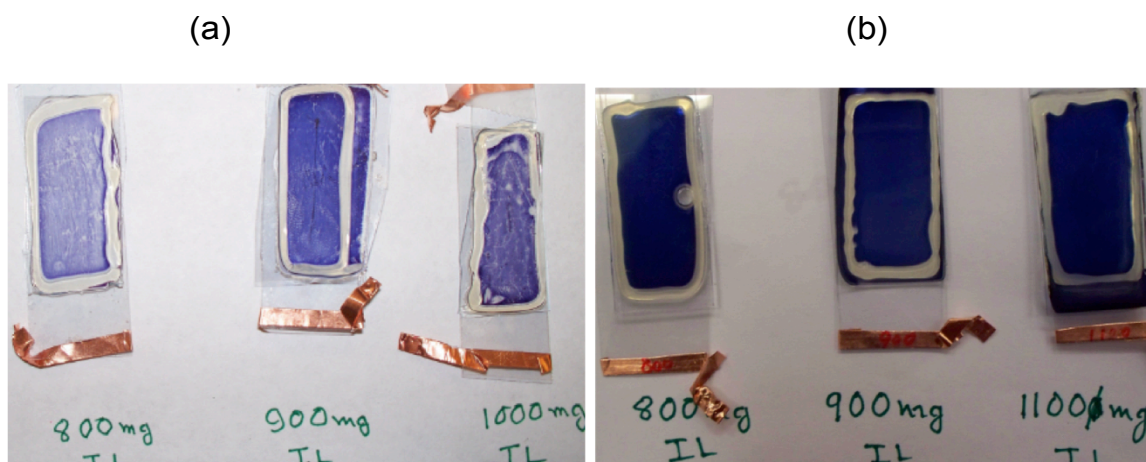


**Figure 4.3** Pictures of assembled ECD via *in situ* approach using a) PProDOT-Me<sub>2</sub> (left) and b) PEDOT (right) using different concentration of ionic liquid 1-butyl-3-methylimidazolium hexafluorophosphate (IL) into 10 gm of polymer gel electrolyte

#### 4.3.2 Effect of propylene carbonate loading

The role of the plasticizer, propylene carbonate (PC) inside the gel matrix is to dissolve the salt and to increase the ionic mobility. As ionic liquids itself can be work as a plasticizer, amount of PC was tried to replace by ionic liquid. But it was noticed that the photopic contrast was reduced significantly by reducing the PC loading. This is because of the reduced ionic mobility by reducing the viscosity of the system. EC devices were assembled using *in situ* method by using 2.5wt% EDOT monomer into the gel electrolyte and polymerized for 40s and the data is shown in **Figure**

**4.4.** It is clear that by increasing the amount of PC inside the solid gel matrix initially helped to increase the photopic contrast after a certain percentage of propylene carbonate the value of photopic contrast gets saturated.

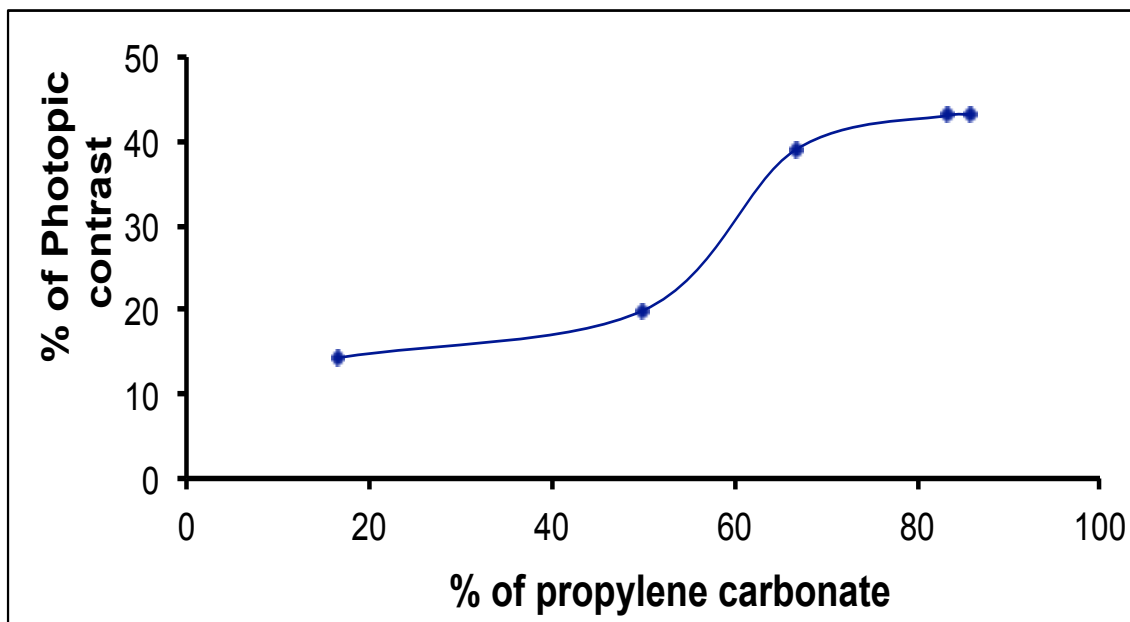


**Figure 4.4** Photopic contrast of PEDOT as a function of propylene carbonate (PC) loading to replace ionic liquid inside the solid gel matrix assemble by *in situ* method

#### **4.3.3 Effect of only EC and tetraethylene glycol dimethyl ether on contrast and switching speed**

For application purpose a wide operation range is always more desirable. For this purpose different plasticizers with higher boiling point were used to understand their effect on EC device parameters. Here two different



solvents ethylene carbonate (EC) and tetraethylene glycol dimethyl ether with higher boiling point were used instead of propylene carbonate. For ethylene carbonate system the solvent to PEGDA ratio was kept same (1:1) by wt% as PC to PEGDA, but for tetraethylene glycol dimethyl ether system the ratio was optimized to 5:2 wt% based upon the molar mass.

**Table 4.1** Shows the ratio between solvent to poly(ethylene glycol) diacrylate used to assemble ECD and the boiling point of each solvents

Solvent	Boiling point (°C)	Solvent : Poly(ethylene glycol) diacrylate
Propylene Carbonate	240	1:1
Ethylene carbonate	260	1:1
Tetraethylene glycol dimethyl ether	275	5:2

*In situ* EC devices were assembled by using 2.5wt% EDOT and ProDOT-Me<sub>2</sub> into the gel electrolyte following above solvent to PEGDA composition with 9wt% LiTRIF that are denoted as system I, system II and system III respectively. 3 V potential was applied to each system for 60s to

polymerize and corresponding photopic contrast without background correction is reported in **Table 4.2**. For ethylene carbonate increasing the conversion time from 60s to 100s could increase photopic contrast. Highest achievable photopic contrast for PProDOT-Me<sub>2</sub> system is 45%T. Same trend has been found for tetraethylene glycoldimethyl ether system. But the problem is with slow switching speed. **Table 4.3** shows an increase of contrast of PEDOT observed at 555 nm by increasing the pulse time.

**Table 4.2** Photopic contrast of PEDOT and PProDOT-Me<sub>2</sub> at 60s polymerization time for three different solvent systems

EC polymer	System I	System II	System Iii
PEDOT	38%	38%	45%
PProDOT-Me <sub>2</sub>	45%	40%	44%

**Table 4.3** Relationship between pulse width and contrast of PEDOT observed at 555nm

PULSE WIDTH	LIGHT	DARK	CONTRAST
2	64.4	25.43	38.97
4	64.59	24.9	39.69
6	64.95	24.7	40.25
8	64.77	24.19	40.58
10	64.78	23.92	40.86
12	64.93	23.62	41.31
15	64.933	23.3	41.633

#### 4.3.4 Effect of solvent mixture on photopic contrast

Because of lower viscosity of ethylene carbonate compare to propylene carbonate, system I takes more time to switch. But ethylene carbonate has higher dielectric constant (89.8 at 25°C) whereas propylene carbonate has dielectric constant (64.92 at 25°C)<sup>22</sup>. By mixing these two solvents into 1:1 weight ratio gives  $\eta_{EC} < \eta_{mix} < \eta_{PC}$  and  $\epsilon_{PC} < \epsilon_{mix} < \epsilon_{EC}$ . Higher dielectric constant provides higher ionic conductivity and lower viscosity facilities the ion movement. As we have seen earlier that ionic conductivity needs to be optimized to achieve maximum photopic contrast. For this purpose, concentration of LiTRIF was to obtain highest ionic conductivity. Ionic conductivity was measured same way like section 4.3.1. Same trend was

noticed as two previous systems. By increasing the salt concentration ionic conductivity increased and reached a maximum value, after that by addition of more salt ionic conductivity decreased due to ion aggregation. For this system, maximum conductivity achieved for 10.7wt% salt concentration. Photopic contrast for each system was measured and the highest photopic contrast was achieved, 48% for 10.7 wt% salt concentrated system.

**Table 4.4** Relation between ionic conductivities for (2.5 g PC + 2.5 g EC +5 g PEGDA + 17.5 mg photo-initiator) and photopic contrast for PProDOT-Me<sub>2</sub> ECDs assembled via *in situ* method at different LiTRIF concentration

Amount of Salt (g)	Salt concentration (wt %)	$\sigma$ (x 10 <sup>-4</sup> S/cm)	ECDs photopic contrast (%)
0.5	4.8	3.8	39
0.8	7.4	4.5	42
1	9.1	5	44
1.1	9.9	5.3	45
1.2	10.7	5.7	48
1.3	11.5	5.4	46
1.5	13	4.8	43

#### 4.4 Conclusions

A systematic method is established to optimize the ionic conductivity for any system. A relationship is established between ionic conductivity and photopic contrast. Ionic liquid, 1-butyl-3-methylimidazolium hexafluorophosphate provides higher ionic conductivity compare to LiTRIF system, as a result it helps to improve the photopic contrast of PEDOT about 2%. But because of low viscosity ionic liquid could not provide color uniformity for systems having electroactive species, like ProDOT-Me<sub>2</sub> with slow diffusion. High dielectric constant and low viscosity of the plasticizer is favorable to enhance the ionic conductivity as well as photopic constant. It is noted that binary solvents works better than a single solvent. As ethylene carbonate has high dielectric constant but low viscosity compare to propylene carbonate, a (1:1) weight ratio mixture of these two solvents helps to increase the photopic constant, 48%.

## References

- (1) Mortimer, R. J. *Electrochim. Acta* **1999**, *44*, 2971.
- (2) Shimano, K. *Solid State Ionics*. **2002**, *147*, 129.
- (3) Granqvist, C. G.; Avendano, E.; Azens, A. *Thin Solid Films* **2003**, *442*, 201.
- (4) Sonmez, G.; Shen, C. K.; Rubin, Y.; Wudl, F. *Angew Chem Int Ed Engl* **2004**, *43*, 1498.
- (5) Choi, M. R.; Woo, S. H.; Han, T. H.; Lim, K. G.; Min, S. Y.; Yun, W. M.; Kwon, O. K.; Park, C. E.; Kim, K. D.; Shin, H. K.; Kim, M. S.; Noh, T.; Park, J. H.; Shin, K. H.; Jang, J.; Lee, T. W. *ChemSusChem* **2011**, *4*, 363.
- (6) Argun, A. A.; Aubert, P. H.; Thompson, B. C.; Schwendeman, I.; Gaupp, C. L.; Hwang, J.; Pinto, N. J.; Tanner, D. B.; MacDiarmid, A. G.; Reynolds, J. R. *Chem. Mater.* **2004**, *16*, 4401.
- (7) Chen, W.; Wu, S.; Ferng, Y. *Materials Letters* **2006**, *60*, 790.
- (8) Kim, W. H.; Mäkinen, A. J.; Nikolov, N.; Shashidhar, R.; Kim, H.; Kafafi, Z. H. *Applied Physics Letters*. **2002**, *80*, 3844.
- (9) Xu, J.; Yang, Y.; Yu, J.; Jiang, Y. *Applied Surface Science*. **2009**, *255*, 4329.
- (10) Hu, B.; Li, D.; Ala, O.; Manandhar, P.; Fan, Q.; Kasilingam, D.; Calvert, P. D. *Advanced Functional Materials* **2011**, *21*, 305.
- (11) Beaujuge, P. M.; Ellinger, S.; Reynolds, J. R. *Adv. Mater.* **2008**, *20*, 2772.
- (12) Seshadri, V.; Padilla, J.; Bircan, H.; Radmard, B.; Draper, R.; Wood, M.; Otero, T. F.; Sotzing, G. A. *Org. Electron.* **2007**, *8*, 367.
- (13) Ding, Y.; Invernale, M. A.; Mamangun, D. M. D.; Kumar, A.; Sotzing, G., A. *J. Mater. Chem.* **2011**, *21*, 11873.

- (14) Kumar, A.; Otley, M. T.; Alamar, F. A.; Zhu, Y.; Sotzing, G. A. *J. Mater. Chem. C* **2014**, 2, 2510.
- (15) Invernale, M. A.; Seshadri, V.; Mamangun, D. M. D.; Ding, Y.; Eilorama, J.; Yavuz, M. S.; Sotzing, G., A. *Chem. Mater.* **2009**, 21, 3332.
- (16) Invernale, M. A.; Ding, Y.; Mamangun, D. M. D.; Yavuz, M. S.; Sotzing, G. A. *Adv Mater* **2010**, 22.
- (17) Song, J. Y.; Wang, Y. Y.; Wan, C. C. *J of Power Sources* **1999**, 77, 183.
- (18) Padilla, J.; Seshadri, V.; Filloramo, J.; Mino, W.; Mishra, S.; Radmard, B.; Kumar, A.; Sotzing, G. A.; Otero, T. *Syn Metals.* **2007**, 157, 261.
- (19) MacCallum, M. A.; Vincent, C. A. *Polymer Electrolyte Reviews*, **1989**, 2, 1989.
- (20) Tomida, D.; Kumagai, A.; Qiao, K.; Yokoyama, C. *Int. J. Thermophys.* **2006**, 27, 39.
- (21) Zhu, Y.; Otley, M. T.; Alamar, F. A.; Kumar, A.; Zhang, X.; Mamangun, D. M. D.; Li, M.; Arden, B. G.; Sotzing, G. A. *Org. Electron.* **2014**, 15, 1378.
- (22) Ahmad, S. *Ionics.* **2009**, 15, 309.

## **Chapter 5**

### **Effect of polymer matrix on optical performance of electrochromic polymer composites in solid-state devices**



**Abstract:** Significant interest has developed over the past few years for using electrochromic devices in the smart window and eyewear industries; high photopic contrast is one of the most desirable specifications for these applications. Herein, the role of the polymer matrix on the formation of the conjugated polymer in a one-step, *in situ* fabrication process was investigated. Unlike the more conventional electrodeposition method, the *in situ* approach functions by having conjugated polymers formed inside the solid polyelectrolyte matrix. Thus, the influences of the conformation of the cross-linked polymer electrolyte matrix on the resulting electrochromic polymer and the effect on photopic contrast of the device were studied. A binary (ethylene carbonate and propylene carbonate mixture) plasticizer system and lithium trifluoromethanesulfonate salt were used as the other components of the solid polyelectrolyte matrix. The ionic conductivity of these systems was optimized, and the glass transition temperature was reported for each system to evaluate the polymeric matrix behavior. An increase of 8% photopic contrast (46%T to 54%T) was observed by changing the molar mass of the prepolymer/oligomeric acrylate, poly(ethylene glycol) methyl diacrylate,  $M_n$  of 700 to 250, using poly(2,2 dimethyl-3,4-propylenedioxythiophene) (PProDOT-Me<sub>2</sub>) as the conjugated polymer. A significant change in the absorption behavior in the oxidized form of the electrochromic device was noticed.

## 5.1 Introduction

Conjugated polymers have garnered interest for the ease of controlling band gap energy, low manufacture cost, high stability, high color efficiency, and mechanical flexibility<sup>1-3</sup>. There are numerous industrial applications, such as photovoltaic cells, batteries, capacitors, light emitting diodes, radio frequency identification sensors; one of the most popular applications is using them as electrochromic materials<sup>1,4-9</sup>. In electrochromic technology, controlling the color is an important aspect. For conjugated polymers, the electronic property of each redox state can be easily tuned by introducing different substituents, putting spacers to reduce the steric hindrance, and by using donor-acceptor approach on the polymeric backbone, among other techniques<sup>7,10,11</sup>.

In general, conjugated polymers are synthesized either chemically or electrochemically. An electrochemical polymerization has an advantage over chemical polymerization procedures as it can be processed easily. In the traditional method, monomers get polymerized from an electrolyte bath on the electrode surface by applying a suitable potential. However, this process is very sensitive to the conductive surface of the substrate. To avoid the difficulty in fabrication of large electrochromic devices, our group has introduced a simple, one-step method, which is known as the *in situ* method<sup>12</sup>. Following this new approach, large defect-free, stable

electrochromic windows with sub-second switching speeds can be assembled with a high success rate and minimal chemical waste<sup>12-16</sup>.

Since conjugated polymers are forming inside the polymer matrix, when using the *in situ* approach, the device performance depends on the device composition<sup>13,14</sup>. It was observed that the optical behavior depends on the morphology and the conformation of conjugated polymer chains. In our previous studies,<sup>13-15</sup> the effect of the ionic conductivity of the gel electrolyte system on device performance was elucidated. To better understand the role of the solid gel electrolyte on the formation of the conjugated polymer, the effect of each gel electrolyte component needs to be studied. The gel electrolyte is a simple, cross-linked matrix of low molecular weight polyethylene glycol based acrylates, bonded with lithium ion of the salt via coordination<sup>17</sup>. Addition of plasticizer helps to dissolve the salt and to increase the ionic mobility throughout the matrix. Salt provides ions, which move in and out to the conjugated polymer regions to assist the electrochemical oxidation and reduction processes; the polymer matrix provides mechanical stability for the device and solvent.

Here, the role of the cross-linked polymer matrix on the formation of the conjugated polymer and the performance of the electrochromic devices was studied. The effect of salt identity was studied and it was found that lithium salts were the best choice for *in situ* electrochromic devices<sup>14</sup>. In this work, lithium trifluoromethanesulfonate and a 1:1 by weight binary mixture of propylene carbonate (PC) and ethylene carbonate (EC) was

used as the plasticizer. For an eyewear application, greater than 50% photopic contrast without any background correction is desired; among various thiophene-based derivatives, poly(2,2 dimethyl-3,4-propylenedioxythiophene) (PProDOT-Me<sub>2</sub>) has the highest contrast because of its more transparent oxidized state<sup>18</sup>. To understand the effect of the polymer matrix on the optical performance of the *in situ* devices, the ionic conductivity of plasticizer and three different molecular weight polyethyleneglycol diacrylate (PEGDA) systems (M<sub>n</sub> = 700 (System I), M<sub>n</sub> = 550 (System II), M<sub>n</sub> = 250 (System III)) were optimized and the photopic contrasts of the electrochromic devices were measured using PProDOT-Me<sub>2</sub> as the conjugated polymer. Figure 1 shows the chemical structures of the materials used in this study.

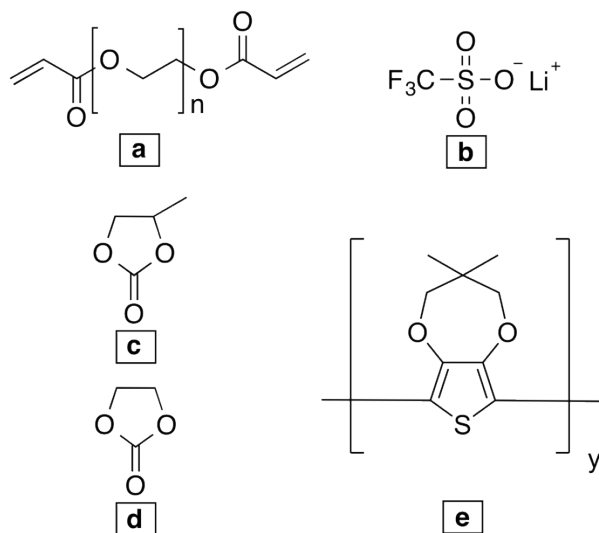


**Figure 5.1** Chemical structures of a) PEGDA, b) LITRIF, c) PC, d) EC and e) ProDOT-Me<sub>2</sub>.

## **5.2 Experimental**

### **5.2.1 Materials**

Poly(ethylene glycol) diacrylate ( $M_n = 700$ ) (PEGDA-700), poly(ethylene glycol) methyl diacrylate ( $M_n = 550$ ) (PEGMDA-550), poly(ethylene glycol) diacrylate ( $M_n = 250$ ) (PEGDA-250), propylene carbonate (PC), ethylene carbonate (EC), lithium trifluoromethanesulfonate (LITRIF), and 2,2-dimethoxy-2-phenyl-acetophenone (DMPAP) were purchased from Sigma Aldrich and used as received. ITO coated polyethylene terephthalate (PET) and glass (resistance 8-12 Ohm/sq) were purchased from Bayview Optics and Delta Technologies, respectively. UV curable adhesive, UVS-91, was purchased from Norland Products Inc. Conductive copper tape was purchased from Newark. ProDOT-Me<sub>2</sub> was synthesized according to the literature procedure<sup>18</sup>.

### **5.2.2 Polymer gel electrolyte preparation**

To prepare different PEG acrylate solid gel electrolyte matrix systems, a 1 to 1 weight ratio of plasticizer to cross-linker system was prepared, LITRIF salt and DMPAP was dissolved, and photo initiation occurred using a CL-1000 Ultraviolet Crosslinker according to literature procedure.<sup>19,20</sup>

### **5.2.3 Electrochromic Device Fabrication**

The highest ionic conductivity gel electrolyte solution for each of the different PEG systems was chosen and 2.5 wt% ProDOT-Me<sub>2</sub> was added.

Electrochromic devices were built according to previously reported methods.<sup>12</sup>

#### **5.2.4 Instrumentation**

##### **5.2.4.1 Ionic conductivity measurements**

To evaluate the highest ionic conductivity of each PEG acrylate system, different weight percentage of LiTRIF salt (4.8 wt% to 13 wt%) was dissolved into 1:1 weight ratio of (plasticizer : PEG-acrylate) and cured using photoinitiator. The ionic conductivity,  $\sigma$ , was measured by placing the solid polymer gel electrolyte in between two stainless steel electrodes using AC impedance spectroscopy over a 20 to 10000 Hz frequency range. Using the Bode plot, the resistance (R) of the solid electrolyte was calculated and  $\sigma$  was calculated using the following equation,  $\sigma = t/RA$ , where t is the thickness of the polymer gel electrolyte and A is the area of the electrodes.

##### **5.2.4.2 DSC analyses**

Differential scanning calorimetric studies were carried out on TMA Q-400 at a scanning rate of 5°C/min, an applied force 0.0200 N, and a final temperature of 50°C.

#### 5.2.4.3 Electrochemical Studies

To electrochemically polymerize ProDOT-Me<sub>2</sub>, a +3 V potential bias was applied in a typical electrochemical cell, where the reference electrode was with the counter electrode. For reversible oxidation and reduction switching, a  $\pm 2$  V was applied. CHI 720c and 400a potentiostats were used to perform all electrochemical studies.

#### 5.2.4.4 Photopic contrast calculations

The photopic contrast ( $\Delta T_{\text{photopic}}$ ) is the transmittance difference between the colored and bleached states. The photopic transmittance for each redox state was calculated as mentioned earlier.

### 5.3 Results and discussion

For the *in situ* assembly method, the monomer is dissolved into the liquid polymer system, which consists of plasticizer, salt, and low molecular weight acrylate functionalized polyethylene glycol. This liquid electrolyte is placed between ITO coated glass and/or PET substrates. It is then put into a UV chamber to crosslink the polymer chains in the presence of a photoinitiator. By applying a +3 V bias, ProDOT-Me<sub>2</sub> gets polymerized inside the solid polymeric matrix, close to the working electrode, in a gradient fashion whereby the highest concentration of conducting polymer is closest to the working electrode and the density decreases with increasing distance. Since conjugated polymers are forming inside the

solid matrix, ionic conductivity is an important factor for controlling the photopic contrast of the electrochromic devices.<sup>13-15</sup> In our previous studies, it was shown that the ionic conductivity of each polymer gel matrix needs to be optimized based upon the salt concentration. The highest ionic conductive matrix will provide the highest photopic contrast within a given gel matrix, though, as shown in this work, the nature of each gel matrix, itself, has an effect on photopic contrast.

The mobility and number of charge carriers' influences ionic conductivity.<sup>21</sup> For the polymeric solid gel matrix, the oxygen atom of the ether linkage forms a coordination bond with a lithium ion. Rearranging the coordination between the Li ion and the oxygen atoms of the polymer backbone increases cation mobility and adds free volume into the matrix where the ion can diffuse. In general, by increasing the mean hole size and/or free volume, the segmental motion of the polymer chains will increase.<sup>22</sup> The probability of finding a hole inside a polymer matrix can be described by the term  $\exp(-\gamma v^*/v_f)$ , where  $v^*$  is the hole volume,  $v_f$  is the mean volume of the hole size distribution, and  $\gamma$  is a numerical factor (0.5 to 1) to correct for the overlapping of holes.<sup>23</sup> By correlating the diffusion of a molecule and the probability of finding the hole, the ionic conductivity can be written according to Nernst-Einstein equation:<sup>24</sup>

$$\sigma = CT^{1/2} \exp(-\gamma v^*/v_f), \text{-----(5.1)}$$

where C is a fitting constant.



Due to the fact that ionic conductivity is related to segmental motion, by adding plasticizer with a low viscosity and a high dielectric constant, one can improve the ionic conductivity of the overall system. Propylene carbonate (PC) is the most common plasticizer used in solid polymeric gel electrolytes because of its high dielectric constant and low viscosity. In our previous study, it was noted that the viscosity of a 1:1 wt% PC:EC binary system has a lower viscosity (2.21 cP at 25°C) compared to the pure PC and EC system,<sup>15</sup> which helps to increase the  $\sigma$  of the polymeric system, as well as the photopic contrast of the electrochromic devices. The dielectric constants for PC and EC are 64.9 and 89.8 at 25°C, respectively, and the boiling points of PC and EC are 242°C and 260.1°C at normal pressure, respectively. To have a wide operational range, plasticizers with less volatility and vapor pressure are always more desirable. In order to have high ionic conductivity and low vapor pressure, the binary system (PC+EC) was used in these experiments.

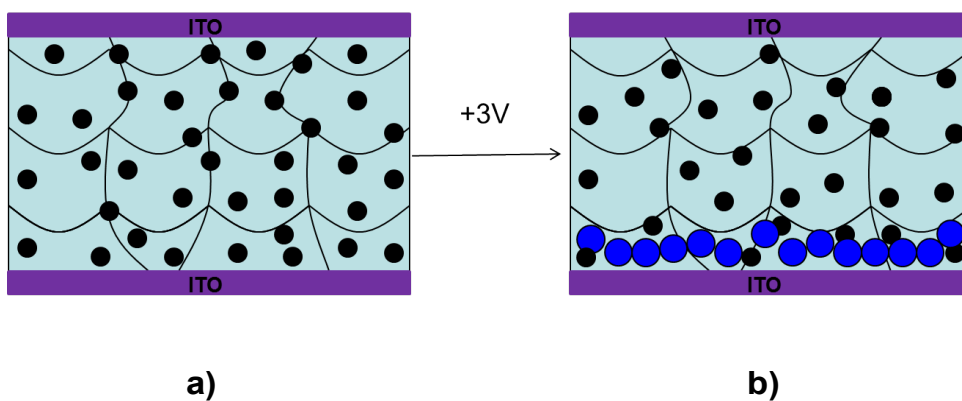


**Figure 5.2** Cross-sectional diagram of an ECD a) before and b) after electropolymerization of electroactive species in the solid state via the *in situ* method.

As previously mentioned, to achieve the best performance of the ECD, the  $\sigma$  needs to be optimized. The highest  $\sigma$  for system I was reported to be  $5.7 \times 10^{-04} \text{ S/cm}^2$  and involved the addition of 10.7 wt% LiTRIF salt into the gel electrolyte.<sup>15</sup> For systems II and III, the  $\sigma$  needs to be optimized based upon the salt concentration. By addition of salts into the solvent-polyethylene glycol system, the number of charge carriers increases. As a result, the ionic conductivity of the system also increases. However, at some point, with an increase in concentration of salt the interaction between the ions is strong enough to form ion-pairs. Due to ion-aggregation, the segmental motion of the system decreases, which results in a lower ionic conductivity.<sup>25</sup> For systems II and III, ionic conductivity was measured as a function of salt loading using 1:1 wt% (PC : EC) and PEGDA. The results are shown in **Figure 5.3**.

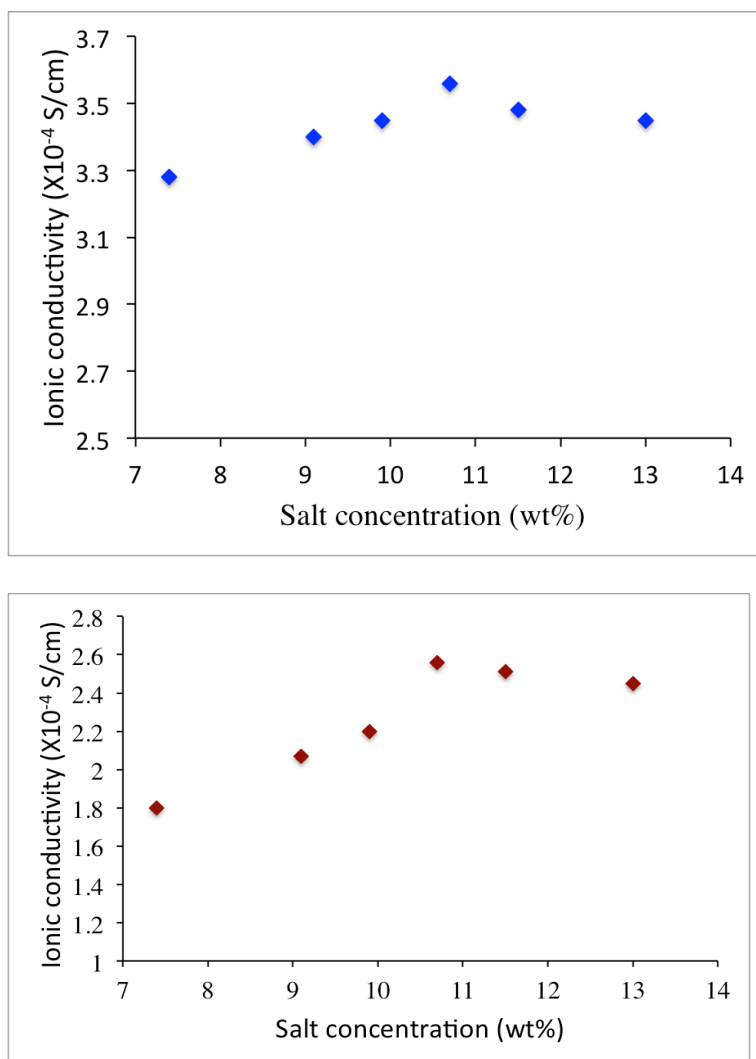


**Figure 5.3** A) and B) shows the relationship between ionic conductivity as a function of salt loading for systems II and III, respectively.

It was observed that the highest  $\sigma$ , which can be achieved for system, I is  $5.7 \times 10^{-4}$  S/cm, which decreases to  $1.8 \times 10^{-4}$  S/cm for system III. By going from system I to III, the chain length of the prepolymer becomes shorter, thus the crosslinking density increases and free volume decreases. As a result, according to equation (2),  $\sigma$  will decrease due to the lowering of segmental motion.

To use these electrochromic devices in daily life, another important feature is to know their operational temperature. Compared to the pure PEGDA system, the polymer gel electrolyte matrix will show an increase in glass transition temperature because the addition of salt into the system causes segmental motion to decrease.<sup>26</sup> TMA was employed to determine the glass transition temperature ( $T_g$ ) of the optimized composition of each polymeric system. Going from system I to III, the  $T_g$  changes from  $-67.4^{\circ}\text{C}$  to  $-58.9^{\circ}\text{C}$  as the segmental motion decreases due to increasing PEG content.

**Table 5.1**  $T_g$  values, ionic conductivity and optical behavior of three optimized PEGDA systems using PProDOT-Me<sub>2</sub> as the conjugated polymer.

System	Optimized ionic conductivity (S/cm <sup>2</sup> )	$T_g(^{\circ}\text{C})$	%T photopic, bleached	%T photopic, colored	$\Delta T_{\text{photopic}}$
I	$5.7 \times 10^{-4}$	-67.4	60	14	46
II	$3.56 \times 10^{-4}$	-61.9	64	14	50
III	$2.4 \times 10^{-4}$	-58.9	68	14	54

Electrochromic devices were built using systems I, II, and III. The thickness of the conjugated polymer composite is related to the transmittance value of each redox state.<sup>13</sup> To achieve the maximum photopic contrast for each system, keeping the monomer concentration constant at 2.5 wt%, optimization based upon the polymerization time was carried out and these optimized photopic contrasts are reported in **Table 1.1**. It was noticed that by lowering the molar mass of PEG, the photopic contrast of the system increased from 46%T to 54%T. The %T<sub>colored</sub> for the neutral state remained almost the same, about 14%T for all three systems, however the oxidized states improved by as much as 8%T (60%T to 68%T). Because the free volume of the polymer gel matrix is increased for higher molecular weight PEG systems, a more expanded conjugated polymer chain will form inside the solid gel matrix with fewer defects as compared to the more compact coil conformation. This will result in less absorption intensity in the oxidized state to give a higher photopic contrast. To explain this behavior, absorption spectra of the oxidized states for each system were taken in the NIR region and are shown in **Figure 5.4**. A significant increase in the absorption intensity was observed between systems I and III in the NIR region. This increased absorption of the free electronic tail supports a compact conjugated coil conformation for low molecular weight PEG systems.<sup>27,28</sup> The high degree of clarity obtained in the bleached state can be seen in the representative electrochromic device image, shown in **Figure 5.5** (right). Since the conjugated polymers are

forming inside the gel matrix, it is difficult to take any kind of SEM images to check the conformation of the polymer chains. Even under the diminutive pressure for atmospheric SEM analysis, the surface of the solid gel matrix was observed to deform.

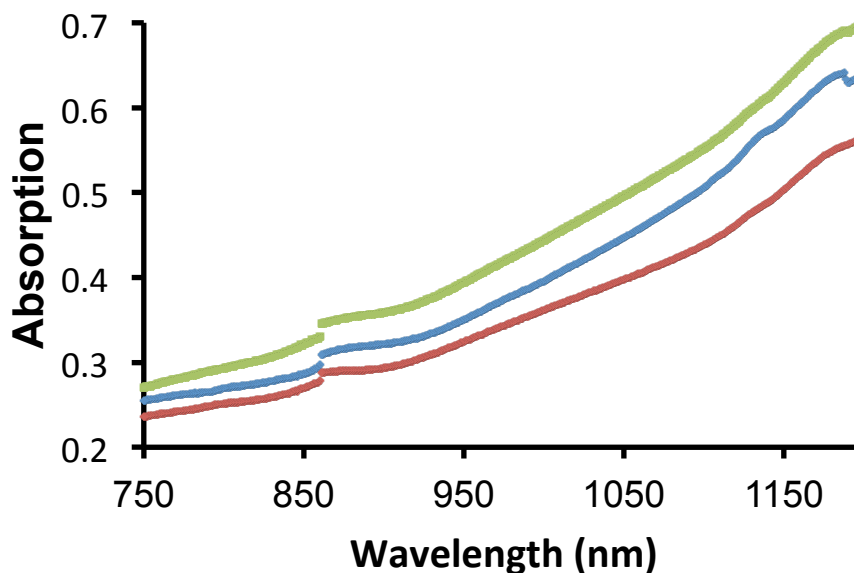


**Figure 5.4** Absorption spectra of electrochromic devices, PProDOT-Me<sub>2</sub> in oxidized state assembled by the *in situ* method using three ionic conductivity optimized PEGDA systems; a)  $M_n = 700$ , b)  $M_n = 550$ , and c)  $M_n = 250$ .

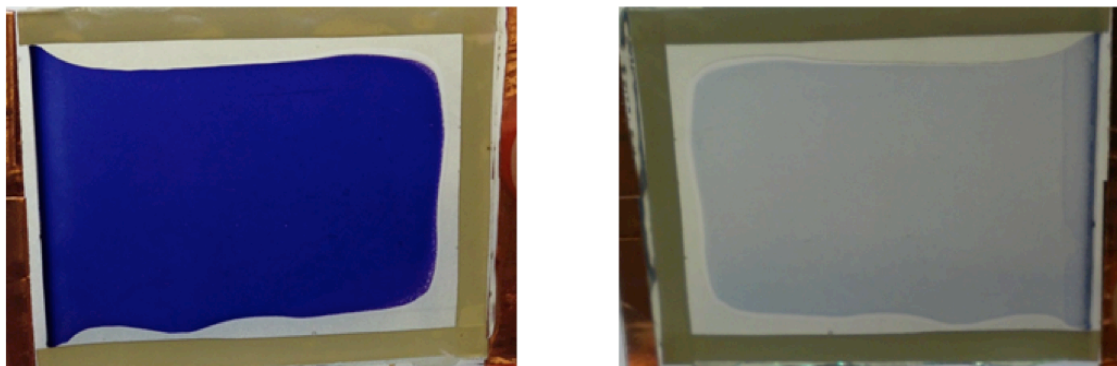


**Figure 5.5** A neutral (left) and oxidized (right) PProDOT-Me<sub>2</sub> electrochromic device with 54% photopic contrast using the optimal gel composition of 1:1 EC: PC, LITRIF, and PEGDA ( $M_n = 250$ ).

## 5.4 Conclusions

The optical performance of single layered solid electrochromic devices assembled using the one-step *in situ* method depends on the ionic properties of the polymeric matrix. In this approach, conjugated polymer composites are forming inside the solid polymeric matrix. Thus, the conformation of the conducting polymer chains also affects the optical properties of the device. This study has shown that an increase in the %T<sub>bleached</sub> of the PProDOT-Me<sub>2</sub> conjugated polymer can be achieved by lowering the molecular weight of the PEGDA crosslinker in the gel electrolyte matrix from  $M_n$  700 to 250. This increase in %T<sub>bleached</sub> impacts on an overall improvement to provide 54% photopic contrast without any background correction.

## References

- (1) Argun, A. A.; Aubert, P. H.; Thompson, B. C.; Schwendeman, I.; Gaupp, C. L.; Hwang, J.; Pinto, N. J.; Tanner, D. B.; MacDiarmid, A. G.; Reyanols, J. R. *Chem. Mater.* **2004**, *16*, 4401.
- (2) Beaujuge, P. M.; Reynolds, J. R. *Chem Rev* **2010**, *110*, 268.
- (3) Gunbas, G.; Toppare, L. *Chem Commun (Camb)* **2012**, *48*, 1083.
- (4) Westenhoff, S.; Howard, I. A.; Hodgkiss, J. M.; Kirov, K. R.; Bronstein, H. A.; Williams, C. K.; Greenham, N. C.; Friend, R. H. *J Am Chem Soc* **2008**, *130*, 13653.
- (5) Liu, R.; Duay, J.; Lee, S. B. *ACS Nano* **2010**, *4*, 4299.
- (6) Bijleveld, J. C.; Zoombelt, A. P.; Mathijssen, S. G.; Wienk, M. M.; Turbiez, M.; de Leeuw, D. M.; Janssen, R. A. *J Am Chem Soc* **2009**, *131*, 16616.
- (7) Shi, P.; Amb, C. M.; Knott, E. P.; Thompson, E. J.; Liu, D. Y.; Mei, J.; Dyer, A. L.; Reynolds, J. R. *Adv Mater* **2010**, *22*, 4949.
- (8) Hamedi, M.; Forchheimer, R.; Inganas, O. *Nat Mater* **2007**, *6*, 357.
- (9) Sonmez, G.; Shen, C. K.; Rubin, Y.; Wudl, F. *Angew Chem Int Ed Engl* **2004**, *43*, 1498.
- (10) Mortimer, J. A.; Dyer, A. L.; Reynolds, J. R. *Displays* **2006**, *27*, 2.
- (11) Roncali, J. *Chem. Rev.* **1992**, *92*, 711.
- (12) Ding, Y.; Invernale, M. A.; Mamangun, D. M. D.; Kumar, A.; Sotzing, G., A. *J. Mater. Chem.* **2011**, *21*, 11873.
- (13) Kumar, A.; Otley, M. T.; Alamar, F. A.; Zhu, Y.; Sotzing, G. A. *J. Mater. Chem. C* **2014**, *2*, 2510.
- (14) Zhu, Y.; Otley, M. T.; Alamar, F. A.; Kumar, A.; Zhang, X.; Mamangun, D. M. D.; Li, M.; Arden, B. G.; Sotzing, G. A. *Org. Electron.* **2014**, *15*, 1378.
- (15) Alamar, F. A.; Otley, M. T.; Zhu, Y.; A., K.; Sotzing, G. A. *Solar Energy Materials and Solar Cells* **2015**, *132*, 131.



- (16) Otley, M. T.; Alamar, F. A.; Zhu, Y.; Singhaviranon, A.; Zhang, X.; Li, M.; Kumar, A.; Sotzing, G. A. *Appl. Mater. Interfaces* **2014**, *6*, 1734.
- (17) Henderson, W. A. *Solid State Ionics* **2012**, *217*, 1.
- (18) Welsh, A.; Kumar, A.; Meijer, E. W.; Reynolds, J. R. *Adv Mater* **1999**, *11*.
- (19) Invernale, M. A.; Seshadri, V.; Mamangun, D. M. D.; Ding, Y.; Eilorama, J.; Yavuz, M. S.; Sotzing, G., A. *Chem. Mater.* **2009**, *21*, 3332.
- (20) Invernale, M. A.; Ding, Y.; Mamangun, D. M. D.; Yavuz, M. S.; Sotzing, G., A. *Adv Mater* **2010**, *22*.
- (21) Bamford, B.; Reiche, A.; Dlubek, G.; Allion, F.; Sanchez.; Alam, M. A. *J. Chem. Phys.* **2003**, *118*, 9420.
- (22) Miyamoto, T.; Shibayama, K. *J. Appl. Phys.*, **1973**, *44*, 5372.
- (23) Pas, S. T.; Ingram, M. D.; Funke, K.; J., H. A. *Electrochimica Acta* **2005**, *50*, 3955.
- (24) Forsyth, M.; Meakin, P.; MacFarlane, D. R.; Hill, A. J. *J. Phys. Condens. Matter* **1995**, *7*, 7601.
- (25) MacCallum, M. A.; Vincent, C. A. *Polymer Electrolyte Reviews*, **1989**, *2*, 1989.
- (26) Hardy, L. C.; Shriver, D. F. *J. Am. Chem. Soc.* **1985**, *107*, 3823.
- (27) Avlyanov, K. J.; Min, Y.; MacDiarmid, A. G.; Epstein, A. J. *Syn Metals*. **1995**, *72*, 65.
- (28) Avlyanov, K. J.; Kuhn, H. H.; Josefowicz, J. Y.; MacDiarmid, A. G. *Syn Metals*. **1997**, *84*, 153.

## **Chapter 6**

### **One step approach towards neutral to neutral color**

**Abstract:** A new approach is demonstrated to achieve neutral colors in both redox states of electrochromic devices (ECDs) by using two different approaches. (I) By using a yellow colored organic dye with electrochromic polymer (PProDOT-Me<sub>2</sub>) and (II) by controlling the diffusional gradient of electroactive monomers, 1,3-di-tert-butyl-3,4 propylene dioxythiophene (ProDOT-*t*Bu<sub>2</sub>) and 2,2-dimethyl-3,4 propylene dioxythiophene (ProDOT-Me<sub>2</sub>), inside the solid gel matrix in one step assemble method. A series of random conjugated co-polymers, [PProDOT-*t*Bu<sub>2</sub>-co-PProDOT-Me<sub>2</sub>] with distinct wavelengths formed inside the matrix, orthogonal to electrodes that include all subtractive colors by controlling the concentration of the co-monomers, which results neutral color. For both approaches a 30%T photopic contrast is achieved for colored to transmissive states for an assembled ECD without any background correction.

## 6.1 Introduction

Electrochromic materials have gained interest because of fast reversible color change process by applying suitable amount of external potential<sup>1,2</sup>. Among different kinds of electrochromic materials,  $\pi$  conjugated polymers like polythiophene, polypyrrole are considered as potential candidates because of availability of different colors with high optical contrast and sub-second switching speed<sup>1-4</sup>. These types of electrochromic devices are easy to fabricate and gives long-term stability<sup>1,2</sup>.

These kinds of material can be used for smart windows, rear view mirrors, privacy glasses, eyewears, electrochromic inks and fabrics<sup>1-13</sup>. A neutral-to-neutral color transition is most desirable for optical application purposes of ECDs. Common neutral colors are black, white, grey, ivory and taupe. According to the 1931 and 1964 CIE XYZ color spaces the chromaticity coordinates [x,y] for achromatic colors [0.333, 0.333] based on standard D65 illuminant<sup>14-16</sup>. From the spectroscopic viewpoint, a chromophore, which is able to absorb the entire visible light homogeneously, will exhibit the black or neutral color. Only very few examples are reported to date where donor-acceptor approach (DA) has used to achieve the black color electrochromic polymer<sup>17-19</sup>. Usually alternative DA polymers have two distinct absorption regions in the visible region with a gap between them<sup>20-26</sup>. This gap can be evaded by using suitable ratio of donor and acceptor leading to formation of black color. Another common approach is to get neutral color by involving multilayer of complimentary colored electrochromic polymer<sup>26,27</sup>. Synthesizing the suitable precursors, controlling the polymerization method to get the desire optoelectronic performances are challenging<sup>28</sup>.

In our previous work, it has been noticed that highest photopic contrast (54%T) could be achieved using di substituted ProDOT polymers via *in situ* approach. This EC polymer has maximum absorption around 577 nm in neutral state. It exhibits a transmissive color in oxidized state. Here in this chapter, our goal is to use some complimentary colored dye or other

electrochromic polymers along with PProDOT-Me<sub>2</sub> to absorb all visible lights in one device to create a neutral color.

For this purpose, yellow colored organic dye was chosen that has absorption around 450nm. Here in this approach, by mixing the yellow dye into the gel electrolyte along with ProDOT monomer. And an ECD was built using *in situ* approach. Another approach was used following all subtractive colors to achieve the neutral color.

In our previous work<sup>29</sup>, a high-throughput screening method was reported, to exhibit a full spectral range of all subtractive colors except green and black. Based upon this work, by controlling the feed ratio of two comonomers, 1,3-di-tert-butyl-3,4 propylene dioxythiophene (ProDOT-*t*Bu<sub>2</sub>) and 2,2-dimethyl-3,4 propylene dioxythiophene (ProDOT-Me<sub>2</sub>) into an acrylate based gel electrolyte matrix following our *in situ* approach<sup>30</sup> entire visible spectral range can be achieved (see **Figure 6.1**). A new approach is introduced to achieve neutral color by orienting all subtractive colors orthogonally to the electrodes. All these ProDOT based copolymers and homopolymers are highly transmissive in bleached state<sup>29,30</sup>. As a result, neutral to transmissive colored ECD with good optical contrast can be made by avoiding the synthesis of any precursor polymer.

In order to achieve the homogeneous broad absorption spectra, *in situ* approach<sup>33</sup> was used. In this method, electroactive monomers are dissolved into a polyelectrolyte solution composed of some plasticizer, salt, low molecular weight polyethylene glycol based acrylate and photoinitiator.

This approach helps to increase the success rate to fabricate large area electrochromic windows with low chemical waste<sup>12,31-33</sup>

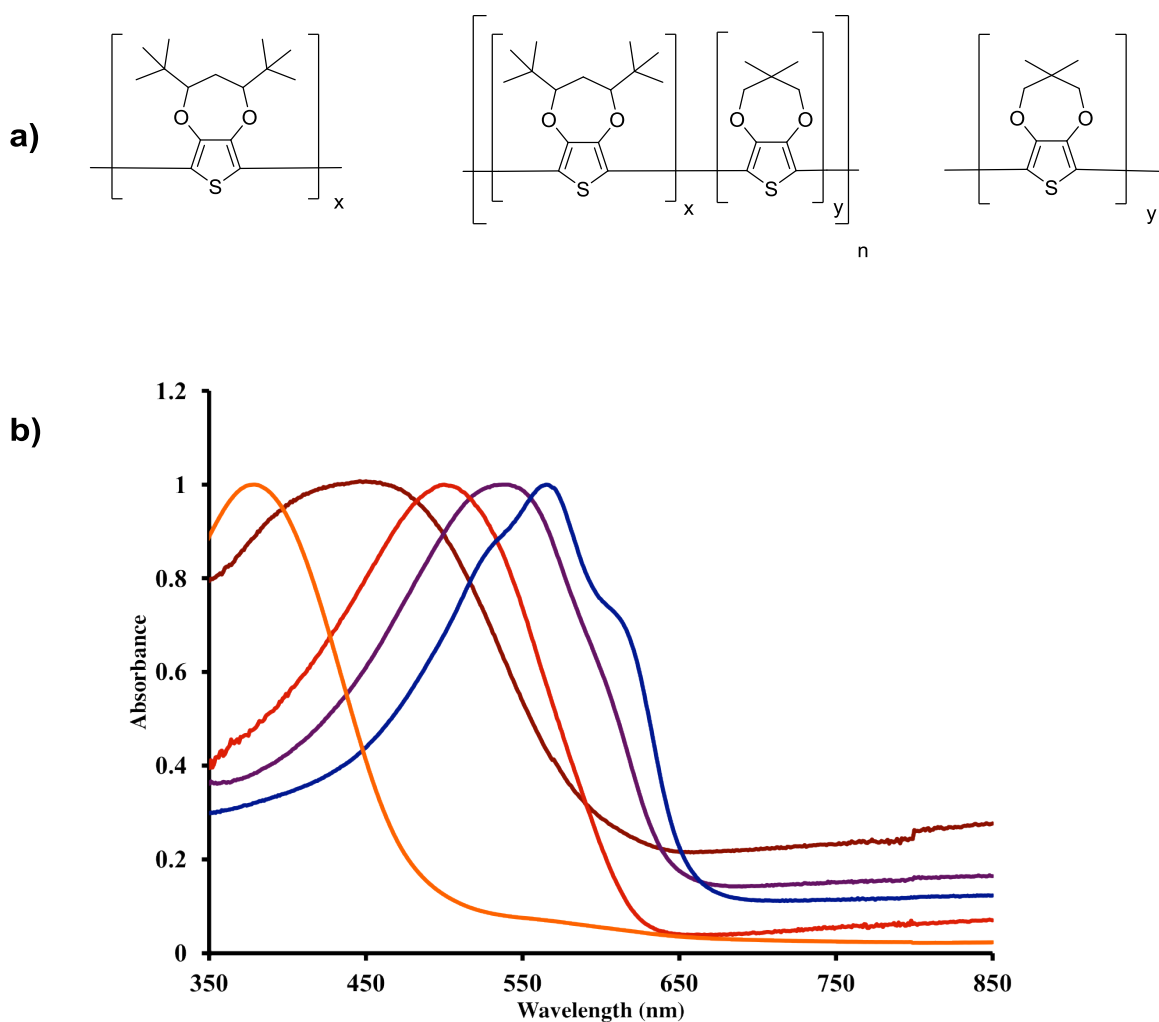


**Figure 6.1** (a) Structures of PProDOT-*t*Bu<sub>2</sub>, PProDOT-*t*Bu<sub>2</sub>-co-PProDOT-Me<sub>2</sub> and PProDOT-Me<sub>2</sub> (b) Absorption spectra of PProDOT-*t*Bu<sub>2</sub>, PProDOT-*t*Bu<sub>2</sub>-co-PProDOT-Me<sub>2</sub> (P<sub>1</sub>, P<sub>2</sub> and P<sub>3</sub> using feed ratio of ProDOT-*t*Bu<sub>2</sub> and ProDOT-Me<sub>2</sub> is 4:1, 3:2, 2:3 respectively) and PProDOT-Me<sub>2</sub> in neutral state (left to right) using *in situ* approach

## **6.2 Experimental**

### **6.2.1 Materials**

Lithium trifluoromethanesulfonate, propylene carbonate, poly(ethylene glycol) diacrylate ( $M_n = 700$ ) and 2,2-dimethoxy-2-phenyl-acetophenone (DMPAP) were purchased from Sigma Aldrich and used as received. ITO coated glass (resistance 8-12 Ohm/sq) was purchased from Delta Tech Inc. UV curable glue was purchased from Norland Products Inc. Yellow dye (Macrolex Yellow G) was purchased from Lanxess, Inc. ProDOT-Me<sub>2</sub> and ProDOT-*t*Bu<sub>2</sub> were synthesized according to reported procedures.<sup>(ref)</sup>

### **6.2.2 Preparation of gel electrolyte**

9 wt% Lithium trifluoromethanesulfonate salt was dissolved into (1:1) wt% propylene carbonate and poly (ethylene glycol) diacrylate mixture. 1.7 mg photo-initiator (DMPAP) was dissolved into per gram of liquid gel electrolyte.

### **6.2.3 Instruments**

A UV cross-linker, UVP CL-1000 was used for curing the liquid gel electrolyte. CHI 720c potentiostats was used to perform the electrochemical study. All optics studies were performed by Varian Cary 5000i UV-Vis-NIR. The corresponding color software, using 1 nm intervals of range 350-850 nm, measured color data.

#### 6.2.4 Device Fabrication

Electrochromic devices were fabricated following our *in situ* fabrication method as described in chapter 3. Here ITO coated glass and PET was used as working and counter electrode. A 3V potential bias was used to electropolymerize the monomers. And  $\pm 2$  V was applied to switch devices.

**For Dye approach:** Organic dye was dissolved into the gel electrolyte solution with 2.5wt% ProDOT-Me<sub>2</sub> monomer and placed the solution in between two ITO substrates like “sandwich method”.

**For all ECP approach:** An 1 mm thick gasket was placed around the perimeter of the conductive surface of the glass substrate to get a uniform thickness of the gel electrolyte. 1 wt% ProDOT-*t*Bu<sub>2</sub> was dissolved into the liquid polyelectrolyte and drop cast it on the ITO surface and cross-linked solid matrix was obtained by exposing UV light at 365nm (5.8mW/cm<sup>2</sup>) for 5 minutes in absence of oxygen. 10 wt% ProDOT-Me<sub>2</sub> polyelectrolyte solution was prepared and put it on top of the first layer and let the monomers diffuse for certain period of time. Another ITO coated glass substrate was placed on the top of the gel electrolyte and cured as before.

#### 6.3 Results and discussion

For dye approach: For this approach it is important to balance the ratio of absorption intensities of yellow dye to PProDOT-Me<sub>2</sub>. To obtain the minimal



effect of the yellow dye in clear state, concentration of dye needs to be optimized. And to achieve the neutral color in dark state color intensity of PProDOT-Me<sub>2</sub> needs to be optimized by controlling the polymerization time. The 0.17 mg of yellow dye into 1 gm of polymer gel electrolyte produces neutral color in both states at 30s polymerization time. By converting the ProDOT-Me<sub>2</sub> monomer for longer period more PProDOT-Me<sub>2</sub> will form and it will be close to the blue color. The highest photopic contrast achieved for neutral-to-neutral colored ECD was 30 % without background correction.

For all ECP approach: To achieve a continuum copolymers and homopolymers inside a solid electrochromic device in one step, ProDOT-*t*Bu<sub>2</sub> and ProDOT-Me<sub>2</sub> were dissolved into polyelectrolyte solution separately. ProDOT-*t*Bu<sub>2</sub> (1st layer) solution was casted on top of an ITO substrate, formed solid matrix by UV irradiation; ProDOT-Me<sub>2</sub> (2nd layer) solution was casted on top of the solid 1st layer and two monomers were allowed to diffuse, to form the concentration gradient. Once the desired concentration gradient is achieved, counter electrode was placed on top and cured the 2nd layer. By applying 3V potential bias electropolymerization was carried out and  $\pm 2$  V was applied to switch devices.

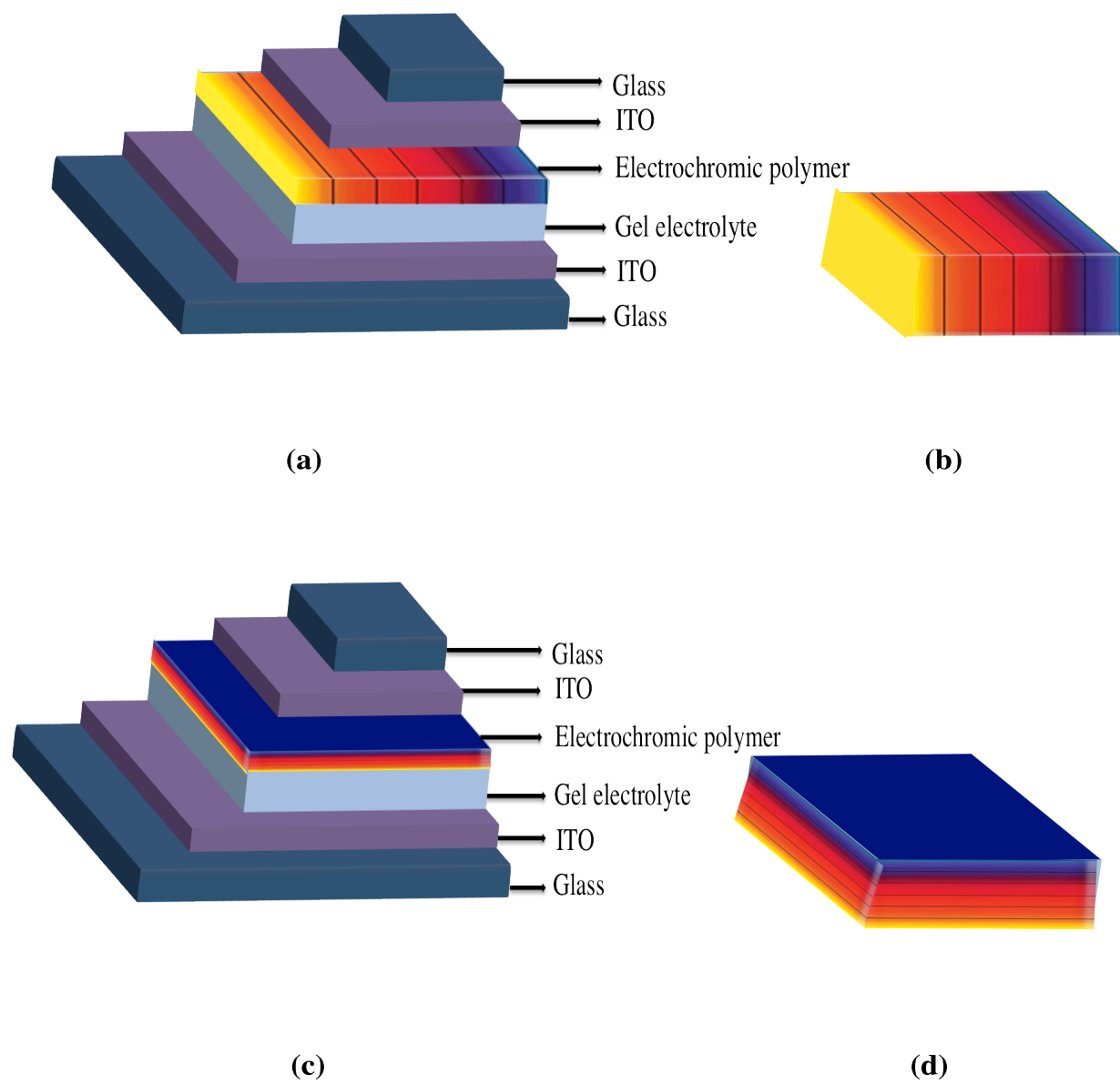


**Figure 6.2.** Schematic diagram of electrochromic window where subtractive color spectrum is (a) horizontal and (c) orthogonal on ITO, (b) and (d) shows the close-up view of electrochromic layer.

To achieve the neutral absorption spectra in neutral state using this abovementioned approach, the diffusional gradient of two monomers need to be controlled. According to Fick's second law, the distance traveled by the electroactive species depends on its diffusion coefficient and diffusion time.

$$x = (2Dt)^{1/2}$$

where x is the distance (in meter) traveled by the electroactive species at t time (in second), D is the diffusion coefficient (in  $\text{m}^2\text{s}^{-1}$ ) of the electroactive species. The value of D also depends on the concentration of electroactive species<sup>29,31</sup>.

To carry out this experiment following parameters are needed to be controlled/optimized: i) thickness of the monomer gel electrolyte layer, ii) concentration of each monomer and iii) diffusion time. To maintain the simplicity, the thickness of the monomer gel electrolyte and the concentration of the monomers were kept constant throughout the experiment. 1 mm thick gasket was used to maintain the thickness of the first layer. Here 1 wt% ProDOT-*t*Bu<sub>2</sub> and 10 wt% ProDOT-Me<sub>2</sub> in gel electrolyte layer was used as the 1st layer and 2nd layer respectively. 10 wt% concentration of ProDOT-Me<sub>2</sub> was chosen as the diffusion coefficient of ProDOT-Me<sub>2</sub> is very close to the saturation limit in the solid polyelectrolyte matrix.<sup>34</sup> Any other solvents like propylene carbonate or acetonitrile were not used to dissolve ProDOT-Me<sub>2</sub> monomer to reduce the swollen effect of the cross-linked polymer matrix.

Monomers were not used as reversed layer because of mainly two reasons, a) the diffusion coefficient of ProDOT-Me<sub>2</sub> is about 2.63 times higher than ProDOT-*t*Bu<sub>2</sub><sup>31</sup> and b) it is hard to dissolve high wt% of ProDOT-*t*Bu<sub>2</sub> into the polyelectrolyte solution. **Figure 6.3** depicted the schematic diagram of the stepwise experimental method.

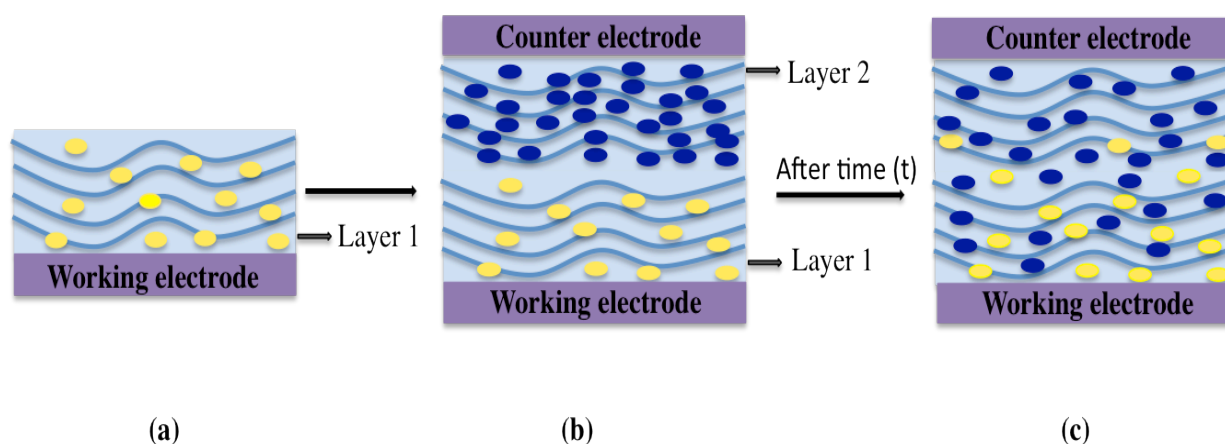
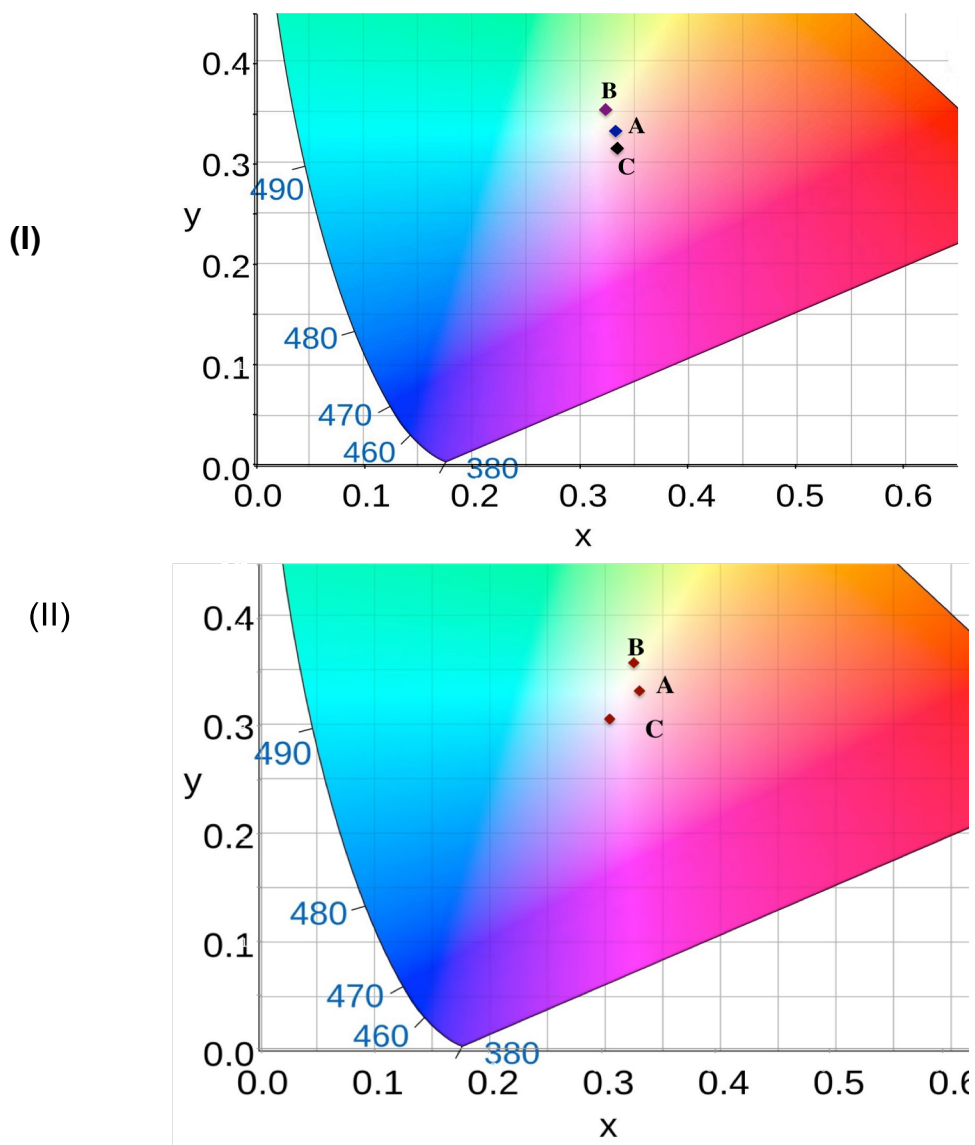


**Figure 6.3.** Schematic diagram of stepwise assemble method (a) polyelectrolyte with 1wt% ProDOT-*t*-Bu<sub>2</sub> (Layer 1) drop casted on ITO surface and cured under UV light, (b) 10 wt% ProDOT-Me<sub>2</sub> into polyelectrolyte (Layer 2) casted on top of layer 1, (c) after time (t) monomers diffused from one layer to another

Distance traveled by 10 wt% ProDOT-Me<sub>2</sub> monomers inside solid gel electrolyte matrix was measured following the diffusion study experiment set up. Here, solid polymer gel matrix (without any monomer) was formed

in between two ITO coated substrate. A hole was created in the middle of solid polymer gel matrix. 10 wt% PProDOT-Me<sub>2</sub> was dissolved into liquid electrolyte and the hole was filled with this monomer gel electrolyte. Then monomers were allowed to travel into the solid matrix for time (t). After time (t) liquid from the hole was pipetted out and applied 3V potential to oxidized the monomers. It was found that 10wt% ProDOT-Me<sub>2</sub> needs 3 hours to diffuse 1 mm. Same experiment was carried out by adding 1wt% ProDOT-*t*Bu<sub>2</sub> into solid polymer gel matrix. It was noticed that there is no significant change in diffusion in presence of ProDOT-*t*Bu<sub>2</sub> into the solid polymer matrix.

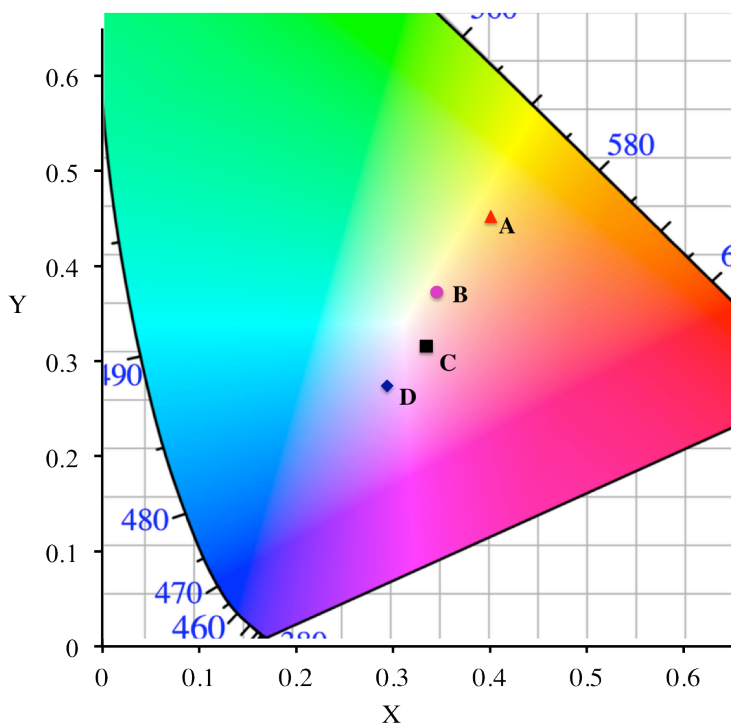
An ECD was assembled as mentioned in **Figure 6.3**, where 1wt% ProDOT-*t*Bu<sub>2</sub> and 10wt% ProDOT-Me<sub>2</sub> were used as 1<sup>st</sup> and 2<sup>nd</sup> layer respectively. And the monomers were allowed to diffuse between two layers for 3 hours before polymerization, so ProDOT-Me<sub>2</sub> has enough time to reach the working electrode. The absorption spectrum of each redox state was taken after switching the ECD using  $\pm 2$  V. A broad absorption spectrum was found which corresponds to neutral color. Color coordinate indicates that about 3 hours diffusion time provided us the neutral color at both redox states. **Figure 6.4(II)** represents the color coordinates for the dark to transmissive state of a neutral to transmissive electrochromic device assembled via *in situ* method.



**Figure 6.4** (I) Color coordinates of A) achromatic white point, (B) and (C) represents bleached and dark state respectively for the neutral-to-neutral ECD assembled via yellow dye approach (top).

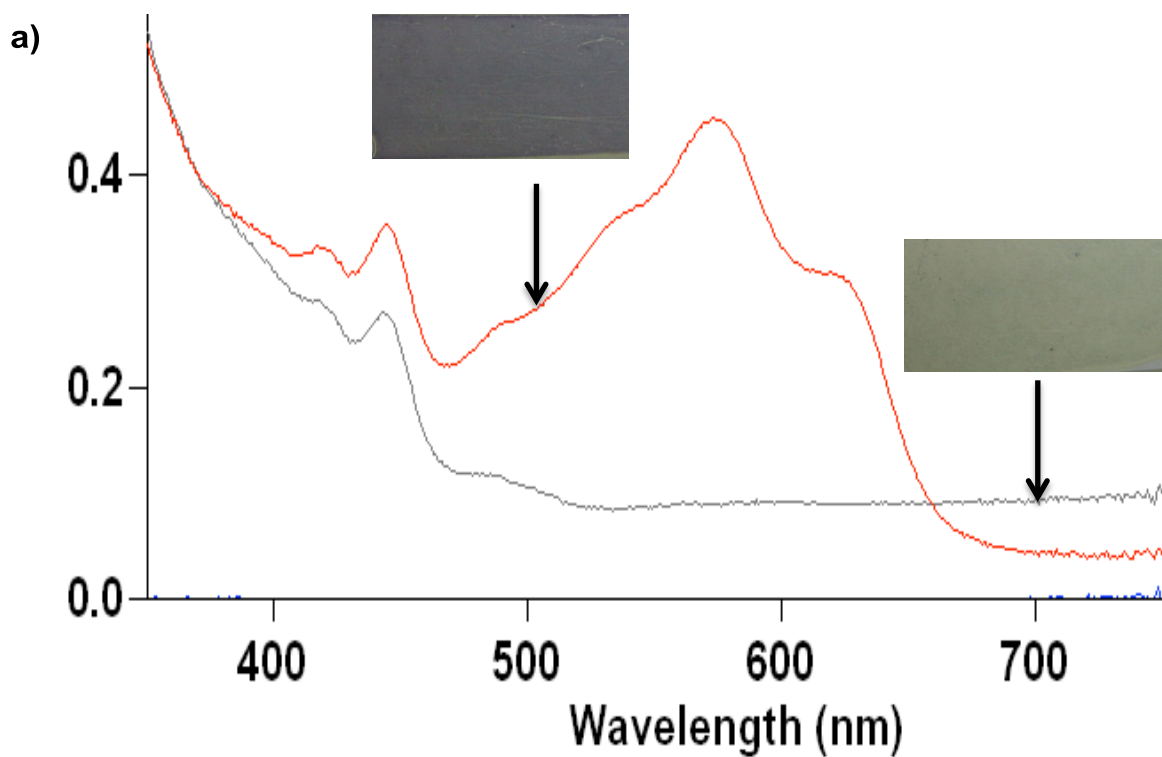
(II) Color coordinates of A) achromatic white point (in blue), (B) and (C) represents transmissive (in red) state and dark state (in black) of the neutral-to-neutral ECD respectively using all ECPs (bottom).

This diffusion time needs to be controlled based upon the concentration of the monomers and thickness of solid gel electrolyte layer; otherwise mostly PProDOT-*t*Bu<sub>2</sub> or PProDOT-Me<sub>2</sub> will be formed for too short or too long waiting period. **Figure 6.5** shows CIE color co-ordinates of different ECD at colored state using abovementioned monomer concentrations and 1 mm polymer gel thickness, where the diffusion time is 0 hrs, 1.5 hrs, 3 hrs and 5 hrs respectively.



**Figure 6.5** Color coordinates of the ECD in dark state at different diffusion time interval 0hr, 1.5hr, 3hr and 5hr denoting by A, B, C and D respectively

The highest photopic contrast was achieved is 30% (24%T in dark state and 53%T in oxidized state) with <2 second switching speed. **Figure 6.6 (b)** shows the absorption spectra and pictures of each redox state.





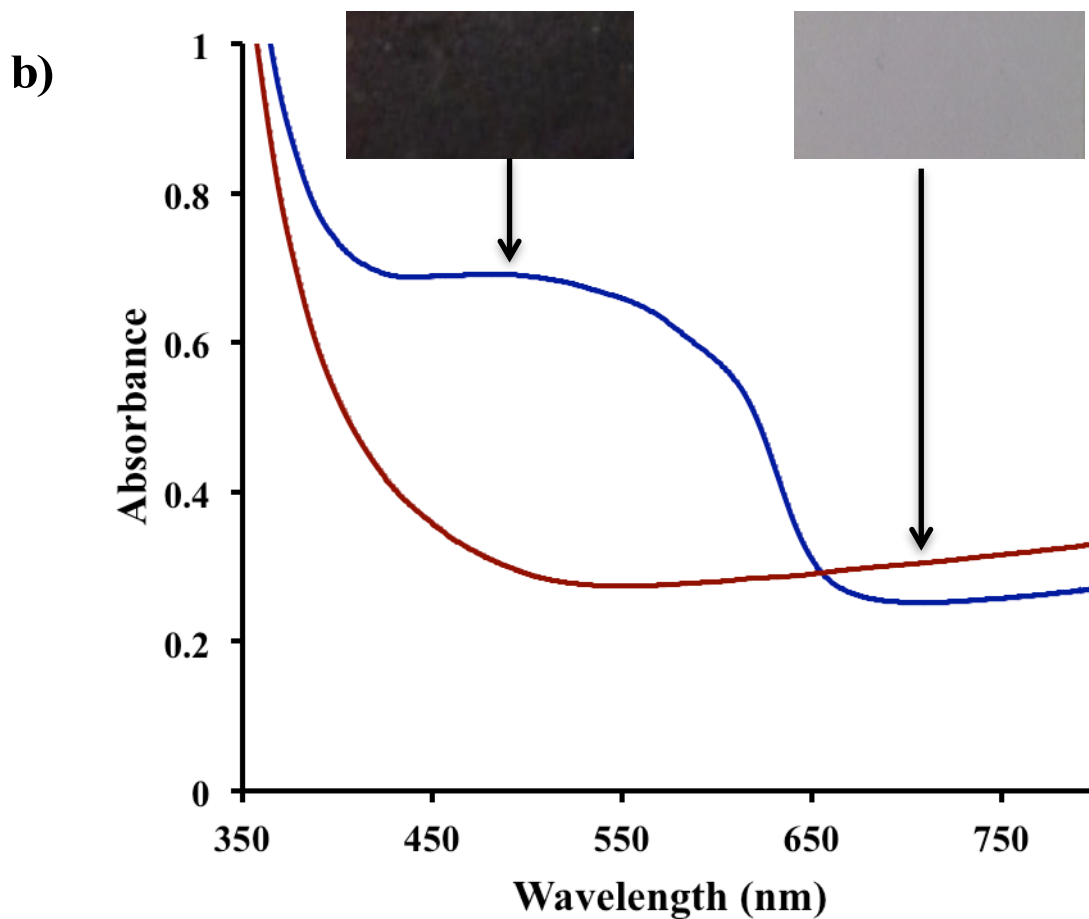


**Figure 6.6** (a) absorbance spectra of dark (red) and transmissive (grey) state using yellow dye approach, and (b) Absorbance spectra of dark (blue) and transmissive (red) state using all ECPs approach; images of corresponding dark and transmissive state of neutral EC devices assembled via *in situ* method are shown

## 6.4 Conclusion

In summary, simple one step method is established to achieve neutral-to-neutral color using *in situ* approach. Neutral to neutral colored ECD with 30%T photopic contrast was achieved without any background correction. It helps greatly to reduce the synthetic and the processing difficulties for the electrochromic precursor or polymers. As there is no need to use the electrolyte bath to form the electrochromic polymer or spray coat the precursor polymer, the success rate of ECD fabrication is high as well. By using inject printing or other sophisticated processing methods, uniform thinner monomer electrolyte layer can be created, As a result large area neutral color ECD can be fabricated in short time period.

## References

- (1) Beaujuge, P. M.; Ellinger, S.; Reynolds, J. R. *Adv. Mater.* **2008**, *20*, 2772.
- (2) Argun, A. A.; Aubert, P. H.; Thompson, B. C.; Schwendeman, I.; Gaupp, C. L.; Hwang, J.; Pinto, N. J.; Tanner, D. B.; MacDiarmid, A. G.; Reyanols, J. R. *Chem. Mater.* **2004**, *16*, 4401.
- (3) Matsushita, S.; Jeong, Y. S.; Akagi, K. *Chem Commun* **2013**, *49*, 1883.
- (4) Yao, Z.; Di, J.; Yong, Z.; Li, Q. *Chem Commun* **2012**, *48*, 8252.
- (5) Zhang, X.; Steckler, T. T.; Dasari, R. R.; Ohira, S.; Potscavage, W. J.; Tiwari, S. P.; Copp, S.; Ellinger, S.; Barlow, S.; Kippelen, B.; Reyanols, J. R. *J. Mater. Chem.* **2010**, *20*, 123.
- (6) Sonmez, G.; Shen, C. K.; Rubin, Y.; Wudl, F. *Angew Chem Int Ed Engl* **2004**, *43*, 1498.
- (7) Hamed, M.; Forchheimer, R.; Inganas, O. *Nat Mater* **2007**, *6*, 357.
- (8) Liu, R.; Duay, J.; Lee, S. B. *ACS Nano* **2010**, *4*, 4299.
- (9) Cirpan, A.; Argun, A. A.; Grenier, C. R. G.; Reeves, B. D.; Reyanols, J. R. *J. Mater. Chem.* **2003**, *13*, 2422.
- (10) Tehrani, P.; Hennerdal, L. O.; Dyer, A. L.; Reynolds, J. R.; Berggren, M. *Journal of Materials Chemistry*. **2009**, *19*, 1799.
- (11) Invernale, M. A.; Ding, Y.; Sotzing, G. A. *ACS Appl. Mater. Interfaces*. **2010**, *2*, 296.
- (12) Ding, J.; Invernale, M. A.; Sotzing, G., A. *ACS Appl. Mater. Interfaces*. **2010**, *2*, 1588.
- (13) Monk, P. M. S.; Mortimer, R. J.; Rosseinsky, D. R.; Cambridge University Press: 2007, p 483.
- (14) Mortimer, R. J.; Dyer, A. L.; Reynolds, J. R. *Displays* **2006**, *27*, 2.
- (15) Balasubramanian, R.; Bouman, C. A.; Allebach, J. P. *J. Electron. Imaging* **1994**, *3*, 45.

- (16) Sonmez, G. *Chemical communications (Cambridge, England)*. **2005**, 5251.
- (17) Beaujuge, P. M.; Ellinger, S.; Reynolds, J. R. *Nat Mater* **2008**, 7, 795.
- (18) Iclia, M.; Pamuk, M.; Algi, F.; Onal, A. M.; Cihaner, A. *Org. Electron.* **2010**, 11, 1255.
- (19) Lee, K. R.; Sotzing, G., A. *Chem Commun* **2013**, 49, 5192.
- (20) Vasilyeva, S. V.; Beaujuge, P. M.; Wang, S.; Babiarz, J. E.; Ballarotto, V. W.; Reynolds, J. R. *ACS Appl. Mater. Interfaces*. **2011**, 3, 1022.
- (21) Shi, P.; Amb, C. M.; Knott, E. P.; Thompson, E. J.; Liu, D. Y.; Mei, J.; Dyer, A. L.; Reynolds, J. R. *Adv Mater* **2010**, 22, 4949.
- (22) Roncali, J. *Macromol. Rapid Commun.* **2007**, 28.
- (23) Fei, Z.; Shahid, M.; Yaacobi-Groos, N.; Rossbauer, S.; Zhong, H.; Watkins, S. E.; Anthopoulos, T. D.; Heeney, M. *Chem Commun* **2012**, 48, 11130.
- (24) Almeataq, M. S.; Yi, H.; Al-Faifi, S.; Alghamdi, A. A. B.; Iraqi, A.; Scratt, N. W.; Wang, T.; Lidzey, D. G. *Chem Commun* **2011**, 49, 2252.
- (25) Izuhara, D.; Swager, T. M. *J. Mater. Chem.* **2011**, 21, 3579.
- (26) Unur, E.; Beaujuge, P. M.; Ellinger, S.; Jung, J. H.; Reynolds, J. R. *Chem Mater.* **2009**, 21, 5145.
- (27) Shin, H.; Kim, Y.; Bhuvana, T.; Lee, J.; Yang, X.; Park, C.; Kim, E. *ACS Appl. Mater. Interfaces*. **2012**, 4, 185.
- (28) Oktem, A.; Balan, A.; Barana, D.; Toppare, L. *Chem. Commun.* **2011**, 47, 3933.
- (29) Alamar, F. A.; Otley, M. T.; Ding, J.; Sotzing, G., A. *Adv. Mater.* **2013**, 25, 6256.
- (30) Dey, T.; Invernale, M. A.; Ding, Y.; Buyukmumcu, Z.; Sotzing, G. A. *Macromolecules* **2011**, 44, 2415.

- (31) Kumar, A.; Otley, M. T.; Alamar, F. A.; Zhu, Y.; Sotzing, G. A. *J. Mater. Chem. C* **2014**, 2, 2510.
- (32) Zhu, Y.; Otley, M. T.; Alamar, F. A.; Kumar, A.; Zhang, X.; Mamangun, D. M. D.; Li, M.; Arden, B. G.; Sotzing, G. A. *Org. Electron.* **2014**, 15, 1378.
- (33) Alamar, F. A.; Otley, M. T.; Zhu, Y.; A., K.; Sotzing, G. A. *Solar Energy Materials and Solar Cells* **2015**, 132, 131.

## **Chapter 7**

### **Development of Flexible Electrode for Photonic application**

**Abstract:** Electrochromic devices were prepared and characterized using flexible free-standing conductive fiber mat as working electrode. Conductive nanofibers were made by coating electrospun poly(ethylene terephthalate)-silica nanocomposite with poly[3,4-ethylenedioxythiophene]-poly[styrene sulfonate (PEDOT-PSS). Electrochromic polymers: [PEDOT], poly(2,2-dimethyl-3,4-propylenedioxythiophene) [PProDOT-Me<sub>2</sub>], poly[2,2'-bithiophene] and random copolymer of 2,2-dimethyl-3,4-propylenedioxythiophene-co-1,3 di-*t*-butyl-3,4-propylenedioxythiophene [PProDOT-Me<sub>2</sub>-co- PProDOT-*t*Bu<sub>2</sub>] were formed on conductive nanofibers via electrodeposition method. Sheet resistance, luminance and electrochromic layer thickness were evaluated for conductive fibers. Switching speed of electrochromic layer on non woven fiber mat with sheet resistivity 90 ohm/sq was reported as <5 mins for an 4cm<sup>2</sup> active area.

## 7.1 Introduction

A recent research interest has been noticed in the smart flexible, wearable, fashionable textile industry<sup>1-4</sup>. Several prototypes were developed by different industries like Philips, Levis, Nokia, SmarTex etc<sup>5</sup>. A flexible electrode using paper substrate was developed by Reynolds group<sup>6</sup>. A reflective-type electronic device was reported using electrochromic materials on conductive fabrics by Sotzing's group<sup>7</sup>. This electrochromic material has advantages over photochromic color changing fabrics due to

the ability of fast switching speed between two-color states and availability of several colors<sup>8,9</sup>.

A conductive fabric can be made by several ways like soaking, spin coating, melt processing, and spray coating the conductive materials on fabric<sup>10-12</sup>. Because of the flexibility, lightweight and ease of processability conductive polymers become ideal choice for electrochromic substrate<sup>7,13,14</sup>.

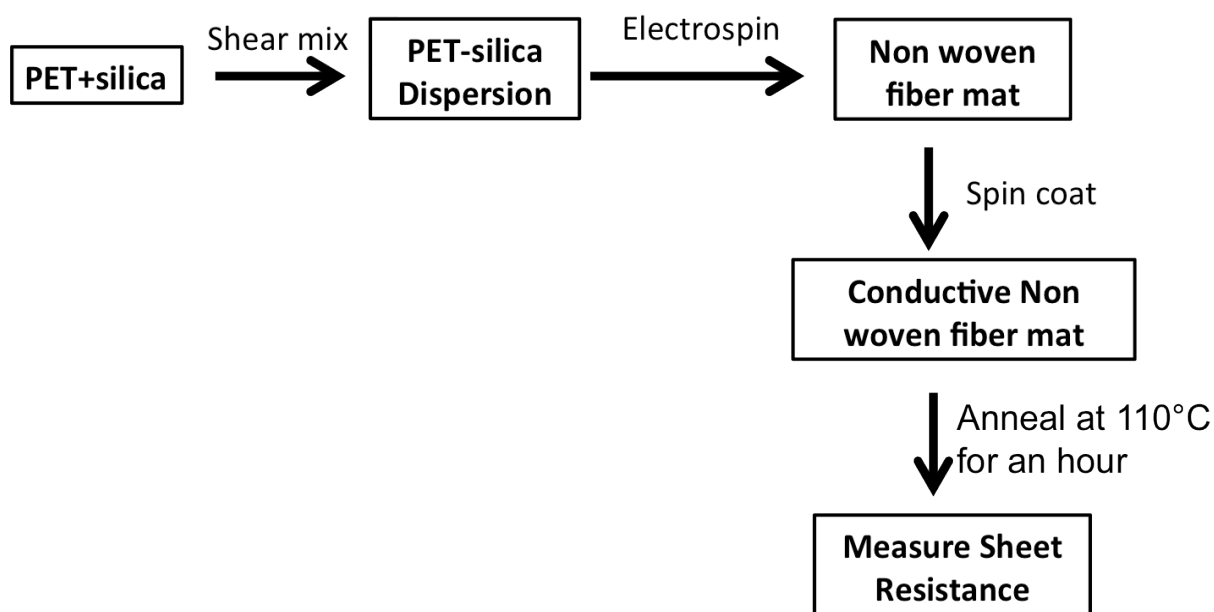
Poly[3,4-ethylenedioxythiophene]-poly[styrene sulfonate], [PEDOT-PSS] has distinct advantages over other conductive systems such as polypyrrole<sup>15</sup>, polyaniline, carbon nanotubes etc.<sup>16</sup> as it's being environmentally stable, easily processable as a film, low cost and relatively transparent<sup>17-20</sup>. Oxidize state of PEDOT is conductive; it is used as an optically transparent conductive material. PEDOT can be synthesis using electrochemically or chemically but the solubility of this polymer into organic solvent is an issue. Bayton P, an ion-complex material was developed by Bell Lab. This is a dark blue colored water dispersion of PEDOT along with polystyrenesulfonate (PSS). This polyanionic part helps to stabilize the oxidized form of PEDOT. PEDOT-PSS is commercially available and different company produces with different conductivity using different commercial sources like Ogacon, Clevios etc. In this study our focus is to make a free-standing conductive fiber mat as a replacement of indium-doped tin oxide (ITO) and assemble an electrochromic device using electrochromic materials. Here in this study several EC materials<sup>21-23</sup> could



be used out of which bithiophene, ProDOT-Me<sub>2</sub> and ProDOT-*t*-Bu<sub>2</sub> was used to study the electrochemical properties. ECDs were assembled using conductive non woven mesh as working electrode via both traditional electrodeposition method and *in situ* method<sup>24</sup>.

Poly (ethylene terephthalate), [PET] is a widely used thermoplastic polymer used to make films and fibers because of its thermal stability, spinnability and chemical resistance. In a separate study, it is noticed that the incorporation of 3 wt% silica nanoparticles inside the PET nano fibers decreases the sheet resistance drastically. To make our conductive nanofibers, a dispersion of PET and silica nanoparticles was prepared by shearing. Then by controlling the electrospinning parameters a fabric mesh was prepared with a desired fiber diameter. SEM was taken to measure the diameter of the fibers and TEM images were taken to analyze how well the silica particles were dispersed inside the fibers. This mesh is simply spin coated with a dispersion of PEDOT-PSS, doped with 5wt% DMSO<sup>8</sup> to lower the sheet resistance and annealed at 110°C for an hour. It was noted that using secondary dopant and annealing process helps to increase the conductivity of PEDOT-PSS film. Other secondary dopants like sorbitol, glycerol etc. could be used to increase the conductivity of PEDOT-PSS film. The exact explanation that helps to increase the conductivity is still controversial. It could be because the dopant will be evaporated after annealing and that will help the electron hopping process<sup>26,27</sup>. Shearing time and electrospinning time was optimized to achieve better sheet resistance of

fiber mesh. In case of reflective type ECDs, besides high conductivity, minimum coloration is desirable for fabric electrodes. For this reason optimization of the sheet resistance was carried out as a function of luminance. The concentration of conductive polymer was controlled to establish a relation between sheet resistance ( $R_s$ ) and color coordinates.



**Scheme 7.1** Schematic diagram for making conductive fiber mesh

## 7.2 Experimental

### 7.2.1 Materials

Polyethylene terephthalate ( $M_v=30,000$ )(PET) was bought from Scientific Polymer. Acetonitrile, propylene carbonate, poly ethylene glycol diacrylate ( $M_n=700$ ), lithium trifluoro methane sulfonate (LiTRIF), dimethoxyphenylacetophenone (DMPAP), dimethyl sulfoxide (DMSO), 2,2'

bithiophene and lithium hydride were purchased from Sigma-Aldrich, silica nanoparticles with surface area  $200\text{m}^2/\text{g}$ , average particle size  $12\text{nm}$  was purchased from AEROSIL. ORGACON S300 and CLEVIOS PH1000 PEDOT-PSS were bought from Agfa and Heraeus, respectively. The metal mesh was from ITP GmbH as generous gift. Copper tape was purchased from Newark. Dichloromethane (DCM) & trifluoroacetic acid (TFA) was from Fisher.

### **7.2.2 Preparation of PET-silica dispersion**

PET was dissolved into TFA and DCM mixture (1:1) wt ratio. 3 wt% silica nano particles were dissolved into this solution. To get a better dispersion the solution was shear mixed.

### **7.2.3 Electrospinning conditions**

A typical electrospinning set up was arranged using model# syringe pump to inject the polymer solution and model## as high voltage power supply. The injection speed of the polymer solution through 18"G needle syringe was  $3\text{ml/hr}$ . The working distance between the electrode and glass collector was  $15\text{ cm}$  and the applied voltage was  $15\text{kV}$ .

### **7.2.4 Spin coating conditions**

A  $2.5\text{cm} \times 2.5\text{cm}$ , PET-silica nanofiber covered glass substrate was placed inside the Spincoater model P6700 and spin coated with 100, 50,

25, 10 wt% of orgacon PEDOT-PSS diluted by distilled water, 5wt% DMSO with respect to PEDOT-PSS solution using 600 rpm for 60 seconds.

#### **7.2.5 Electrochemical study**

Electrochemical conversion of electroactive monomers to conjugated polymers was carried out by CHI700C and 400A. For electrodeposition of electrochromic polymers on the conductive nanofibers, 0.1M LiTRIF/ACN solutions were used as an electrolyte solution. Lithium hydride inside a porous glass tube was placed into the electrolyte solution. For electrodeposition of electrochromic polymer a 10 mM monomer solution was used.

**7.2.6 Colorimetric analysis:** A PR-670 colorimeter was used to analyze the colors and the luminance of different samples. A reference was run on only PET-silica fiber mesh (without PEDOT-PSS) on white background under D65 standard illuminant lamp inside a black box. 360-860 nm measurement range with 1 nm intervals and a 1/2degree aperture MS-5X zoom lens was used.

#### **7.2.7 Conductivity measurement**

A four-line was used to measure the sheet resistance varying the applied current. Keithley 224 was used as current source. At least 10 data points were taken per sample.

### **7.2.8 Scanning electron microscopy (SEM)**

SEM imaging was done on the Jeol JSM-6335F at 2.5 kV, probe current: 14  $\mu$ A to induce charging on the surface of a cross-sectioned sample. Charging allowed differentiation between the conducting and non-conducting regions via charge contrast imaging. Cross-sectioning was done by cutting the free-standing fiber mesh submerged in liquid nitrogen with a razor blade.

### **7.2.9 Transmission Electron Microscopy characterization**

Bright field TEM images were taken using a FEI Tecnai-T12 at 80 kV. EDS measurements were performed on a EDAX silicon crystal detector (30 mm<sup>2</sup>) operated by FEI TIA software. EDS was used to identify the SiO<sub>2</sub> within the PET fiber cross-sections.

PET fiber mesh was cut into 2 mm X 6 mm sections that were then embedded into an epoxy resin (SPI-Chem Araldite 6005 kit), and cured at 80°C for at least 12 hours. Next, samples were cut into ultrathin sections, 20  $\mu$ m, slices using 45° Diatome diamond blade on a Reichert–Jung Ultra Cut E microtome and collected on a 400 mesh carbon coated copper grids. Excess water was wicked off of the copper grid/sample then TEM was immediately done.

### **7.2.10 Device assembly**

Once the electrochromic polymer was deposited on PET-silica conductive nanofiber, substrates were washed with ACN and allowed to dry in air. A

gel electrolyte solution (5g PC, 5 g PEGDA, 1g LiTRIF, 17.5 mg DMPAP) was drop casted on it and another piece of ITO coated PET or metal mesh was placed on top of it. Whole assembly was exposed under 365 nm UV light for 5 minutes to make a crosslinked polymeric gel matrix.

## **7.3 Results and Discussion**

### **7.3.1 Optimization of PET loading to prepare fiber**

To prepare the PET –silica fibers, 3wt% of silica nanoparticles were dispersed into 15wt% PET solution according to section 6.2.2. Electrospinning of the above solutions were carried out following section 6.2.3 using aluminum foils as collectors. Diameter of the fibers was measured using the SEM analysis. Average diameters for 10wt%, 15wt% and 20wt% PET-silica fibers are about 0.42 $\mu$ m, 1.18  $\mu$ m and 1.69  $\mu$ m respectively. Due to the intermediate values, 15wt% PET-silica fibers were chosen for rest of the studies. SEM images were taken for fibers made with 15 wt% PET with and without silica nanoparticles and it is clear that the sample without silica has a smoother surface compare to other. **Figure 7.1** shows the SEM images of 15 wt% PET fiber with and without silica. TEM images were taken and shown in **Figure 7.2**. It confirms the presence of silica particles on surfaces.

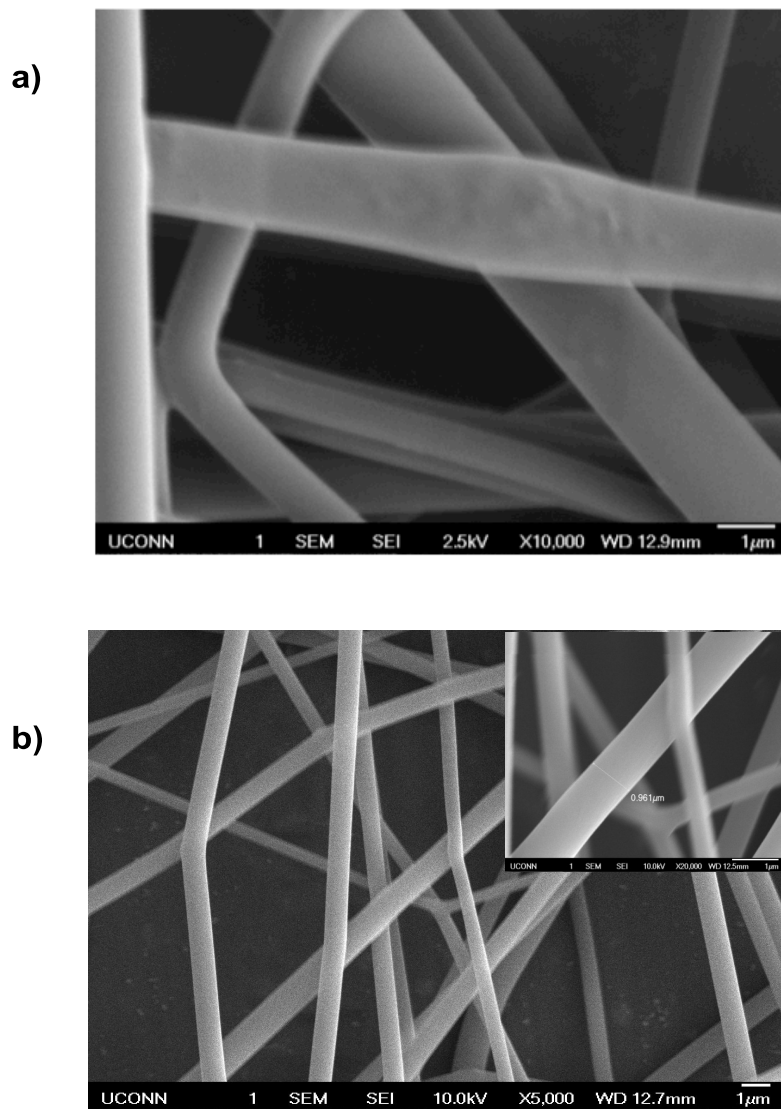


**Figure 7.1** a) and b) are SEM images of 15wt% PET fiber mesh with and without silica.

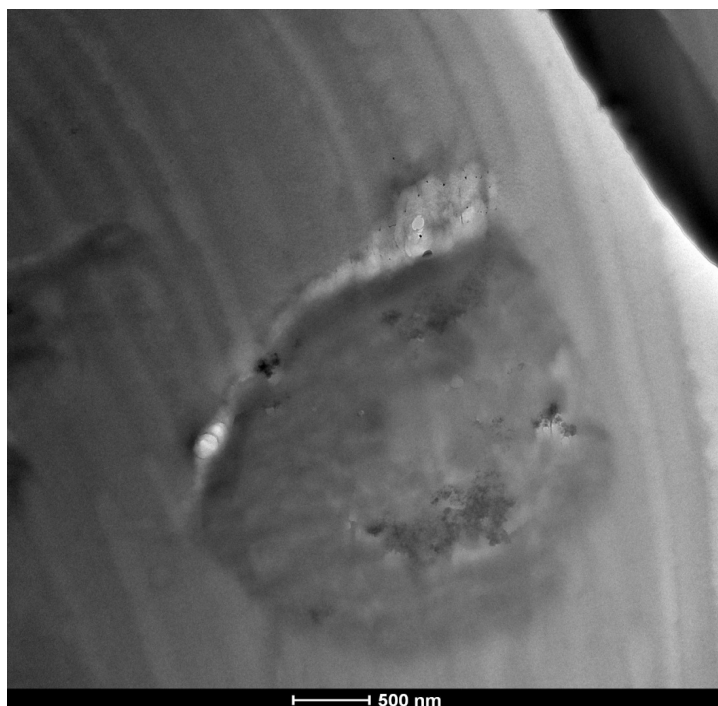


**Figure 7.2** TEM image of silica nanoparticles on surface of 15wt% PET fiber mat

### 7.3.2 Optimization of shearing time

To get a good dispersion of silica particles inside the PET solution 5, 10 and 15 minutes shearing time was used and fiber mesh was collected on glass using 2 minutes electrospinning time. CLEVIOS PEDOT-PSS was used to spin coated the substrates using 600rpm for a minute and sheet resistance was measured using 4-probe line. From **Table 7.1**, it is clear



that longer shear time improves the sheet resistance of the mesh. Longer shearing time, > 15 minutes was not tried due to significant solvent loss.

**Table 7.1** Relation between shearing time of PET-silica dispersion and sheet resistance of corresponding fiber mat coated with PEDOT-PSS (Clevios) with 5wt% of DMSO for a minute at 600rpm

Formulation	Electrospinning time (min)	Shearing Time (min)	Average sheet resistance $R_s$ (ohm/sq)
15wt%PET-3wt%silica	2	5	250
15wt%PET-3wt%silica	2	10	151
15wt%PET-3wt%silica	2	15	99

### 7.3.2 Optimization of run time and waiting time

To get a freestanding flexible mesh electrospinning time was increased from 2 minutes to 10 minutes keeping the flow rate (3ml/hr) and applied voltage (15kV) constant. This mesh was made conductive using abovementioned

method and sheet resistance was measured. The sheet resistance was increased from 99 ohm/sq to 167 ohm/sq. As the thickness of the fiber mesh obtained after 10 min electrospinning is around 0.2mm and during spin coating process, there was no waiting period, so the PEDOT-PSS can penetrate through the sample. To resolve this problem, after drop casting PEDOT-PSS on top of mesh inside the spin coater and started to wait which is denoted as “waiting time”. It was noticed that by increasing the waiting time prior spun coating improved sheet resistance. The sheet resistance value reaches to threshold at 34 ohm/sq at 45 minutes. **Table 7.2** shows the relation between waiting time and sheet resistance of conductive mesh made of 15wt% PET-3wt% silica for 10 minutes electrospinning run time. To improve the sheet resistivity, electrospinning run time was increased to 8 hour to get a densely packed fiber mat. By following the same above-mentioned procedure a conductive fiber mesh was prepared with sheet resistivity 3 ohm/sq. But because of brittle nature of PEDOT, it was not possible to make a flexible electrode using that low sheet resistive (3 ohm/sq) non woven mat.

**Table 7.2** Relation between sheet resistance and waiting time prior spin coating of PEDOT-PSS (Clevios) with 5wt% of DMSO on PET-silica non woven fiber mat

Formulation	Run time(min)	Waiting time(min)	$R_s$ ohm/sq
15%PET-3%silica	2	0	99
15%PET-3%silica	10	0	167
15%PET-3%silica	10	2	152
15%PET-3%silica	10	10	95
15%PET-3%silica	10	15	80
15%PET-3%silica	10	45	34

#### 7.3.4 Relation between sheet resistance and luminance of conductive mesh

As per application purpose luminance needs to be optimized based on sheet resistance. PEDOT-PSS, itself has a dark blue color and PEDOT-PSS from CLEVIOS has a darker color than ORGACON. Color coordinates (LAB) on 15wt% PET-silica fibers electrospun by CLEVIOS and ORGACON solution doped with 5wt% DMSO for a minute at 600 rpm are (0.0464, -0.0300,-0.1279) and (0.0925,-0.0418, -0.1104) respectively. Corresponding average sheet resistance value for both substrates were 34 ohm/sq and 90 ohm/sq. Although the sheet resistance for PET-silica mesh

made from ORGACON is higher than CLEVIOS, it was chosen as this has close value compare to ITO coated PET ( $R_s=60$  ohm/sq).

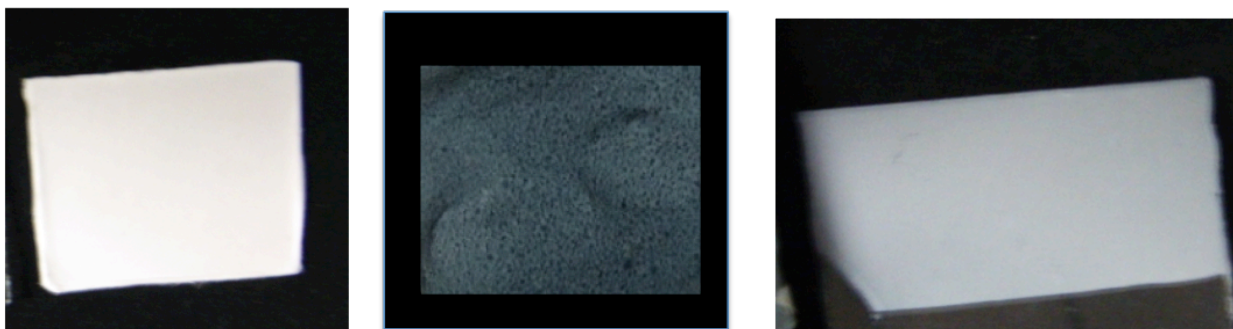


**Figure 7.3** PET non woven mat (a) before PEDOT-PSS coating, (b) after Clevious PEDOT-PSS coating, (c) after Orgacon PEDOT-PSS coating

To get minimal color interferences from the PEDOT-PSS, the rest of the studies were carried out using ORGACON solution. To establish a relation between sheet resistance and luminance, various concentration of ORGACON PEDOT-PSS, diluted with 0wt%, 50wt%, 75wt%, and 90wt% distilled water were prepared and doped by using 5wt% DMSO. 15wt% PET-silica fiber mesh, collected on glass substrate was spun coated with abovementioned PEDOT-PSS solution using 600rpm for a minute. The sheet resistance ( $R_s$ ) and color co-ordinates (LAB) were measured and shown in **Table 7.3**. Thicknesses of the mesh were about 0.20mm and all LAB were reported using a reference fiber mesh without any PEDOT-PSS. It can be seen that the  $R_s$  value is going down by increasing the

concentration of the PEDOT-PSS but at the same time the samples are getting enhanced color.

**Table 7.3** Relation between various concentration of ORGACON PEDOT-PSS with luminance and  $R_s$

Sample #	wt% of PEDOT-PSS	Color coordinates (LAB)	Sheet resistance $R_s$ (ohm/sq)	EC polymer deposition
1	100	0.0925, - 0.0418, -0.1104	90	Deposited
2	50	0.1146, - 0.0534, - 0.1234	177	Deposited
3	25	0.1419, - 0.0672, -0.142	688	Not deposited
4	10	0.1566, 0.0779, -0.1411	5805	Not deposited

### 7.3.5 Electrochemical study

All of these four different types conductive fiber mesh were placed inside a typical electrolyte bath setup using 2,2-dimethyl-3,4-propylenedioxythiophene [ProDOT-Me<sub>2</sub>]/ACN monomer solution. A cyclic voltagram was carried out to deposit PProDOT-Me<sub>2</sub> on several conductive substrates using 0 to +1.7V potential at 50 mV scan rate. For sample 3 and 4 deposition of PProDOT-Me<sub>2</sub> was not observed because of low conductivity. But for sample 1 and 2 electrochromic polymerization of PProDOT-Me<sub>2</sub> occurred and the cyclic voltagrams are shown in **Figure 7.4**.

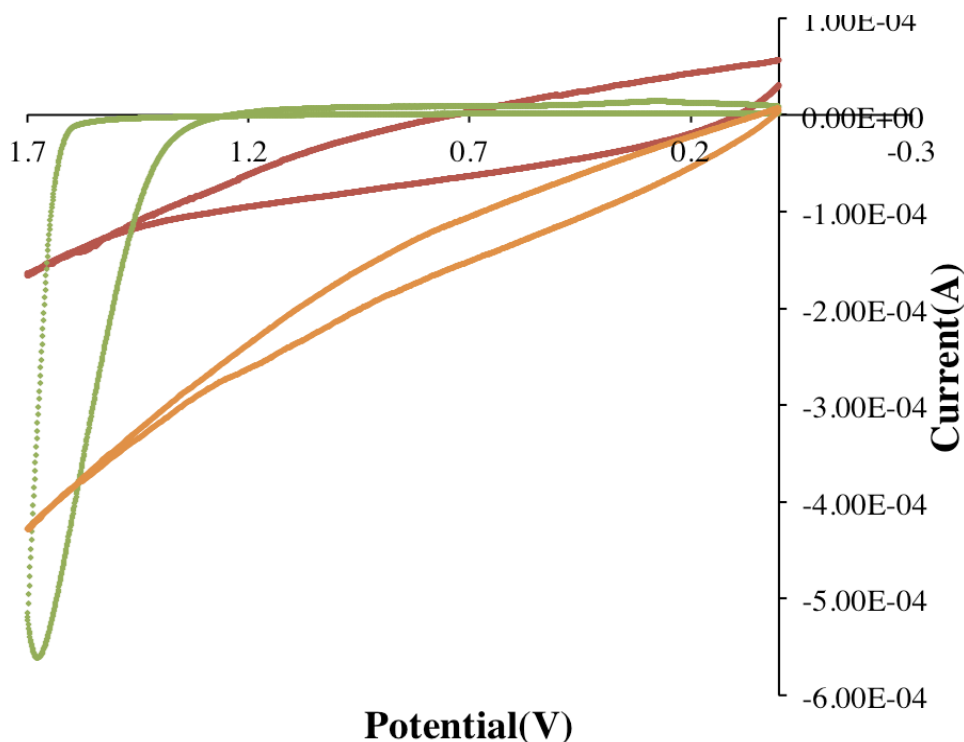


**Figure 7.4** Cyclic voltagrams for PProDOT-Me<sub>2</sub> on a) ITO coated glass substrate (green), b) sample 1 (yellow) and c) sample 2 (red) using 50mV scan rate

Same experiment was carried out using 2,2' bithiophene monomer and same trend was noticed. Using the same monomer concentration, sample 1 consumed  $8.386 \text{ mC/cm}^2$  charge while sample 2 consumed  $2.125 \text{ mC/cm}^2$  at 30 s conversion times for 2-electrode system where PET-ITO used as counter electrode. Because of the lower  $R_s$  value of sample 1, the amount of polymer grown on the mesh is less than the other using same monomer concentration and conversion time. **Figure 7.5 and 7.6** shows the images and color coordinates of sample 1 and 2 after deposition of poly 2,2' bithiophene. Fiber diameter was measured by SEM analysis and **Figure 7.7** shows the images. It was found that the thickness of the PEDOT-PSS and electrochromic polymer on sample 1 is  $0.31 \text{ }\mu\text{m}$  and  $0.4 \text{ }\mu\text{m}$  respectively. Electrochemical studies were performed after deposition of poly 2,2' bithiophene and they undergo electrochemical redox switching and the images at two redox state are shown in **Figure 7.8**

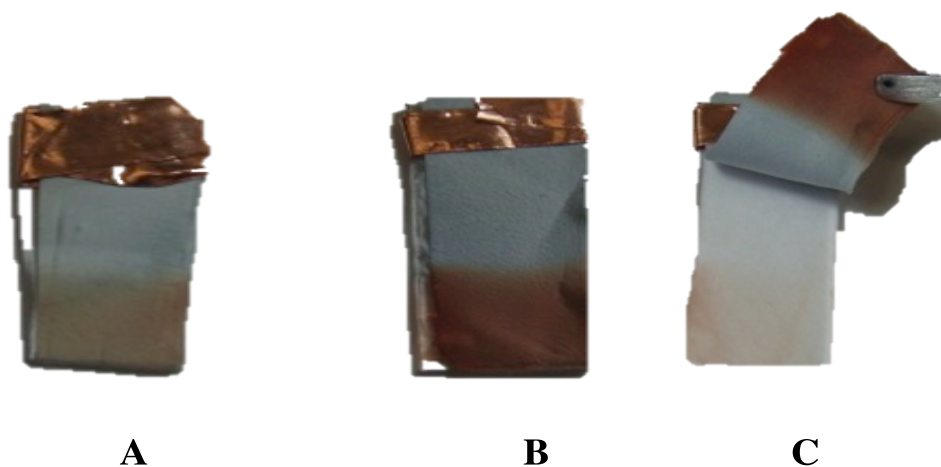


**Figure 7.5** Poly 2,2'bithiophene deposited on conductive PET-silica fiber mesh (A) sample 1, (B) and (C) sample 2 using ACN/LiTRIF electrolyte bath front and back

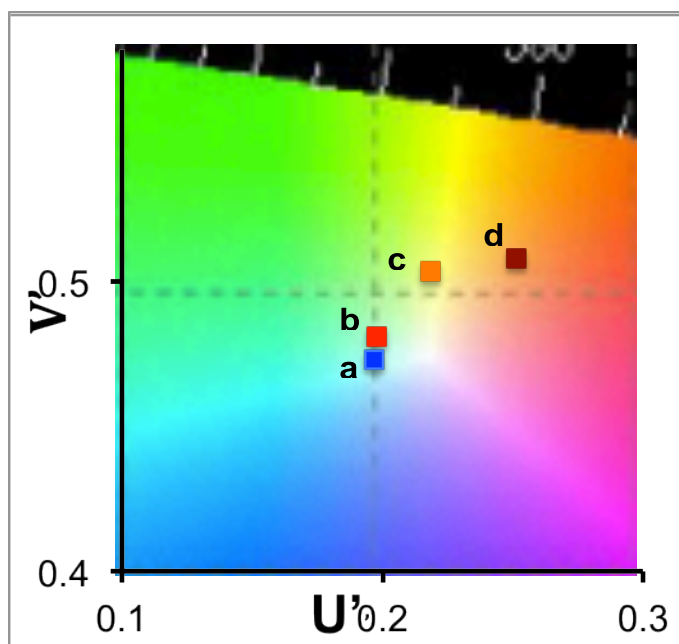


**Figure 7.6** Represents the color coordinates of fiber mesh (a) sample 1 before, (b) sample 2 before, (c) sample 1 after and (d) sample 2 after Poly 2,2'bithiophene deposited by blue, red, orange and dark red respectively.

Same electrochemical experiment was performed using a mixture of two monomers, 2,2-dimethyl-3,4-propylenedioxythiophene and 1,3 di-*t*-butyl-3,4-propylenedioxythiophene to get a random copolymer of PProDOT-Me<sub>2</sub>-co- PProDOT-*t*-Bu<sub>2</sub>.



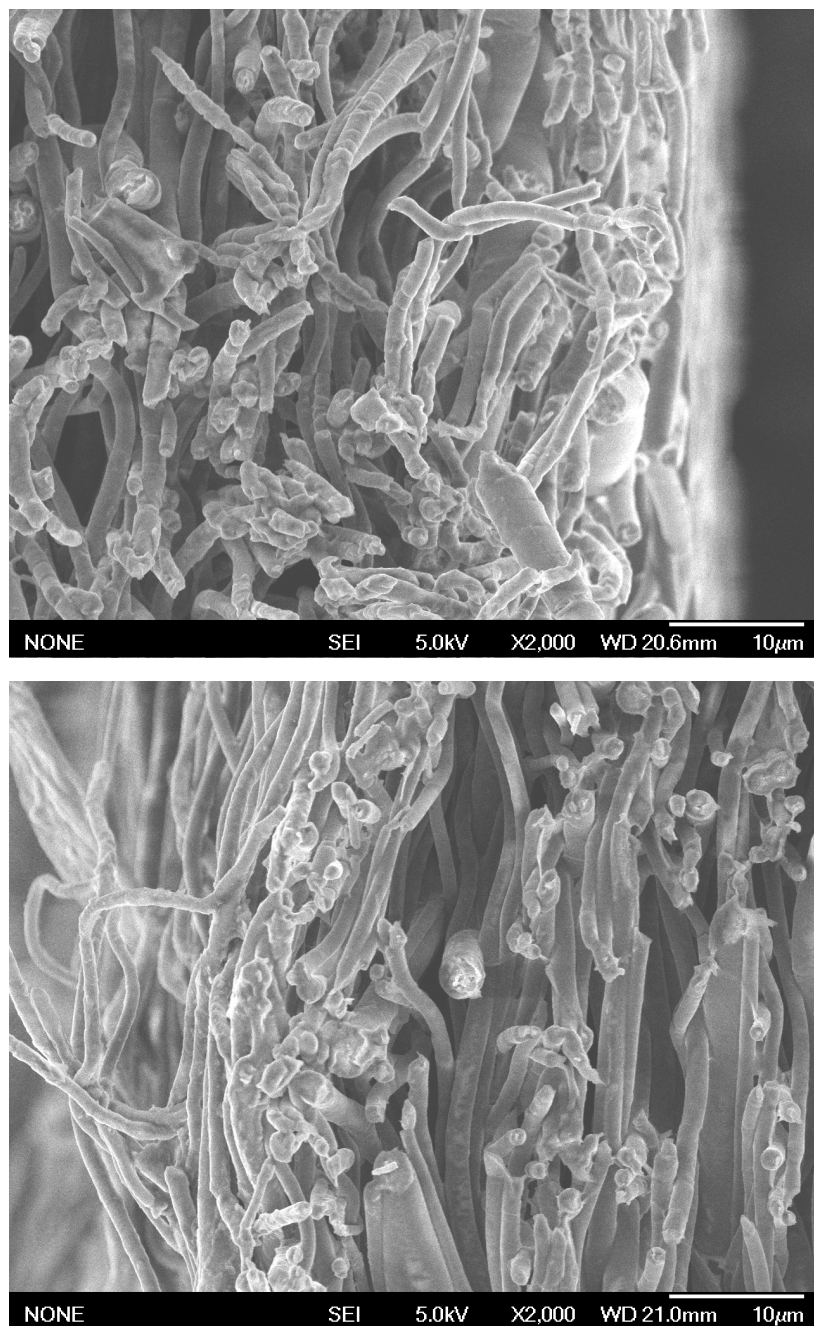


**Figure 7.7** SEM images of 15wt% PET-silica after spun coated with 100wt% Orgacon (top) and after electrodeposition of poly 2,2' bithiophene (bottom).

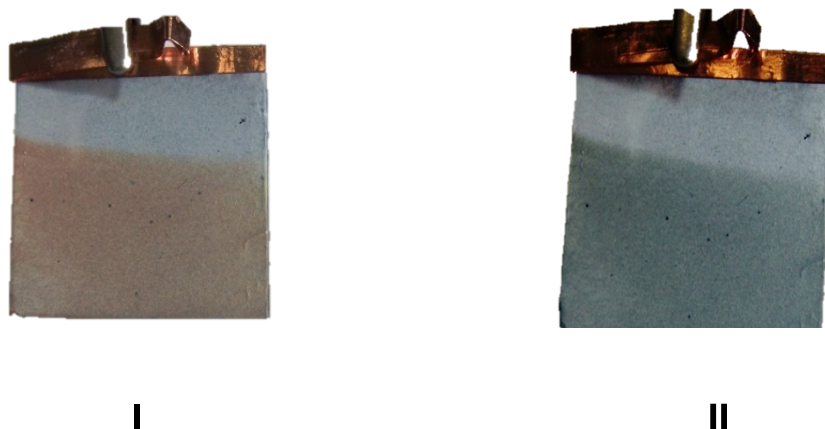


**Figure 7.8** (I) and (II) showing electrochemically switched neutral and oxidized state of Poly 2,2'-bithiophene deposited on conductive fabric mesh respectively

### 7.3.5 Electrochromic device assemble

Electrochromic devices were assembled using conductive fiber mat as working electrode as reported previously. Device 1 and 2 were made by electrodepositing poly 2,2'-bithiophene and copolymer PProDOT-Me<sub>2</sub>-co-PProDOT-*t*Bu<sub>2</sub> on conductive fiber mat and placing a polymer gel electrolyte in between working and counter electrode. For device 1 and 2 stainless steel mesh and ITO coated PET were used as counter electrode. An electrochromic device (denoted as 3) was assembled using *in situ* approach using 100wt% PEDOT-PSS concentrated fiber mat as working electrode and ITO coated PET was used as counter electrode. ProDOT-Me<sub>2</sub> monomer was dissolved into polymer gel electrolyte and a 3 V bias was used to form the electrochromic polymer onto conductive mesh.

Assembled electrochromic devices 1, 2 and 3 are shown in **Figure 7.9**. A  $\pm 2$  V potential is subjected to switch the devices between two-redox states. Third switching cycle of device 2 is shown in **Figure 7.10**. The ECD needs about 4-5 minutes to switch completely from one state to other with 4 cm<sup>2</sup> active area.

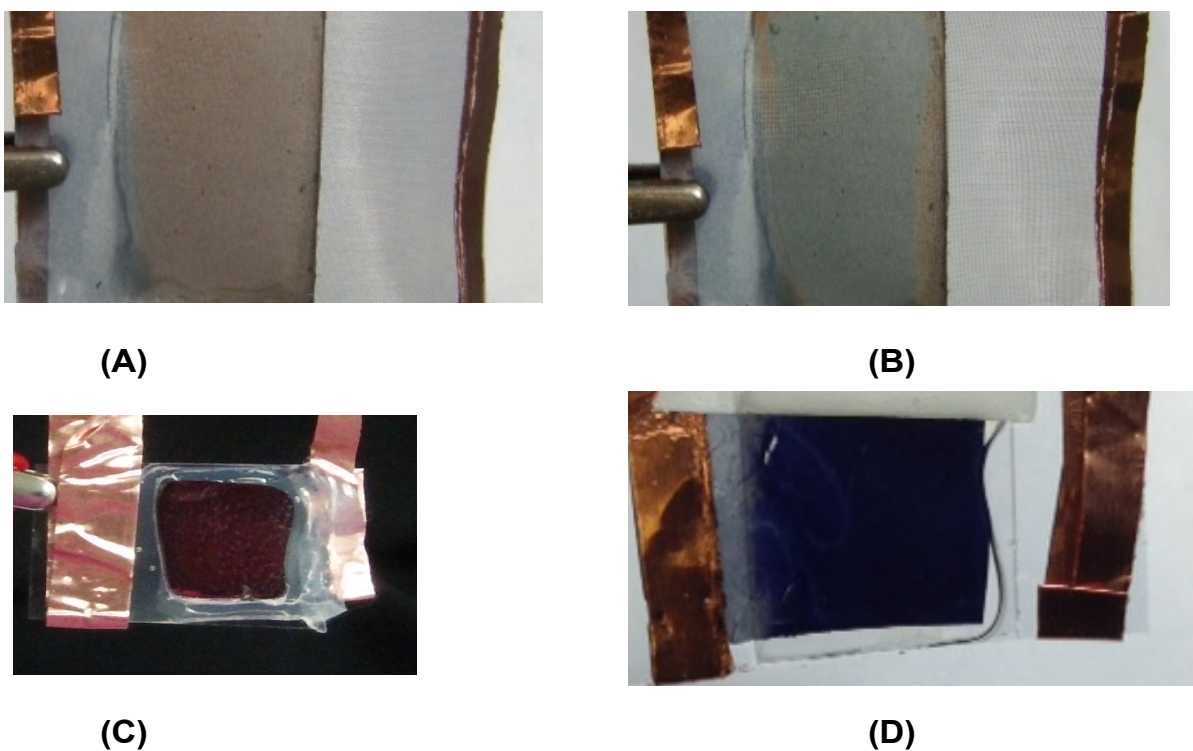


**Figure 7.9** Assembled ECD using PET-silica fiber mesh as the working electrode: (A) neutral state of device 1, (B) oxidized state of device 1, (C) neutral state of device 2 and (D) neutral state of device 3

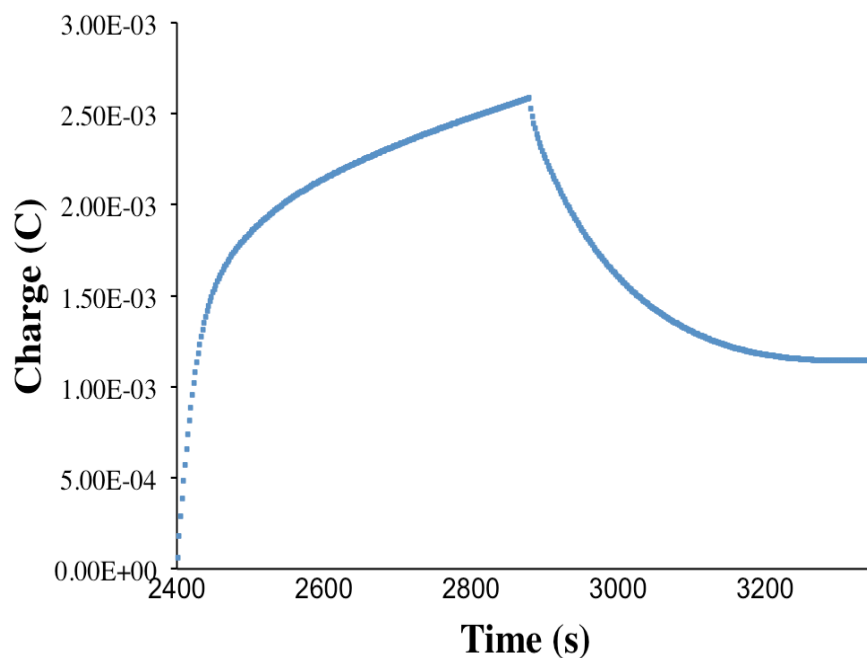


**Figure 7.10** Third switching cycle of copolymer, PProDOT-Me<sub>2</sub>-co-PProDOT-*t*Bu<sub>2</sub> deposited on PET-silica fiber mat

#### 7.4 Conclusions

This process demonstrates a novel approach to prepare conductive nonwoven fiber mesh with sheet resistivity 34 ohm/sq. By optimizing the electro spinning parameters flexible electrode was made with 90 ohm/sq sheet resistivity. A relationship was established between luminance and sheet resistivity and the effect of conductivity on coloration of electrochromic polymer. Reflective type electrochromic device was assembled using non woven fiber mat as working electrode.

## References

- (1) Rossi, D. D. *Nature Materials* **2007**, 6, 328.
- (2) Mattila, H. R. C. N. L. T. *Intelligent textiles and clothing; Cambridge: Boca Raton* **2006**, p. xviii.
- (3) Tao, X. C. N.-L. Q. *Wearable electronics and photonics; Boca Raton FL: Cambridge* **2003**, p. xiv.
- (4) Malinauskas, A. *Polymer* **2001**, 42.
- (5) Carpi, F.; Rossi, D. D. *IEEE TRANSACTIONS ON INFORMATION TECHNOLOGY IN BIOMEDICINE* **2005**, 9, 295.
- (6) Tehrani, P.; Hennerdal, L. O.; Dyer, A. L.; Reynolds, J. R.; Berggren, M. *Journal of Materials Chemistry*. **2009**, 19, 1799.
- (7) Invernale, M. A.; Ding, Y.; Sotzing, G. A. *ACS Appl. Mater. Interfaces*. **2010**, 2, 296.
- (8) Hu, B.; Li, D.; Ala, O.; Manandhar, P.; Fan, Q.; Kasilingam, D.; Calvert, P. D. *Advanced Functional Materials* **2011**, 21, 305.
- (9) Argun, A. A.; Aubert, P. H.; Thompson, B. C.; Schwendeman, I.; Gaupp, C. L.; Hwang, J.; Pinto, N. J.; Tanner, D. B.; MacDiarmid, A. G.; Reyanols, J. R. *Chem. Mater.* **2004**, 16, 4401.
- (10) Jang, S. Y.; Sotzing, G. A.; Marquez, M. *Macromolecules* **2004**, 37, 4351.
- (11) Bokria, J. G.; Kumar, A.; Seshadri, V.; Tran, A.; Sotzing, G. A. *Adv Mater* **2008**, 20, 1175.
- (12) Kumar, A.; Jang, S. Y.; Padilla, J.; Otero, T. F.; Sotzing, G. A. *Polymer* **2008**, 49, 3686.
- (13) Kim, W. H.; Mäkinen, A. J.; Nikolov, N.; Shashidhar, R.; Kim, H.; Kafafi, Z. H. *Applied Physics Letters*. **2002**, 80, 3844.
- (14) Xu, J.; Yang, Y.; Yu, J.; Jiang, Y. *Applied Surface Science*. **2009**, 255, 4329.

- (15) Hu, L.; Pasta, M.; Mantia, F. L.; Cui, L.; Jeong, S.; Deshazer, H. D.; Choi, J. W.; Han, S. M.; Cui, Y. *Nano letters* **2010**, *10*, 708.
- (16) Wu, J.; Zhou, D.; Too, C. O.; Wallace, G. G. *Syn Metals*. **2005**, *155*, 698.
- (17) Groenendaal, L.; Jonas, F.; Freitag, D. *Adv Mater* **2000**, *12*, 481.
- (18) Kim, J. Y.; Jung, J. H.; Lee, D. E. *Syn Metals*. **2002**, *126*, 311.
- (19) Huang, J.; Miller, P. F.; Wilson, J. S.; Mello, A. J. D.; Bradley, D. C. *Adv. Funct. Mater* **2005**, *15*, 290.
- (20) NA, S. I.; Kim, S. S.; Jo, J.; Kim, D. *Adv Mater* **2008**, *20*, 4061.
- (21) Beaujuge, P. M.; Ellinger, S.; Reynolds, J. R. *Nat Mater* **2008**, *7*, 795.
- (22) Gunbas, G. E.; Durmus, A.; Toppare, L. *Adv. Funct. Mater.* **2008**, *18*, 2026.
- (23) Sonmez, G.; Shen, C. K.; Rubin, Y.; Wudl, F. *Angew Chem Int Ed Engl* **2004**, *43*, 1498.
- (24) Ding, Y.; Invernale, M. A.; Mamangun, D. M. D.; Kumar, A.; Sotzing, G., A. *J. Mater. Chem.* **2011**, *21*, 11873.
- (25) Nardes, A. M. **2007**
- (26) Huang, J.; Miller, P. F.; Wilson, J. S.; Mello, a. J. d.; Mello, J. C. d.; Bradley, D. D. C. *Advanced Functional Materials*. **2005**, *15*, 290.
- (27) Nardes, A.; Kemerink, M.; Dekok, M.; Vinken, E.; Maturova, K.; Janssen, R. *Org. Electron.* **2005**, *9*, 727.

## **Chapter 8**

### **Conclusion and future work**

In this dissertation, we have seen that  $\pi$ -conjugated electrochromic polymers can be formed inside the solid matrix via one step assemble method that is known as *in situ* process. For this process, there is no need to synthesize the ECPs before assembling the device. That helps to avoid complicated synthesis procedure. The only criterion for this process is, the monomer needs to be dissolved into the gel electrolyte to give a colorless solution. There is no need to electrolyte bath that led to minimal chemical waste. As the electropolymerization process is a nucleation growth process, it is diffusion controlled. And the diffusion rate of any electroactive species is slow inside the solid matrix compare to liquid electrolyte. As a result the rate of success for *in situ* process to make a defect-free device is very high compare to traditional electrodeposition method. There is no need to have a vigorously cleaned electrode surface. An ECD can be easily assembled within 15 minutes under open atmosphere. In chapter 3, it has been shown that large area defect-free device about a size of a goggle,  $>100\text{ cm}^2$  was assembled via *in situ* with a 46% photopic contrast without any background correction. In this chapter it has mentioned that as the ECPs are growing inside the device, the optical behaviors like contrast, switching speed are very much dependent on both material and device characteristics. A relationship is established to achieve best performance by optimizing the material and device properties. Rate of the electrochemical reaction could be affected by several factors, among them concentration of is very important. As this reaction is diffusion controlled,



any kind of change in electro active species; like by changing the size of the molecule or by varying the concentration the rate of ECP formation will be affected. That will affect the optical properties of the device. For any kind of change in material behavior the polymerization time needs to be controlled to achieve highest photopic contrast. As it has been noted that each ECP system has a saturation value based on the polymer layer thickness, to have a device with high optical value with fast response time the thickness needs to be controlled. Other variables like thickness of the gel electrolyte, temperature also can affect the photopic contrast.

Also, the ionic conductivity of the gel electrolyte has an important role to increase the photopic contrast. It has been found that highest conductivity produces highest contrast. Here different types of salt and solvents were used and it is noticed that lithium salts works better than other salt system. Instead of using a single solvent system binary system has higher conductivity as well as higher photopic can be achieved.

As these ECPs are forming inside the solid matrix, by changing the cross-linking density of the system affect the morphology of the ECPs. Although morphology of these ECPs could not be studied under SEM but the spectroscopic data at oxidized state supports the fact. By changing the molecular weight of PEGDA, photopic contrast increased to 54% for PProDOT-Me<sub>2</sub> with out any background correction.

Here only PEGDA systems were used for this section (chapter 5) but other oligomeric systems with different repeating unit and active group could be used to enhance the photopic contrast of ECPs as well.

It has been seen that color of the copolymer can be tuned pretty easily by changing the concentration of corresponding monomer via *in situ* method. All subtractive colors can be achieved following this method. Even neutral color can be achieved by forming all subtractive colors in one step. Here we have seen that by addition of small amount of organic yellow dye with PProDOT-Me<sub>2</sub> was able to provide neutral color. So, it could be possible by synthesizing suitable ECP that has close  $\lambda_{\max}$  to yellow dye and transmissive bleached state would enhance the photopic contrast of neutral color device from 30%.

On my last project, we were able to develop a flexible non woven fiber mat with 90 ohm/sq sheet resistance. That resistance value is very close to the commercially available ITO that is used to build ECDs. In future by changing the size and concentration of silica nano particle or by using different technique like plasma effect, flexible fibers with low sheet resistivity (<90 ohm/sq) could be achieved.